ADDIS ABABA UNIVERSITY
INSTITUTE OF TECHNOLOGY
CENTER OF ENERGY TECHNOLOGY

INTEGRATION OF SOLAR THERMAL SYSTEM FOR IMPROVED ENERGY CONSUMPTION IN LOW TEMPERATURE INDUSTRIAL PROCESSES, CASE: HARAR BREWERY.

FINAL

Advisor: Dr. Ing. Abebayehu Assefa
&
Dr. Abdulkadir Aman

By: Ashenafi G/Hawariat

THIS IS SUBMITTED TO SCHOOL OF GRADUATE STUDIES, ADDIS ABABA INSTITUTE OF TECHNOLOGY, IN PARTIAL FULFILMENT FOR THE DEGREE OF MASTERS OF SCIENCE IN ENERGY TECHNOLOGY

MAY 2016

ADDIS ABEBA

ETHIOPIA

Certification

I, the undersigned, certify that I read and hear by recommend for acceptance by Addis Ababa University Institute of Technology Energy Center a thesis entitled “Integration of Solar Thermal System for Improved Energy Consumption in Low Temperature Industrial Processes, Case: Harar Brewery.” In partial fulfillment of the requirements for the degree of Masters of Science in Energy Technology.

Dr. Abdulkadir Aman

(Supervisor)

Declaration

I, Ashenafi G/Hawariat, First, I declare that this thesis is the result of my own work and that all sources or materials used for this thesis have been duly acknowledged. This thesis is submitted in partial fulfillment of the requirements for Masters' Degree' in Energy Technology at Addis Ababa University and to be made available at the University's Library under the rules of the Library. I confidently declare that this thesis has not been submitted to any other institutions anywhere for the award of any academic degree, diploma, or certificate.

Ashenafi G/Hawariat

Signature --------------------

Addis Ababa University

Institute of Technology

School of Graduate Studies

Energy Center

This is to certify that the thesis prepared by Ashenafi G/Hawariat, entitled: "Integration of Solar Thermal System for Improved Energy Consumption in Low Temperature Industrial Processes, Case: Harar Brewery" and submitted in partial fulfillment for the requirement of degree of Master of Science in Energy Technology compiles with regulation of Addis Ababa University and meets the accepted standards with respect to originality and quality.

Board of Examining Committee:

Advisor: - Dr. Abdulkadir Aman Signature……………Date ………………

External Examiner: ____________________________Signature…………..…Date……………….

Internal Examiner: _____________________________Signature…………..…Date …………..……

…………………………………………………………

Chair of Department or Graduate Program Coordinator

Abstract

The objectives of this paper are to analyze thermal energy production of heat pipe evacuated tubes solar collector and investigate the integration of solar thermal system with conventional system in low-temperature industrial processes in Harar Brewery Factory. In this study, Matlab program and RET Screen software were implemented to identify technical and financial feasibility of the system.

Six low temperature processes, such as feed water pre-heating, kegging, CIP, Mashing at 78^0C, bottle cleaning and mashing at 52^0C were selected in the industry for integration of solar thermal system. The total annual conventional thermal energy consumption of the selected processes is 11,176.18MWthr. This covers 54.15% of the annual total thermal energy consumption in the industry from the chemical energy of fuel (20638.23MWthr).

The solar thermal system of a single heat pipe evacuated tubes solar collector was analyzed. The maximum outlet water temperature is 80^0C for mass flow rate of 47.52 kg/hr through the manifold. However, the maximum outlet water temperature is 52^0C in mashing process for the mass flow rate of 75.60kg/hr. and, the maximum outlet water temperature for bottle cleaning at 65^0C. It should have a mass flow rate of 66.6kg/hr. The maximum instantaneous efficiency is during sun shine and sun set hours. And, the minimum instantaneous efficiency is 84.96% on March 31 at 11:00 in the morning for the mass flow rate of 47.52kg/hr. However, the minimum instantaneous efficiency is 83.02% when the mass flow rate is 66.6kg/hr. And, the minimum instantaneous efficiency of the system is 62.19% when the mass flow rate of water is 75.60kg/hr. The maximum solar thermal energy harvested form a single collector at a mass flow rate of 47.52kg/hr is 3.19KWt on March 31 at 11:00 in the morning. However, the highest daily solar thermal energy produced on March 12 is 22.01KWthr and the lowest daily solar thermal energy produced on July 19 is 3.66KWthr.

The appropriate location of solar collectors is identified to harness the maximum possible solar energy. The optimal number of collectors needed for partial supply of thermal energy to the industry are 368 (30 for mashing at 52^0C, 62 for mashing at 78^0C, 59 for bottle cleaning, 22 for feed water pre heating, 168 for CIP and 27 for kegging).

The Annual solar thermal energy production was analyzed for all processes. Those are 127.03MWhr, 333.47Mwhr and 1613.98MWhr for mashing at 52^0C, bottle cleaning and other thermal processes at $78\text{-}80^0$C respectively. The total annual solar thermal energy harvested for all selected processes is 2074.48MWhr.

Due to the integration of solar thermal system in low temperature industrial processes, the consumption of conventional thermal energy for the selected processes are reduced to 9101.70MWhr/year. Which means 18.56% of thermal energy consumption for selected processes in the industry could be saved. However, the total annual thermal energy consumption of the industry is reduced to 18147.76MWthr. This means 12.07% (10.05% from selected processes, 2.01% from overall heat loss and 0.01% from pre heating of fuel) of the fuel consumption in the industry is saved. In other way, 205,840.65 liter of furnace oil is saved every year.

The total initial investment cost of the project is $440,864 (50% is project equity and the remaining is project debt). This project saves $165,813 of the annual cost of the industry for thermal energy application and reduces 729.54 tons of carbon dioxide (CO2) emission per year. The project equity is returned back with 1.6 years.

Acknowledgment

A lot of thanks to the Almighty God for His willingness without which this thesis work is unthinkable.

First of all I would like to express my sadness for the passes away of my former advisor Dr. Ing. Abebayehu Assefa. I am deeply grateful for his support, feedback and encouragement. He had given time for my work until the last day. I really wish him rest in peace. And also, I gratefully acknowledge my new advisor Dr. Abdulkider Aman for his positive responds to see and comment my thesis.

I pull-out my gratitude to all Harar Brewery S.C workers who have devoted their time to give me all necessary information and valuable data for this thesis (particularly Ato Zemichael technical head of HBF and Ato Kidus Maintenance Section staff member).

Thanks go also to Dr. Solomon Abebe head of Energy Center in Addis Ababa University, Institute of Technology wrote a letter to Harar Brewery Factory and other organization to get the necessary data for this work.

I am deeply grateful to all of my friends in Haramaya University, Institute of Technology (particular Ato Habitamu Hailu for his valuable support and Ato Asmelash Tilahun for editing this paper) for their everlasting support throughout this thesis work.

Table of Contents

List of Tables

List of Figures

Abbreviations

IEA	International Energy Agency
SWH	Solar water heating
ETC	Evacuated tube collectors
ETSCs	Evacuated Tube Solar Collector
FPC	Flat Plate Collector
WBF	Walliya Kilinto Brewery Factory
BBF	Bedelle Brewery factory
HBF	Harar Brewery Factory
NOC	National Oil Company
Abv	Alcohol by Volume
CIP	Clean In Place
ODE	Ordinary Differential Equation
PDE	Partial Differential Equation
GCV	Gross Calorific Value
GHG	Green House Gases
HPETSc	Heat Pipe Evacuated Tube Solar Collector
DBE	Development Bank of Ethiopia

Nomenclature

ω	Hour Angle (^{0})
ST	Solar Time (hr)
N	Number of Day of the Year /Number of Solar Collector/
k_T	Hourly Clearness Index
I	Irradiation/Global Irradiance/ $\left(\frac{W}{m^2}\right)$
R	Ratio
I_o	Extraterrestrial Irradiance (W/m^2)
Isc	Solar Constant (1367W/m^2)
ΔP	Pressure Drop
h	Heat Loss Coefficient ($\frac{W}{m^2K}$)/ Enthalpy (J/Kg) /
T	Temperature (^{0}C)
U	Heat Loss (W/m^2)
D	Diameter (m)
L	Length (m)
k	Thermal Conductivity (W/m C)
K_p	Permeability of Wick (m)
t	Thickness (m)
V	Velocity (m/s) (Volume (m^3))
Cp	Specific Heat (J/kg C)
re	Effective Radius of Heat Pipe

A Area (m^2)

Q Thermal Energy (W)

ṁ Mass Flow Rate (Kg/s)

η Efficency (%)

h_{fg} Latent Heat of Vaporization (KJ/Kg)

l Length (m)

T_{bf} Temperature of heat pipe working fluid (^0C)

Hr Hydraulic Radius of Porous Media.

ke Conductivity of the Wick Material

R Heat Transfer Resistance (m^2K/W)

Po Working Pressure (bar)

r_e Effective Radius of Heat Pipe (m)

r_h Hydraulic Radices of Porous Media (m)

Greek Symbols

δ Declination Angle

θ Incident Angle(Angle)

Ø Latitude

β Inclination Angle

γ Surface Azimuze Angle /Specific Heat Ratio/

ρ Graund Reflective Coefficient (Density)

σ Stephen Boltsman Constant (surface Tension)

ε Emmisivity

μ Viscosity

τ Trnsimitivity

α Absorvitvity

Subscripts and Superscripts

o Exterterstorial

d Diffuse

b Beam

T Total on Tilted Surface

pg Plate to Glass

ga Glass to Ambient

r Radiation Heat Transfer /Reflective/

bt Beam on Tilted Surface

dt Diffuse on Tilted Surface

z Zenith

p Plate

g Glass/gravity

a Ambient /adiabatic

i Inner/ Instantaneous

o Outer

e Evaporation Section

sc Saturated Liquid to Condensation Section

cov Convention

CHAPTER ONE

1. Introduction

1.1. Background Information

1.1.1. Energy Demand

Energy is a critical input to the socio-economic development of any nation as well as to the protection of the nation's environment [1]. It fuels the industry, commerce, transportation, agriculture and other economic activities.

The energy crises (the oil shocks of the 1970's) occasioned by sudden sharp increases in the price of petroleum and its products had devastating impacts on the economies of many countries, both developed and developing, but in particular the latter [2]. A number of factors have brought to the fore the importance of, and urgency for alternative energy resources. These include the high energy prices, insecurity of energy supply, concern about adverse environmental and health impacts and unease over the rate at which the major energy resources are being depleted.

Concern has, furthermore, been mounting about the spiraling depletion of the environment as exemplified by local air pollution and acid precipitation from ever growing fossil fuel combustion. Associated with these are emerging global issues such as potential climate change as a result of greenhouse gases emissions. All these as well as the attendant adverse health impacts have become important drives for increased alternative source of energy.

1.1.2. Thermal Energy in the Industrial Sector

Heat energy is one of the most important production factors in the industry. Thermal energy accounts for 37 percent of energy consumed within most developed countries, and 47 percent of the world's energy consumption. The industrial sector is the leading source of energy consumption in the United States. At nearly one third of total energy use, it exceeds both the transportation and residential sectors. Within the industrial sector, nearly two thirds of energy used is consumed as heat [3].

Depending on how industrial thermal energy is defined, nearly 90 percent of the energy comes from burning fossil fuels, but biomass can count for up to 11 percent. The remaining 10 percent of thermal industrial energy comes from electricity, which is often generated by power plants that burn fossil fuels. This situation affected the environment from extracting fossil fuels, the air pollution emitted after their combustion, and large emissions of greenhouse gases [4].

In connection with increasing energy costs advanced and efficient energy supply systems are required. Additionally, a sustainable production attracts the consumer's attention more and more. Hence, the reduction and replacement of fossil fuels are major objectives for industrial production, as the industry consists of various branches for heat energy demand. Solar thermal process heating systems are a very encouraging renewable technology for fuel replacement. It is possible to cover the low-temperature heat demand up to 100 °C and energy for hot service water with sophisticated, market available solar-thermal systems [5]. It is obvious that there are also sub-sectors with mainly heat energy demands above 100 °C, for example the metal production and processing or the production of glass and ceramics. However, there remain many sub-sectors with large low-temperature energy demand [6].

According to the International Energy Agency (IEA), solar thermal energy is a practical technology with much room for innovation which has been largely unexploited for industrial needs. As of 2008, there were only 90 solar thermal plants for industrial process heating worldwide, comprising a combined 25 thermal megawatts (MWth) of output. When compared to the 118 GWth of solar output worldwide, this constitutes less than 0.02% of total solar thermal capacity [7].

1.1.3. Thermal Energy in Brewery Industries

A comprehensive review identified solar energy is currently an underutilized renewable energy source that has the potential to supply a portion of industrial thermal energy demand for the food industry and especially its sub-sectors breweries as very promising for solar-thermal applications [8]. Solar thermal systems, when correctly integrated within an industrial process, could provide significant progress towards both increased energy efficiency and reduction of carbon dioxide emissions. With efficient production technology more than 90 % of the required thermal energy demand in brewery industry is below 100 °C [9]. As Table 1:1 illustrates, only a few processes, e. g. evaporation (beer production) need temperatures above 100 °C and is not suitable for low temperature solar-thermal energy supply. However, low-temperature processes like; pre-heating, bottle cleaning, mashing and clean in place applications dominate the production of beer.

Table 1:1: Exemplary Process Temperatures in Brewery industries [10]

S.N	Processes	Sub- sector	process	Max. operating temperature
1	<100^0c	brewery	Mashing	65
		brewery	Bottle cleaning	85
		brewery	CIP	90
2	>100^0c	brewery	Evaporation of water	100

This study "Integration of Solar Thermal System for Improved Energy Consumption in Low Temperature Industrial Processes, Case: Harar Brewery factory" is designed to the development of heat energy supply systems for low-temperature energy demand focusing on solar-thermal energy. In this paper the potential of heat pipe evacuated tube solar thermal system to provide low temperature process heat demand of a plants were investigated. The general concerns of integrating solar thermal energy into a non-continuous and continuous process were discussed and a review of how the solar collector system can be operated to meet specific output water temperatures for specific thermal process. Specific integration strategies that could be applied to the Harar Brewery Factory were examined and the energy saving potential of each integration strategy was analyzed based on local meteorological data and market available heat pipe evacuated tube solar collector's specification. In addition, the economic feasibility of the system was analyzed.

1.2. Statements of the Problem

Currently, Ethiopia is one of the fastest growing countries in the world and has planned to transfer agricultural leading economy to industrialization. Accordingly, many different industries are launching in the country each year and the majority of newly established industries are using energy intensively. Almost all of those industries are dependent on the electrical power supplied by EPECO, fuel and natural gases imported from abroad.

The electrical power supplied for industrial application is 839MW which is 37% of the total production capacity of the country [11, 12]. However, it is not enough to cover the total energy demand of the industries. And, the imported fossil fuel charged the country a huge amount of foreign currency and exposed for carbon dioxide and other flue gases emission. Therefore, the country should search other technical and economical feasible options or means of thermal energy production systems.

Solar thermal process is the best environmental friendly source of energy for the countries located in between tropic of Cancer and tropic of Capricorn. These countries have high potential of solar irradiation and average sun light length of more than 10hour per day throughout the year [13]. Ethiopia is one of these naturally gifted countries having enormous amount of solar energy potential. But, the country didn't use this source of energy as expected.

In the meantime, the heat pipe evacuated tube solar collector for industrial processes has been identified with a number of technical problems that have become the obstacles to their advancements, e.g., low collector efficiency, high heat loss and poor solar energy harvesting capability. Some challenges also relate to the non-continues nature of thermal energy demand in the industries, variable nature of solar resources in short and long term bases, their installations to the buildings and capital costs. So to fix the country energy scarcity, the study on "**Integration Solar Thermal System for Improved Energy Consumption in Low Temperature Industrial Process**" with these unaddressed heat pipe ETSC problems is mandatory.

1.3. Objectives of the Study

1.3.1. General Objectives

The general objective of this study is to analyze thermal energy production of heat pipe evacuated tubes solar collector and investigate the integration of solar thermal system with conventional system for improved energy consumption in low-temperature industrial processes, Case: Harar Brewery Factory.

1.3.2. Specific Objectives

1. To analyze conventional thermal energy consumption in low temperature processes for Harar brewery industry.
2. To analyze hourly outlet water temperature and instantaneous efficiency of heat pipe evacuated tubes solar collector, designed for this specific purpose.
3. To determine optimal solar collectors size and its micrositting for selected thermal processes in the industry
4. To analyze the solar thermal energy production of the system for selected thermal processes in Harar brewery industry.
5. To analyze the improved energy consumption of integrated solar thermal system for selected thermal processes in the industry.
6. Financial analysis of the integration of solar thermal system in the industry.

1.4. Research Questions

This research has planned to answer the following questions:

- How much is the conventional thermal energy consumption of the selected thermal processes in the industry?
- How much is hourly outlet water temperature from heat pipe evacuated tube solar collector for Harar, Ethiopia weather condition?
- How much is hourly instantaneous efficiency of heat pipe evacuated tube solar collector?
- How much solar thermal energy is harvested by a single solar collectors?
- How much collector's area is needed to satisfy the thermal energy demand of low temperature thermal processes in the industry?
- Where is the suitable place for installation of solar collectors?
- How much solar thermal energy is harvested by solar collectors for selected thermal processes in the industry?
- How much the conventional thermal energy is saved due to the integration of solar thermal system in low temperature processes?
- How much tonnes of CO2 emission is reduced due to saving of fuel consumption in the industry?
- How much money is required for integration of solar thermal system for Harar Brewery Factory?
- How long is the payback period to regain the organization equity?

1.5. Scope and Significance of the Study

This study will give a detail knowledge on the integration of solar thermal system in low temperature industrial processes. A five years every fifteen minuet weather data of solar irradiance, ambient temperature and wind speed of Harar, Ethiopia weather condition were used for this study. And, the information of materials property data were collected from different literatures. This study were analyzed theoretically hourly temperature variation of each elements such as external glass cover, absorber plate, saturation fluid in evaporation section, condensation section and useful outlet water in manifold of evacuated tube solar collector for one year period. The conventional thermal energy consumption for six selected low temperature processes (such as Mashing at 52^0 C and 78^0 C, Bottle Cleaning, Make up Water Pre-heating, Kegging and CIP) were analyzed. And, hourly instantaneous efficiency for one year period and the optimal number of collector needed for partial thermal energy supply in the industry were determined. The appropriate location for collector installation was identified. Finally, annual fuel saved and greenhouse gases emission reduction potential were calculated. Mathematical developed model was validated against previous study on the same solar irradiance potential and heat pipe evacuated tubes solar collector specification.

However, this study did not include thermal energy storage for the night time energy consumption in the industry, experimental test for validation of this theoretical analysis, primarily data collection of thermal devices, the steam energy delivering pipes and boiler combustion efficiency in the industry, Stratification in thermal storage tank, solar thermal system integration for processes like pasteurization, temperature gradient of glasses cover and heat pipe perimeter, temperature gradient of along longitudinal axis of evaporator and condensation section and evaporation in the industry and tracing solar collector design.

Confidently, this study will improve energy consumption pattern of the industries. And this study could also suggest some points for further improvement of the system based on theoretical point of views. The results of this research will open an opportunity for further application of solar thermal system for industrial processes in the country. In addition, the result can be used as reference and base for future expansion plans and by policy-maker.

1.6. Organization of the Study

The rest of this paper is organized in to five chapters each having a distinct and related purpose. The next chapter, Chapter Two, explains the theoretical and empirical literature review. Chapter Three is prepared to description of the organization. The appropriate methodology and method is developed at Chapter Four that clearly identifies the empirical techniques and software tools used. Chapter Five is devoted to the analysis and its outcome related to the result. Chapter Six draws conclusions, recommendations.

CHAPTER TWO

2. Literature Reviews

2.1. Introduction

Solar water heating (SWH) systems have a widespread usage and applications in both domestic and industrial sectors. According to Renewable Energy Policy Network data (2010), 70 million houses worldwide were reported to be using SWH systems. Solar water heating is not only environmentally friendly but requires minimal maintenance and operation cost compared to other solar energy applications. SWH systems are cost effective with an attractive payback period of 2–4 years depending on the type and size of the system. Extensive research has been performed to further improve the thermal efficiency of solar water heating [14].

Conventional flat plate collectors are suited for warmer climates and for the times when the intensity of the solar radiation is substantially high. Their benefits are however reduced when they are exposed to cold, cloudy and windy days. Furthermore, when exposed to weathering conditions, the tubes and the insulation has a tendency to deteriorate thereby causing loss of performance [15].

An evacuated tube collector is slightly more efficient than a flat plate system due to lower heat losses. With less heat loss through the vacuum air layer in the evacuated tubes, these systems are more efficient at lower ambient air temperatures. Compared to flat plate collectors, evacuated tube collectors require a smaller roof area than comparable flat plate collectors. Maintaining vacuum is difficult in case of evacuated tube collector. For the purpose of high temperature applications like industrial application and steam generation evacuated tube collectors are best suited because of its minimum heat loss [16].

Evacuated tube collectors (ETC) have been commercially available for more than 20 years. Though they have better performance in producing high temperatures when compared to flat-plate collectors, they are not competitive because of high initial costs. ETC consists of: evacuated tubes (glass-glass seal) to minimize heat losses, copper heat pipes for rapid heat transfer, and aluminum casing to provide durability and structural integrity to the system [17]. ETC minimizes the heat losses due to convection and radiation [18].

The efficiency of solar thermal conversion is around 70%. Solar water heating systems are classified in to two broad categories as passive and active systems. The active solar water heating systems generally have higher efficiencies, their values being 35–80% higher than that of the passive systems [19].

Numerous authors [20, 21, 22] have noted that ETSCs have much greater efficiencies than the common FPC, especially at low temperature and isolation. For instance, Ayompe et.al. [23] Conducted a field study to compare the performance of FPC and a heat pipe ETSC for domestic water heating system. With similar environmental conditions, the collector efficiencies were found to be 46.1% and 60.7% and the system efficiencies were found to be 37.9% and 50.3% for FPC and heat pipe ETSC, respectively.

2.2. Plant Layout and Beer Making Processes

2.2.1. Beer Processes Description

The brewing process uses malted barley and/or cereals, unmalted grains and/or sugar/corn syrups (adjuncts), hops, water, and yeast to produce beer. Depending on the location of the brewery and incoming water quality, water is usually pre-treated with a reverse osmosis carbon filtration or other type of filtering system. Figure 2.1 shows a block diagram flow of the main stages of beer production in a brewery [24].

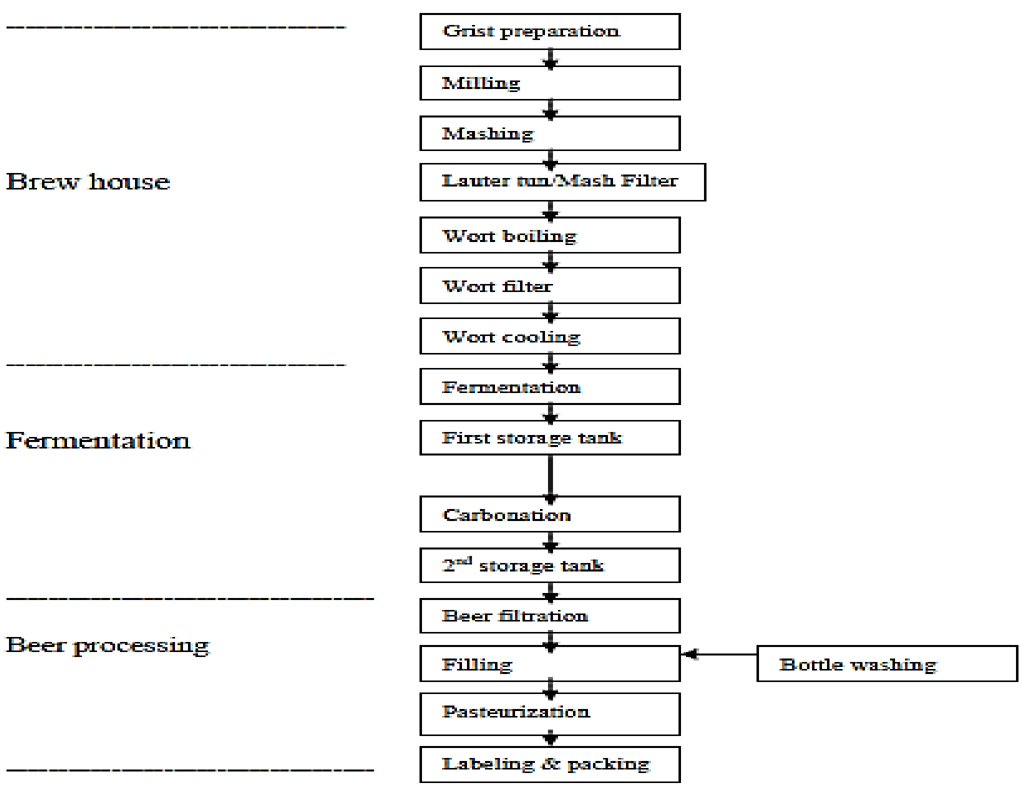

Figure 2. 1: Main Stages of Beer Production [24]

2.2.2. Energy Use in the Brew House

Brewery processes are relatively intensive users of both electrical and thermal energy, and the target for every brewing company should be the development of a sustainable process with efficient energy consumption to achieve savings in fuel and energy costs. Energy consumption is equal to 3-8% of the production costs of beer [24], making energy consumption improvement an important way to reduce costs, especially in times of high-energy price increases.

Thermal energy is used to produce steam, which is used largely for wort boiling, mashing and water heating in the brew house, and in the bottling hall. The major consumers of electricity in breweries are refrigeration (44%), packaging (20%), and compressed air (10%). The process refrigeration system is typically the largest single consumer of electrical energy, but the brew house, bottling hall, and waste water treatment plant can account for substantial electricity demand. The specific energy consumption of a brewery is heavily influenced by utility system and process design; however, site-specific variations can arise from differences in product recipe and packaging type, the incoming temperature to the brewery of the brewing water and climatic variations. Specific energy consumption in a brewery can vary from 100–200 mega joules per hectoliter (MJ/hl), depending on size, sophistication, and other factors [24].

2.3. Solar Thermal for Industrial Processes Heat

The industrial application of solar thermal technology is often erroneously regarded as simply an extended residential domestic hot water installation, albeit on a larger scale. However there are significant, non-trivial differences between the needs and constraints of industrial and residential users that must be considered. Industrial applications typically require higher temperatures and greater volumes than both residential and commercial applications. Where, and at what temperature the heat produced via a solar installation is used and integrated into plant processes must be carefully contemplated. Finally, the variable nature of both the solar energy supply and the process heat demand need to be considered during the design process. While a significant amount of research have been undertaken on the subject of solar equipment [25], a comparatively small amount of research has been conducted into the optimal integration of solar technologies with industrial sites [26].

2.4. Integration of Solar Thermal into Industrial Processes

There are several important issues that need to be considered before an optimal solar thermal installation can be used to provide process heat. Due to the non-continuous nature of the solar resource, storage and control strategies need to be carefully considered as they can add significant extra cost to a system. The process heat demand is also commonly non-continuous in many industrial processes. As a result the temperature/enthalpy profile as well as the pinch temperature may be changing over time as demand varies.

There are two main scenarios that the solar collector system can be designed for [27]. There is the case where the system provides all of the process heat demand at a target temperature. And, the system can be designed to provide some of the process heat demand at a target temperature or at a variable temperature which maximizes solar collector efficiency.

In the first scenario the variable daily demand profile for the site, as well as the site specific solar radiation and ambient temperature profiles need to be known to calculate the required collector area and the thermal storage requirements. The site specific solar radiation and micro-meteorological factors are extremely variable both in the short term and long term (i.e. seasonal variations). These variations need to be quantified in a statistical manner so the tradeoff between thermal storage and solar collector area can be carried out with a degree of confidence. Ultimately attempts to supply all of the heat demand at the target temperature will result in large costly systems that will be significantly underutilized a large proportion of the time unless demand and supply have a matching seasonal variation.

In the second scenario, the system supplies a portion of the heat demand and designing for short term variations in supply and demand and for overall seasonal differences is of less importance. Solar energy is captured whenever it is available and the balance of the heat demand needs to be supplied via other hot utility. The supply profile is therefore the critical factor for determining hot utility savings and hence the cost benefit of using a solar collector system.

From an operational point of view, the opportunity exists to run the collector in one of two ways. Heat can be supplied at the target temperature by manipulating the mass flow rate through the collectors, or a fixed mass flow rate can be supplied with a variable outlet temperature. The outlet temperature from the collector will vary but the system should be integrated such that the inlet is at or above the cold pinch temperature therefore ensuring heat is supplied above the pinch temperature. Operating at a fixed mass flow rate through the collectors will be advantageous because the collector temperature will be lower than for the fixed temperature case and the overall collector efficiency will be higher. The effect of process variables such as mass flow rate and fluid temperatures on collector efficiency is important for maximizing the amount of solar energy recovered [27].

The integration of solar energy into an industrial process requires studying and analyzing the existing heat supply system and determining the potential energy savings and the energy flows and temperatures levels of the process [28].

Integrating solar heat into industrial process is a complex operation compared to others conventional heat supply systems. The best integration of a solar process into an industrial process requires taking into consideration all aspects related to energy efficiency and heat recovery that could lead to economical, technical and organizational improvements. Solar integration into industrial process needs to pay particularly attention to energy saving potentials through a technological optimization of the process in itself and a system optimization of the whole production.

In general, the solar system will provide only a part of the overall process energy demand. While conventional heat systems most often do not pay attention to the temperature level (and consequently are over dimensioned), the integration of solar heat systems in the process implies taking care of the temperature levels of the whole system.

2.4.1. Integration of Solar Thermal for Preheating of Water

In most factories, the central system for heat supply is working with hot water or steam at a pressure corresponding to the highest temperature needed among the different processes. Thus solar systems can be coupled with the conventional heat supply system for preheating water (or other fluids) used for processes or for steam generation or by direct coupling to an individual process working at lower temperature than that of the central steam supply. Figure 2.2 shows the integration of solar thermal for preheating of water [28].

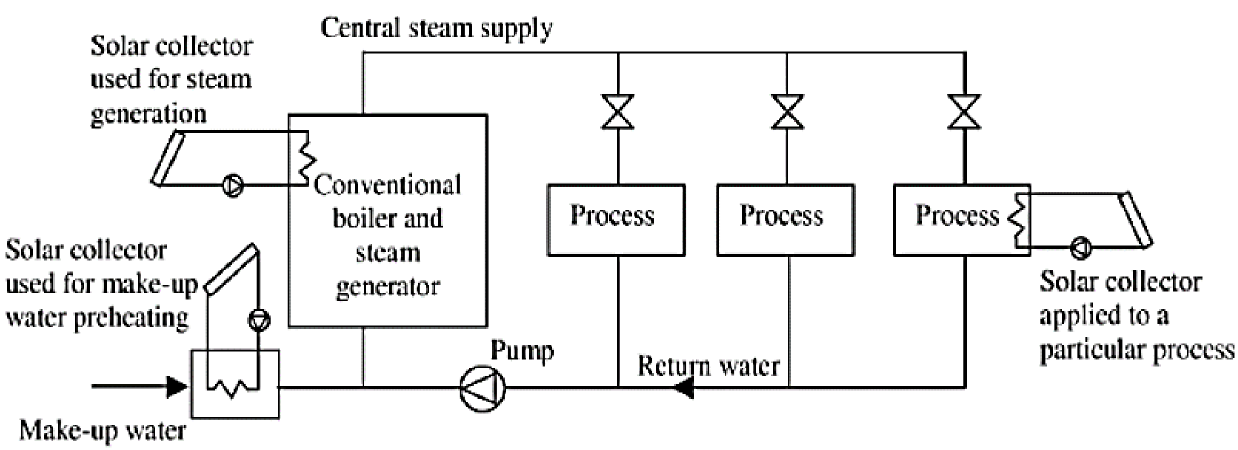

Figure 2. 2: Integration of Solar Thermal for Preheating of Water [28]

2.4.2. Integration of Solar Thermal into the Existing Heating System

The integration of solar thermal heat into industrial processes can also be done by integrating the solar heat directly into the existing heating system (Figure 2.3). Such integration requires that the solar collector operates at the same temperature with the existing heating system. While it is the easiest way to integrate solar thermal into the process both in terms of installation and control, the thermal efficiency should be lower, and the best heat transfer medium would be water to the largest extant [28].

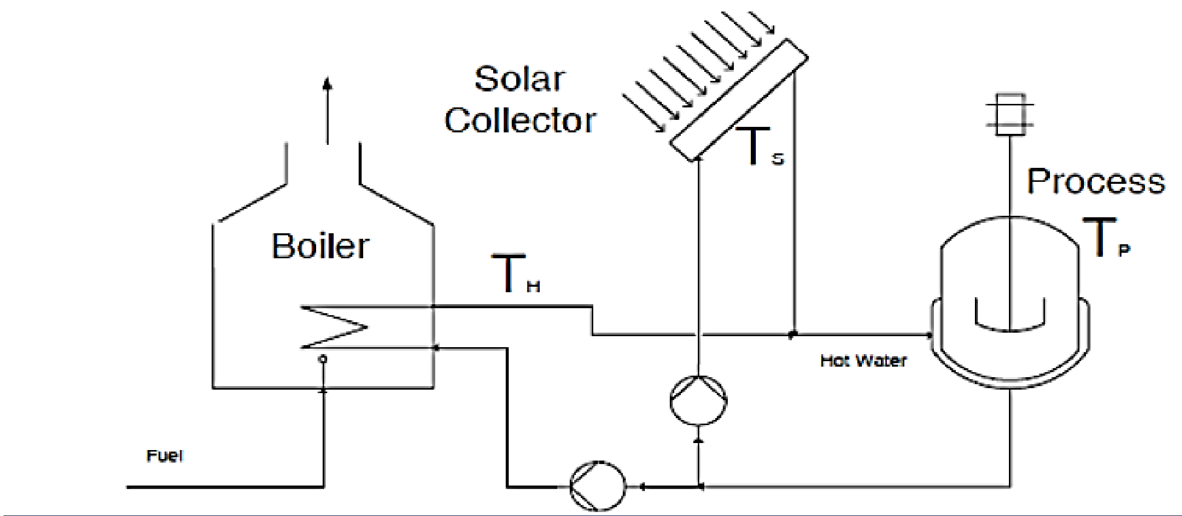

Figure 2. 3: Integration of Solar Thermal into the Existing Heating System [28]

2.4.3. Integration of Solar Thermal into Process Heat

Another possibility of integrating solar system in the conventional heat system is to integrate it directly in the process heat (Figure 2.4). This implies to integrate another heat transfer in the production area if the temperature from solar system differs from the temperature coming from the heating medium. In this configuration, the efficiency of the solar collector can be boosted when the temperature of the process is close to the temperature from the solar collector [28].

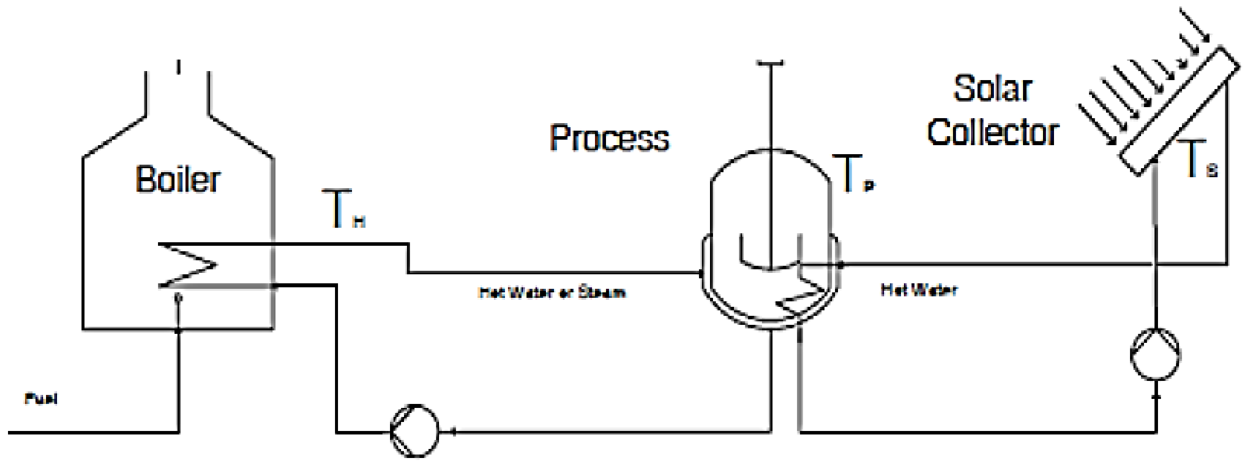

Figure 2. 4: Integration of Solar Thermal into Process Heat [28]

2.4.4. Industrial Solar Systems without Storage

In a lot of industries, the implementation of solar system does not require a storage system as the heat needed is higher than the heat provided by the solar system. This could happen when the process requires a continuous operation and/or a load always higher than the supply of heat by the solar system. In this case, the installation of solar energy system remains low cost, avoiding high storage related costs. In such configuration, the solar heat will be fed directly to the process or to the already existing heat supply [28]. Figure 2.5 is representing a system which needs a heat exchanger as the working fluid of solar system is a special fluid to protect the collector from freezing and corrosion.

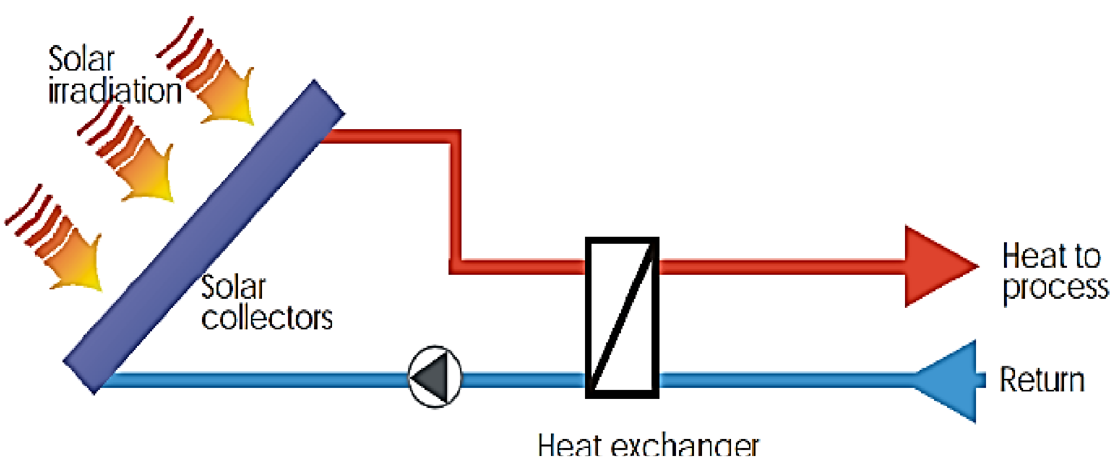

Figure 2. 5: Industrial Solar Systems without Storage [28]

2.4.5. Solar Systems with Heat Storage

Most industrial processes do not operate in a continuous mode over time, being ticked over at some time with strong fluctuation of the process heat demand during the operational periods. In these cases, a storage tank can be coupled to the solar system (Figure 2.6), which will store the unused solar energy collected during the operating-breaks (week-ends, short break of operation…) and will restore this energy collected to the process system during the working process periods. The sizing of the storage tank will depend on the fluctuation of the demand over time [28].

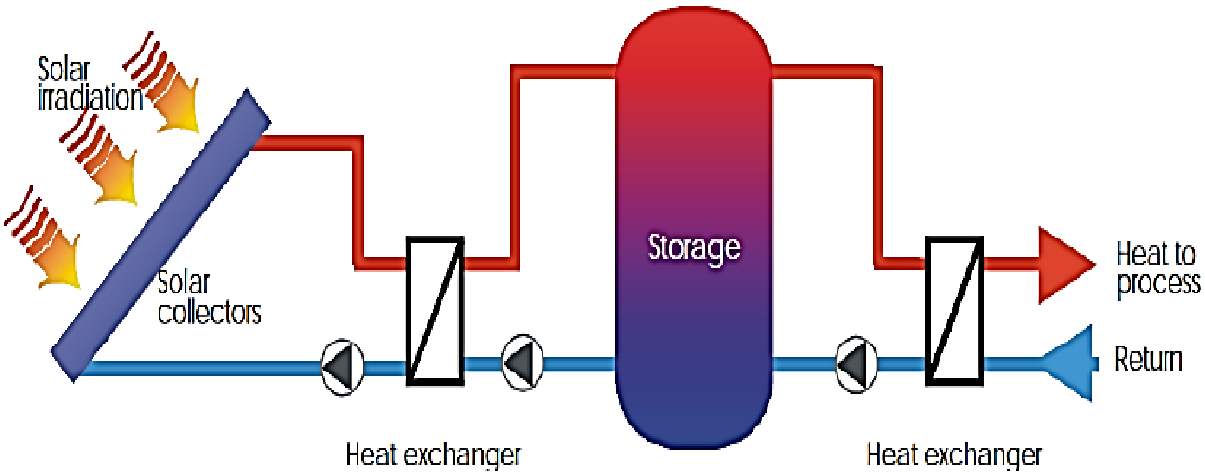

Figure 2. 6: Solar Systems with Heat Storage [28]

2.5. Description of Evacuated Tube Solar Collectors

An ETC is made of parallel evacuated glass pipes. Each evacuated pipe consists of two tubes, one is inner and the other is outer tube (Figs. 2.7 and 2.8). The inner tube is coated with selective coating while the outer tube is transparent. Light rays pass through the transparent outer tube and are absorbed by the inner tube. Both the inner and outer tubes have minimal reflection properties. The inner tube gets heated while the sun light passes through the outer tube and to keep the heat inside the inner tube, a vacuum is created which allows the solar radiation to go through but minimize the heat transfer .In order to create the vacuum, the two tubes are fused together on top and the existing air is pumped out. Thus the heat stays inside the inner pipes and collects solar radiation efficiently. Therefore, an ETSC is the most efficient solar thermal collector [29].

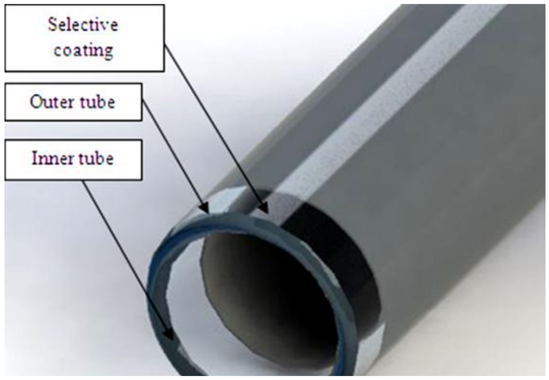

Figure 2. 7: Evacuated Tube Solar Collector [30]

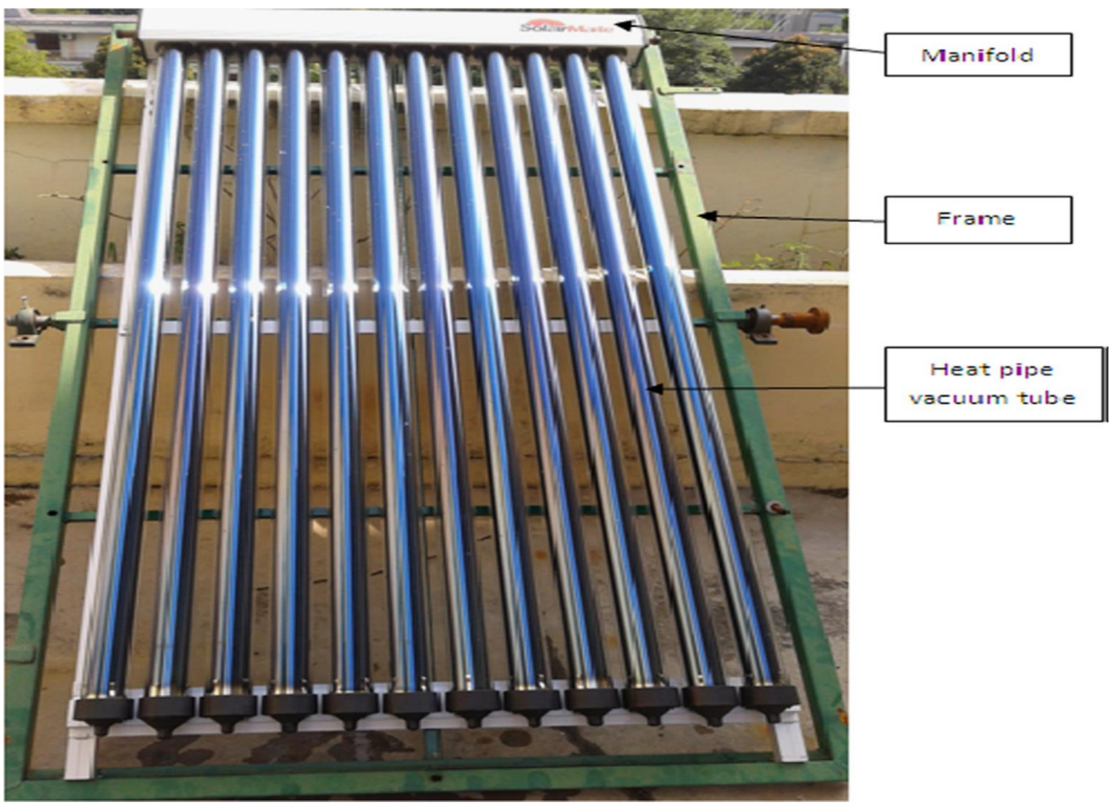

Figure 2. 8: Evacuated tube solar collector [29]

2.6. Factors Affecting the Performance of Evacuated Tube Solar Collectors

2.6.1. Collector Design

It's very common that for active solar-heating systems, solar collectors are the key components. They collect the energy in form of radiations from the sun, convert it into heat and then transfer that heat to a colder fluid (usually water). That energy can be utilized in solar pool heaters, and solar water-heating systems [31]. There are a large number of solar collector designs that have been shown as to be functional. These designs are classified in two general types of solar collectors:

Non Tracking Collector Design: These collectors remain stationary irrespective of position of the sun in the sky. However, they are installed at a particular tilt and orientation angles, whose magnitudes are dependent upon the geographical location (latitude), to maximize the harnessing of solar radiation. These system are classified in to two types such as flat collector evacuated tubes and concentrator collectors evacuate tubes [32].

Tracking Collector Design: The position of sun needs to be tracked for the maximum utilization of the incoming solar radiation. The intensity of solar radiation varies during the day as well as with seasons. The tracking collectors can be divided into two categories: one axis tracking and two-axes tracking collectors [32].

Mousazadeh et al. [33] reviewed the works on tracking systems. It was mentioned that the use of a tracker in a solar collector can enhance the collected energy in the range of 10–100% depending up on the time and geographical location of the site. The use of tracker increases the power consumption and it was recommended not to use trackers in low capacity solar collectors.

2.6.2. Fluid Transfer Pipes or Absorber Tube (Heat Pipe and U Tube)

One of the important design factors for the glass ETC is the shape of absorber tube [34]. For instance, Perez et al. [35] confirmed that the glass ETC with a semi-cylindrical shaped absorber tube could absorb about 16% more energy than ETC with a flat plate shaped absorber tube.

Over the years, different designs of ETC have been reported in several research papers [35, 36]. Two basic ETC designs are the simple fluid-in-glass and fluid-in-metal designs. The fluid-in-metal design can be further classified into heat pipe ETC and U-tube ETC. Heat pipe ETC and U-tube glass ETC are the two most widely- used solar collectors in domestic water heating. Research on the different designs of ETC has focused on the enhancement of the solar collector's performance.

In 2009, Rittidech et al. [37] constructed a simple closed-loop, oscillating, heat-pipe ETC to overcome issues concerning corrosion and freezing (during winter). The system attained a comparable efficiency of about 76%. For a heat-pipe, a vacuum environment is essential to attain high thermal frequency [36]. However, there exist several issues in providing perfect vacuum conditions since the non-condensable gases, released during the operation, remain in the heat-pipe and affect its performance [37]. Hence, there exists a limitation for the usage of heat-pipe ETC systems.

2.6.3. Absorber Coating

An efficient way to maximize the harnessing of solar insolation is to apply coatings of some specific materials on the absorber surface. Coatings are broadly classified as non-selective coatings, and solar selective coatings.

The optical properties like reflectivity, absorptivity, emissivity of non- selective coatings are spectrally uniform, that implies optical characteristics of such coatings are independent of wavelength over a particular wave length range. These coatings have poor solar selectivity and also they are thermally unstable at an elevated temperature resulting in poor absorber efficiency.

Solar selective coatings, on the other hand, have different absorptivity and emissivity in different spectral regions. It means that the optical properties are spectrally dependent [32].

2.6.4. Heat Transfer Fluid

The selection of working fluid considers a number of factors. The working temperature range is the first criteria to be fulfilled by the working fluid. In solar collector, this is a crucial step as it determines the minimum and the maximum temperature for the heat pipe operation. The following are other main criteria for selecting the right working fluid [38].

- Compatibility with the wick and the container
- Good thermal stability
- Wettability of wick and wall materials
- Vapor pressure not too high or low over operating temperature
- High latent heat
- High thermal conductivity

- Low liquid and vapor viscosities
- Higher surface tension
- Acceptable freezing or pour point

Organic solvents are the most widely used working fluid for low temperature applications because of lower vapor pressure, less susceptible for freezing and material compatibility. For example Ethanol has been used in many works for solar applications [39]. But their advantage is degraded by low heat transport capacity. In solar application, the efficiency of heat transport capacity overcomes other selection criteria as for the working fluid. Hence, the use of working fluid with higher latent heat is beneficial. Water gives superior property most of the organic solvents. Water is compatible with copper which is the most common container and wick material used today [40].

2.6.5. Tilt Angle

One of the way to maximize the harnessing of solar insolation is appropriate inclination (tilt) angle of the collectors. Bracamonte et al. [41] studied the effect of several tilt angles (10^0, 27^0 and 45^0) with the same energy input at 10^0 N of latitude in Venezuela. It was found that the tilt angle has significant effect on daily solar energy gain. A 10^0 tilted plane received more irradiation than the horizontal plane, while the 45^0 tilted plane received about nine percent (9%) less irradiation than the horizontal surface.

According to Tang et al. [42] the annual collectible radiation at a given site is related to the tilt-angle, and an optimal tilt-angle can be found for maximizing the annual energy harvesting of the collectors. For areas with abundant solar resources the optimal tile-angle of collector is close to the site latitude, whereas for the areas with poor solar resources the optimal tilt-angle is much less than the site latitude. All-glass evacuated tube collectors should be generally installed with a tilt-angle less than the site latitude in order to maximize the annual collectible radiation, especially in the areas with poor solar resources.

2.6.6. Effects of Azimuth Angle

The annual collectible radiation is affected by its azimuth angle. To investigate such effects Tang et al. [42] studied the ratio of the annual collectible radiation on collectors with any azimuth angle to that on south facing collectors for a given tilt-angle is introduced. The increase of azimuth angle from due south, the annual collectible radiation decreases, and furthermore, with the increase of tilt-angle, such effect becomes more significant. Results also indicate that 20^0 of deviation of azimuth angle from due south brings insignificant reduction of annual collectible radiation on collectors.

2.6.7. Central Distance between Tubes

Effects of central distance between tubes on the annual collectible radiation were presented by Tang et al. [42]. Obviously, the annual collectible radiation increases with the increase in, central distance between tubes. Such increase is slow and almost comes to a stop when center distance between tubes is 2.5 times higher than the outer diameter of collector tube. This is because increase in center distance between tubes will reduce shading between adjacent tubes. Recent years, with the decrease in production cost of solar tubes, the attempt to collect more radiation by increasing center distance between tubes is no longer employed by solar engineers. For most collectors available in the market, center distance between tubes is set at 80 mm for collectors with outer diameter of collector tube is 58 mm, and 70 mm for those with outer diameter of collector tube is 47 mm [42].

2.6.8. Mass Flow Rate

The flow rate is one thermal parameter that affects collector efficiency. The effect of collector mass flow rate per aperture area (kg/h m2) on the useful energy was analyzed by Gao et al. [43]. They recommended that the standard mass flow rates should be ranging from 10 to 70 kg/h m2. According to Hobbi et al [44] studied on the effect of collector's mass flow rate on the annual and monthly collector efficiency, the results also indicates that the mass flow is around 5–60 kg/hm2.

2.6.9. Effect of Tubes Size

The efficiency of the collector increase with increase of tube length but the optimal length of the collector should be ranging 1.5-2m. Gao et al. [45] investigated the effect of tubes size on collector efficiency, the efficiency of the collector initially increased with an increase in tube length and then decreased when the length increased above 1.5 m, but the efficiency varied less 0.02 for a tube length variation from 1.5 to 2.5 m.

2.7. Working Principle of Heat Pipe

The components of a typical cylindrical wicked heat pipe are copper tube with end sealed, wick structure, and a small amount of working fluid in thermal equilibrium with its vapor. It has three main sections as shown in Figure 2.9: the evaporator, adiabatic and the condenser sections. In solar collectors, the evaporator is bonded with the absorber of the collector and the condenser section is inserted in to the heat exchanger. The heat picked by the evaporator sinks at the condenser section. Heat loss in the adiabatic section is mostly ignored for good insulation. The working fluid is maintained at lower pressure in the heat pipe. The working fluid evaporates at the evaporator section and creates a vapor pressure to flow to the condenser section to condense. The evaporation and condensation happens at saturated temperature. The wick develops a capillary pressure to pump condensed liquid from condenser to evaporator to complete the circulation. The pumping can also be done by gravitation in gravity assisted heat pipes.

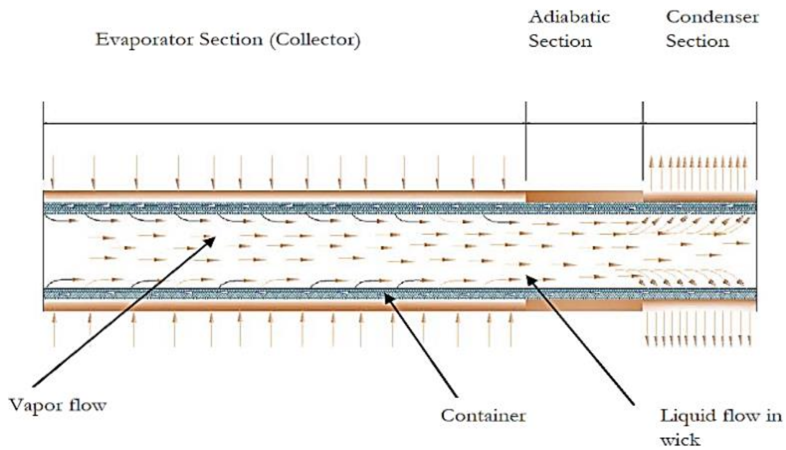

Figure 2. 9: Main Sections of Heat Pipe [38]

2.7.1. Heat Pipe Theory and Design

In the design of heat pipe, the characteristic of the three main components: the working fluid, the wick and the container are of important to attain the required heat transport capacity. In order the heat pipe to work, the pressure drop in the fluid flow has to be compensated by the pumping pressure in the wick by capillarity [38]. In equation form

$$\Delta P_P = \Delta P_v + \Delta P_l + \Delta P_g$$

2.7.2. Heat Transfer Limits

The physical properties of the fluid used and the wick properties determine the design to achieve a working heat pipe with required heat flux. Capillary, sonic, entrainment, boiling, frozen start up, continuum vapor, vapor pressure and condenser effects are physical phenomena that limit heat pipe heat transfer. The heat transfer limit for heat pipe can be caused by any of the above phenomena depending on the construction of the heat pipe and the operating environment. The lowest limit of these phenomena is considered as a design limit. The main design limitations are discussed as follows [38].

Capillary limit (Wicking limit):

The circulation of working fluid between the end zones happens due to the presence of wick structure. This limitation is very common in low temperature heat pipes for instance in hot water production. The limitation occurs when the capillary pumping power is not enough to overcome the pressure drops. The evaporator dries out if heat transfer above this capillary limit is attempted. The maximum heat transfer (Qmax) calculation is based on the hydrodynamic properties of the working fluid, wick and the orientation of heat pipe [46].

$$Q_{max} = \left[\frac{\rho_l \sigma_l h_{fg}}{\mu_l}\right]\left[\frac{K_P A_w}{l_e}\right][\frac{2}{r_e} + \frac{\rho_l\, g l_t \sin\beta}{\sigma_l}]$$

Sonic Limit

Heat pipe operation is accompanied with extraction and addition of mass in the evaporator and condenser. The vapor velocity increases along the evaporator and reaches maximum at the end of the evaporator. Since the vapor diameter is constant the heat pipe can act a nozzle at the end of the evaporator. Since the vapor velocity cannot be greater than the speed of sound, a sonic limit develops [46].

$$Q_{max} = A_v \rho_v h_{fg}\, [\frac{\gamma_v R_v T_s}{2(\gamma_v + 1)}]^{0.5}$$

Entrainment Limit

This limitation happens when water droplets are transported by the fast moving vapor due the shear force between the vapor and liquid at the interphase. If the heat transfer is too high, the evaporator dries out and the heat pipe stops working. Therefore, the maximum heat transfer possible with this limit is [46].

$$Q_{max} = A_v h_{fg} [\frac{\sigma_l \rho_v}{2r_h}]^{0.5}$$

Boiling Limit

Heat pipe wall temperature in the evaporator can become too high when the liquid in the wick starts to boil due to high radial heat flux. The vapor bubbles in the wick prevent the liquid for uniform wetting and a hot spot produces. This leads a dry out in the evaporator and limits the heat transfer [46].

$$Q_{max} = \frac{2\pi lt\ ke\ T_s}{h_{fg}\rho_v \ln(\frac{D_{cui}}{D_v})}\ [\frac{2\sigma_l}{D_{cuo}} - P_o]$$

2.7.3. Selection of Heat Pipes

Heat pipe are classified based on construction and operation. Two-phase closed thermosyphon wickless gravity assisted and capillary driven are the most common heat pipe types used in solar application. Gravity is the main mechanism in the thermosyphon type to return the condensate from the condenser which is located above the evaporator. The entrainment limit is more profound in gravity assisted than capillary driven due to the free liquid surface. The opposite of entrainment, flooding is also a problem in thermosyphon heat pipe. Filling ratio is also very important factor in thermosyphon than capillary driven heat pipe. Dry out occurs because of pool type and non-distributed working fluid. Gravity assisted wickless are difficult in solar collectors with high degree of inclination because of pooling which create non-uniform liquid distribution along the absorber length. This creates an increase wall temperature in some part of the heat pipe [48].

In a capillary driven heat pipe, a wick placed circumferentially in the internal of the sealed container is used to pump the working fluid from the condenser to the evaporator. Appropriate amount of working fluid is put inside the container to saturate the wick. It has better performance in transferring heat with a small temperature drop and long distance. The capillary limit is the main heat transfer limit in capillary driven heat pipe. A combination of wicked and gravity assisted heat pipe gives a compromised performance especially for solar application where the evaporator is long compared to other sections and need a uniform wetting properties [48].

2.7.4. Dimensioning Heat Pipe Selection

The heat collected at the evaporator (solar absorber) has to be dissipated in the condenser. This needs a careful design of evaporator and condenser length. The condenser length depends on the amount of heat collected and the condensation mechanisms. High heat transfer coefficient in condenser heat exchanger results small condenser length. This can be attained by increasing the velocity of the condensing fluid or any other mechanisms which can increase the heat transfer. The size of the evaporator and the cooling fluid temperature also determine the condenser length. Critical design values have to be considered in sizing the sections of the heat pipe. The adiabatic section depends on how long should be the heat transferred from the evaporator. In solar water heaters the length of adiabatic section doesn't have a merit mostly. Therefore, it is desirable to reduce the adiabatic length as small as possible to minimize the heat loss. For the heat collected from the solar absorber, the condenser length can be optimized [46]:

$$\frac{\dot{Q}_{collector}}{k(T_{bf} - T_w)} = \pi D_{cuo} l_c$$

2.8. Previous Works on Heat Pipe Solar Collector

The transient nature of solar energy during operation time makes evacuated tubes solar collector to work in transient heat transfer. This is more pronounced in batch type of solar water heaters where the temperature of the condensing media increases in time. Hassein et al. [47] and Hussein et al. [48] have studied the performance of wickless heat pipe for solar water heating using transient heat transfer models and optimized different system parameters. On the other side, most studies on heat pipe application for solar application consider one-node model adapted from Duffie and Beckman [13] where the heat pipe fluid inside works wholly saturated. Mathioulakis and Belessiotis [49] investigated both theoretically and experimentally new ethanol heat pipe solar collector for water heating by assuming a steady state operation of heat pipe fluid at saturated pressure and temperature. The evaporation heat transfer resistance has been considered in the study. But no information was given concerning condensation and vapor heat transfer resistances. Chen et al. [50] have also studied a two phase thermosyphon solar collector with alcohol as a working fluid both theoretically and experimentally. The thermal resistance of the working fluid vapor resistance was found very small compared to evaporation and condensation thermal resistances. Ismail and Abogderah [51] have also studied heat pipe for thermal storage and solar collector, respectively. Saturated temperature and pressure were assumed in the heat pipe working fluid. Only evaporation and condensation thermal resistances have been considered in their models. The working fluid capacitance and vapor thermal resistance are assumed negligible in this study too. Only evaporation and condensation thermal resistances are considered as heat pipe thermal resistances. Two phase thermosyphon solar collector with distilled water working fluid was investigated both numerically and experimentally and was found to have small temperature variation on absorber, cover and heat pipe during the test hours [52] This can help as to assume that the collector and the heat pipe works in quasi-steady state condition.

CHAPTER THREE

3. Description of the Study Organization

3.1. Introduction to Harar Brewery S.C. Factory

Harar Brewery factory was a governmental organization which produces potable fine beer. The factory was initially established in 1984. After a few years of establishment, it starts production of alcohol and continues until 2011 [53].

Harar Brewery produces Harar Beer, a 4.25% abv pale lager, as well as *Hakim Stout*, a 5.8% abv stout. The brewery also makes *Harar Sofi*, a non-alcoholic beverage that it markets toward the Muslim population. Harar Brewery uses water from the Genela spring, which is situated on its premises. It supplements this with water that it pumps from Finkile, located 33 km from the site. The brewery is capable of producing 250,000 hectolitres per year [53].

In 2011, the state-owned Harar Brewery became a subsidiary of Heineken International through a buyout costing $78 million USD [53]. Harar Brewery Factory is administrated under Heineken International groups that have three Brewery factory branches in Ethiopia namely Walliya Kilinto Brewery Factory (WBF), Bedelle Brewery factory (BBF) and Harar Brewery Factory (HBF). HBF has four departments namely Production, Logistics, Technical Department and Human Resource Development, and Administration Departments [Interview].

3.2. Location and Weather Condition

Geographical Location of Harar Brewery Share Company is located at 530Km east of Addis Ababa with an elevation of about 1870 meter above sea level. Harar brewery Share Company is located 9.30 north of latitude and 42.110 east of longitude with annual average solar irradiation of 230.21W/m2.The climate of the area is typical of the tropical wet and dry class, which is characterized by three temperature periods.

3.3. Staff Profile

The total number of employees of the factory is 243, out of which:

- 155 are permanent employees including the administrators, and
- 88 are temporary laborers‟ (this is the maximum number seen in my study time) and this number varies based on the day today activity of the factory).

3.4. Operating Hours

The factory operates throughout the year and throughout the day with three shifts. However, the operation in the industry stops only 8 hours per week for cleaning and maintenance purpose [Interview].

- Morning shift (from 8:00 AM to 4:00 PM)
- Afternoon shift (from 4:00 PM to 16:00 PM) and
- Night shift (from 16:00 PM to 24:00 AM) with 8 hours operating times for each shift.

3.5. Utilities

The utility systems which the factory uses are:

A, Steam Generation and Distribution Utility Systems: The major fuel supplier of the factory is National Oil Company (NOC) and its main use is to produce steam in the boiler. To produce steam by using furnace oil and to distribute it for the end-use devices, these utilities are essential.

B, Water Distribution Utility Systems: The source of much amount of water used in HBF is water from the Genela spring, which is situated on its premises. It supplements this with water that it pumps from Finkile, located 33 km from the site. The factory consumes water: Hence; to have these functions in the factory from water, the presence of water distribution utility systems is must.

C. Electricity Utility Systems: The factory uses electricity for lighting and to operate electrical appliances (such as pumps motors, air compressor fans, computers and refrigerator) in the factory.

3.6. Boiler, Steam and Hot water Distribution Systems

The feed water system provides water to the boiler and regulates it automatically to produce the specified capacity of steam in the boiler. The steam system collects and controls the steam produced in the boiler. Steam is directed through a piping system to the different points of end use. Steam pressure is regulated using automatic valves from the main distributer and checked with steam pressure gauges at the end use systems. During these times the amount of steam delivered to end use systems may or may not be sufficient enough in comparison with their design as well production capacity.

The fuel system provides furnace oil to boiler and the required heat will be generated as steam. The amount of fuel required to boiler is adjusted automatically with a gauge mounted on boiler.

The thermal energy is obtained from steam-generator (boiler). The main function of boiler is to supply superheated steam to the end use devices. While the boiler performs its function, it consumes a large amount of fuel [Inspection]. The boiler has had the following specifications [Catalogue]:

Table 3. 1: Boiler Specifications

	Specification	**Data Collection Method**
Type	Fire Tube	Catalogue
Model	S202	Catalogue
Manufactured Year [G.C.]	1980	Catalogue
Designed Capacity [Kg/hr] @ 15 Bar	2000	Catalogue
Working Pressure (Max/Min) [Bar]	11/8	Catalogue
Diameter [m]	1.88	Catalogue
Length [m]	3.53	Catalogue
Area [m^2]	26.4	Catalogue
Boiler Efficiency	80	Catalogue

3.7. Major Thermal Energy Consuming Processes

Steam is generated by Boiler and used for thermal processes such as Wort, Lauter Turn, Evaporation, Kegging, Bottle Washing, Pasteurizing, CIP, Feed Water Pre-Heating and Pre-Heating of furnace oil .This steam is delivered to all processes through three delivery canal which has its operation pressure which are preheating pipe, bottling pipe and brewing pipe. Figure 3.1 shows the schematic diagram of steam supply system and pipe line arrangement in the industry.

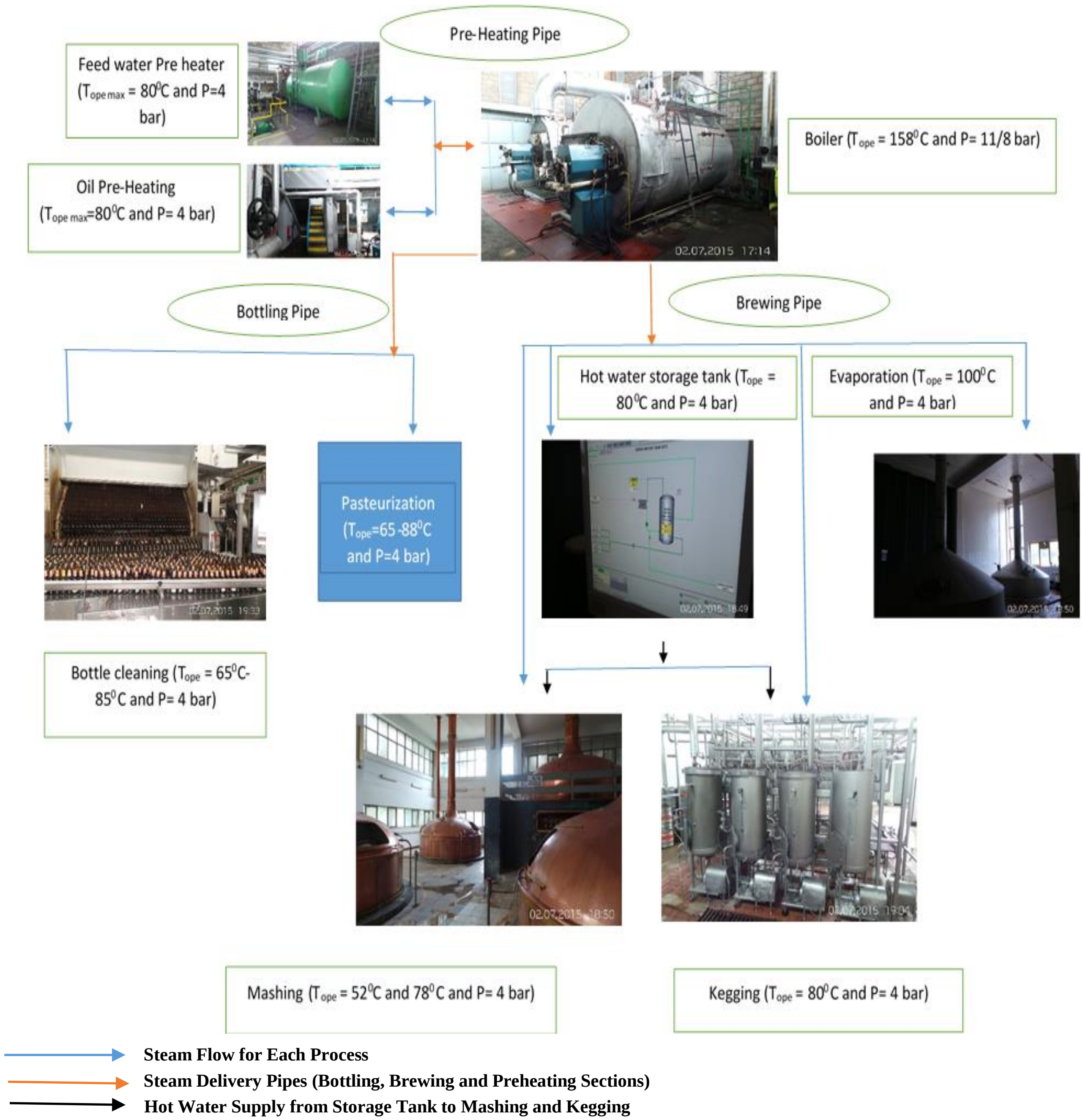

Figure 3. 1: The Schematic Diagram of Steam Supply System and Pipe Lines Arrangement

CHAPTER FOUR

4. Methodology

4.1. Conceptual Framework of the Study

The methodology of this study was separated into six parts. The three parts (such as data collection and analysis, solar irradiance analysis and analysis of thermal system) used to study the useful energy harvest from a single heat pipe evacuated tubes solar collectors. These parts were analyzed based on the specification of the collector and weather data in the study area. A Matlab script was developed for analysis of these parts. Finally, outlet temperature of the fluid on heat exchanger or manifold, system efficiency, conventional thermal energy consumption, solar thermal energy production and integration of solar thermal system with conventional system were simulated using the developed Matlab program.

The next part explained the conventional (furnaces oil) energy analysis in the industry both for the boiler and thermal processes. Part five discusses how solar collectors were arranged and determines the number of solar collectors which needed for the fulfillment of hot water demand for the selected processes in the industry. And, this part identified the suitable place for installation of solar collector in the industry. Financial analysis of the integration of solar thermal system in the industry was mentioned in part six. Figure 4. 1 shows the conceptual framework of this study.

The following assumptions were considered in mathematical models of heat pipe solar collectors:

- Heat pipe working fluid is assumed at saturated temperature and pressure during operation.
- The vapor thermal resistance is assumed negligible.
- The adiabatic section of the heat pipe is well insulated so that heat loss is assumed negligible
- There is no temperature gradient in the cover of the collector.
- Since the heat pipe works at saturation temperature, temperature gradient along the longitudinal direction of evaporator is neglected.
- Temperature gradient on the perimeter of the absorber and across the heat pipe thickness is neglected.
- The solar collector and the heat pipe works at quasi-steady state.

- The edges of the collector are well insulated and the thermal resistance is only by insulation. The same is true for the water tanker.
- No temperature gradient in along condenser and evaporator sections.
- Water tubes are well insulated and the heat loss is neglected
- The heat exchanger (manifold) is well insulated to consider the heat loss neglected.
- Cross flow heat exchanger condensing water flows fully perpendicular to the condenser section of heat pipe.

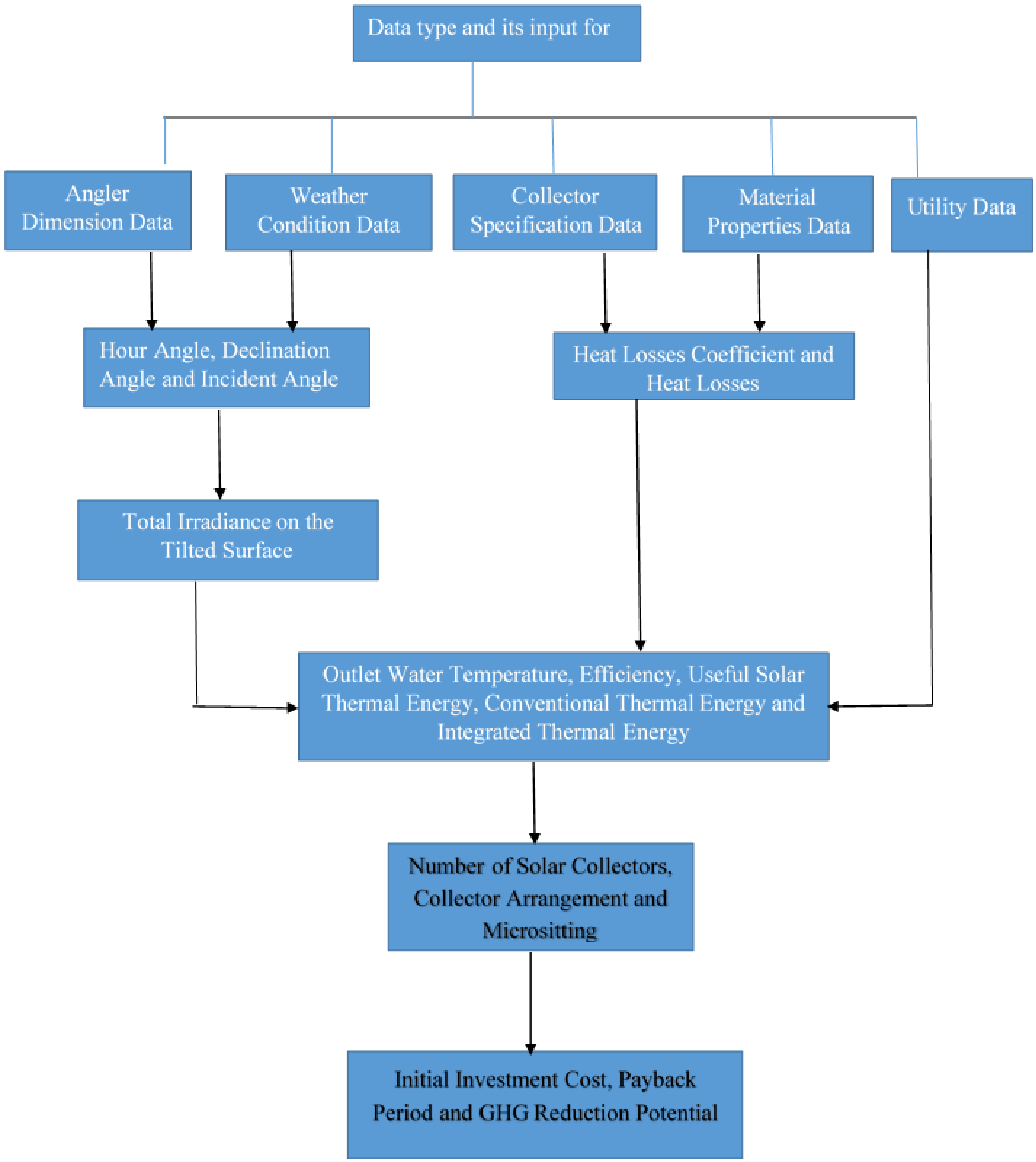

Figure 4. 1: Conceptual Framework of the Study

4.2. Data Collection

4.2.1. Method of Weather Data Collection

The weather data was collected from National Metrological Agency such as Global Irradiance, Wind Speed and Ambient Temperature for every fifteen minutes time interval. These data have included a five years meteorological information from 2010 up to 2014. All available data were converted into average Hourly Global Irradiance, Hourly Ambient Temperature and Daily Average Wind Speed for one year time period.

4.2.2. Method of Utility Data Collection

A secondary utility data was collected from the record in utility section of Harar Brewery factory. These utility data have included daily water consumption for each process, Monthly Fuel Consumption of a Boiler and Maximum Processes Operation Temperature.

4.2.2.1. Daily Water Consumption

A secondary Daily water consumption data was collected for different thermal processes from June 01, 2014 up to January 26, 2015, which means 8 months daily water consumption information. This paper focuses on the selected thermal processes hot water consumption such as Mashing (both at a temperature of 52^0C and 78^0C), Bottle Cleaning, Washing Machineries (CIP), Make up Water Preheating and Kegging. All available water consumption information in the selected processes were converted into average daily consumption basses. The average daily water consumptions for Mashing, bottle cleaning, Make up Water Preheating, Washing Machineries (CIP) and Kegging in meter cubic are 123.87, 93.4, 25.09, 191.1 and 29.55 respectively. Figure 4. 2 shows water distribution line in the industry.

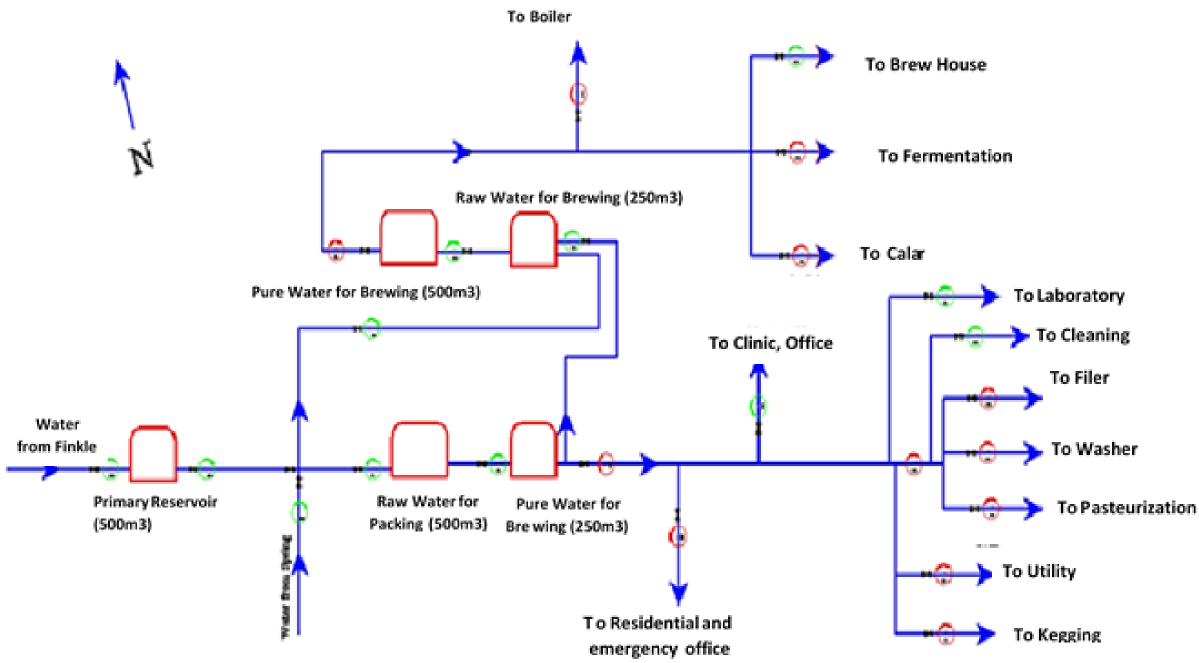

Figure 4. 2: Water Distribution Line in the Industry

4.2.2.2. Daily Fuel Consumption

The industry uses furnace oil boiler for thermal energy application. The boiler works at 80^0 C inlet water temperature supplied from pre-heater, 149^0 C temperature dry steam delivered to all processes at 11/8 bar pressure and 157^0 C flue gases temperature. A secondary monthly fuel consumption data was collected from utility section of Harar Brewery factory from January 2014 up to June 2015. The total amount of fuel consumed during the indicated period is 2,558,086 litter. This work converted the available data in to average daily consumption bases. It is estimated that 4905.25 litter/day of oil consumed in the industry for thermal energy application.

4.2.2.3. Processes Operation Temperature

The processes in the industry work at different maximum operation temperature. There is a process which is operated at a temperature higher than 100^0 C such as evaporation of water which is not suitable for solar water application. And, all other processes such as Mashing, Bottle Cleaning, CIP, feed water Preheating, Kegging and Pasteurization operate at a temperature lower than 100^0 C. The Processes of Mashing and Bottle Cleaning work at a temperature of $52^0/78^0$ C and 65-80^0 C, respectively. And, other processes such as Washing of Machineries, Preheating and Kegging work at a temperature of 80^0 C. This study selected all processes except pasteurization (which is operated in low temperature however it not part of this study) solar water heating application.

4.3. Solar Irradiance Analysis

4.3.1. Estimation of Angular Dimensions

The solar irradiance analysis is done for Harar Ethiopia weather condition in Harar Brewery factory. The Hour Angle and Declination Angle are investigated based on the number of hour of the day (ST) and the number of days of the year (N), respectively.

4.3.1.1. Hour Angle

The hour angle of a point on the earth's surface is defined as the angle through which the earth would turn to bring the meridian of the point directly under the sun. The hour angle at local solar noon is zero, with each 360/24 or 15° of longitude equivalent to 1 h, afternoon hours being designated as positive**.** The hour angle can also be obtained using Madison equation [13].

$$\omega = (ST - 12) * 15 \ldots\ldots\ldots\ldots\ldots\ldots\ldots\ldots\ldots\ldots\ldots\ldots\ldots\ldots\ldots\ldots \quad (4.1)$$

4.3.1.2. Declination Angle

The earth axis of rotation (the polar axis) is always inclined at an angle of 23.45° from the ecliptic axis, which is normal to the ecliptic plane. The ecliptic plane is the plane of orbit of the earth around the sun. As the earth rotates around the sun it is as if the polar axis is moving with respect to the sun. The declination for any day of the year is given as copper equation [13].

$$\delta = 23.45 \mathrm{Sin}\left[\frac{360(284 + \mathrm{N})}{365}\right] \ldots\ldots\ldots\ldots\ldots\ldots\ldots\ldots\ldots \quad (4.2)$$

4.3.2. Solar Geometry

Surface Azimuth Angle: the deviation of the projection on a horizontal plane of the normal to the collector from the local meridian (with zero due south, east negative and west positive). This paper considered 20^0 east surface azimuth angle.

Angle of Inclination: the angle between the plane of the collector and the horizontal. In this study 9^0 angle of inclination was taken.

Zenith Angle: the angle between the vertical (zenith) and the line of the sun.

Angle of Incident: the angle between the beam radiation on the collector and the normal. The incident angle on the inclined surface is calculated by the following equation [13].

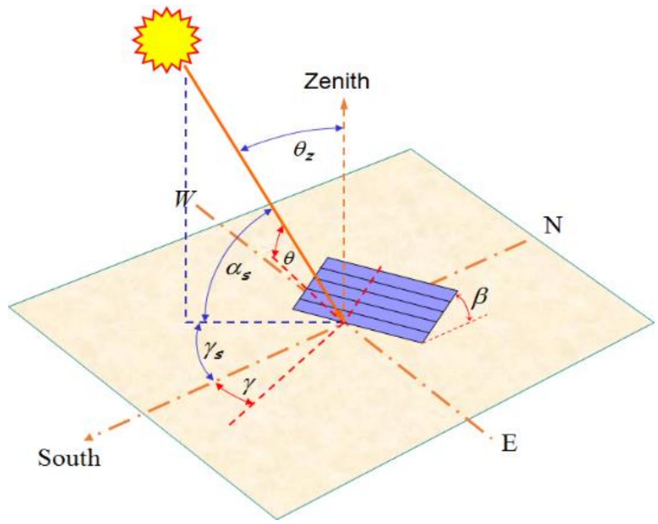

Figure 4. 3: Solar Geometry Angles on Inclined Surface [13]

$$\begin{aligned}\text{Cos}\theta = \sin\delta\sin\emptyset\cos\beta - \sin\delta\cos\emptyset\sin\beta\cos\gamma + \cos\delta\cos\emptyset\cos\beta\cos\omega \\ + \cos\delta\sin\emptyset\sin\beta\cos\gamma\cos\omega \\ + \cos\delta\sin\beta\sin\gamma\sin\omega \ldots \ldots \ldots \ldots (4.3)\end{aligned}$$

4.3.3. Estimation of Beam and Diffuse Irradiance

Hollel, et.al. (1976) [13] presented a simple model for the estimation of the transmittance of beam irradiance in clear sky conditions.

4.3.3.1. Clearness Index

The hourly clearness index k_T during a particular hour is the ratio of the hourly global irradiance on horizontal surface to the hourly extraterrestrial irradiance on horizontal surface during the same time period [13].

$$k_T = \frac{I}{I_O} \ldots \ldots \ldots \ldots (4.4)$$

Where the extraterrestrial irradiance is calculated using equation (4.5)

$$I_o = I_{sc}(1 + 0.033\cos(\frac{360N}{365}) \ldots \ldots \ldots (4.5)$$

4.3.3.2. Prediction of Hourly Diffuse Irradiance

The fraction of the hourly diffuse irradiance on a horizontal plane can be correlated to the hourly clearness index, k_T, and the ratio of the total radiation to the extraterrestrial radiation for the hour. The equations for the correlation Orgill and Hollands, (1977) [13] are:

$$\frac{I_d}{I} = \begin{cases} 1 - 0.249k_T & \text{for } k_T < 0.35 \\ 1.557 - 1.84k_T & \text{for } 0.35 < k_T < 0.75 \\ 0.177 & \text{for } k_T > 0.75 \end{cases} \quad \ldots\ldots\ldots\ldots (4.6)$$

4.3.3.3. Hourly Beam Irradiance

Hourly global irradiance on the clearness index is the sum of beam irradiance and diffuse irradiance [13].

$$I_b = I - I_d \ldots\ldots\ldots\ldots\ldots\ldots\ldots\ldots (4.7)$$

4.3.4. Global Irradiance on the Tilted Surface

The following formula was given by Liu and Jordan (1962) [13] for evaluating the total Irradiance on a tilted surface of arbitrary orientation from knowledge of beam and diffuse irradiance on horizontal surface.

$$I_T = I_b R_{bt} + I_d R_d + \rho R_r (I_b + I_d) \ldots\ldots\ldots\ldots (4.8)$$

Where: R_{bt} is Ratio of Beam Irradiance normal to the earth's surface to Beam Irradiance normal to a tilted surface is given by.

$$R_{bt} = \frac{cos\theta}{cos\theta_z} \ldots\ldots\ldots\ldots\ldots\ldots (4.9)$$

R_d is Ratio of diffuse Irradiance normal to the earth's surface to diffuse Irradiance normal to a tilted surface and the reflective ratio (R_r) are given by.

$$R_d = \frac{1 + \cos\beta}{2} \ldots\ldots\ldots\ldots\ldots\ldots (4.10)$$

$$R_r = (1 - cos\beta)/2 \ldots\ldots\ldots\ldots\ldots\ldots (4.11)$$

4.4. Conventional Thermal Energy Analysis

Furnace oil is used for conventional thermal energy application in Harar brewery factory. It is used for steam generation in the boiler and the steam is transformed for all processes for the supply of the required thermal energy.

4.4.1. Mass Balance Check

In order to calculate the boiler input and output energy, the mass flow rate of furnace oil, feed water and steam must be determined first.

4.4.1.1. Determination of Mass Flow Rate of Furnace Oil

Since the factory uses furnace oil as fuel source to generate steam, determining the mass flow rate of furnace oil is important to know the boiler input energy. The mass flow rate can be determined based on the fuel consumption data, number of working hour and the density of fuel. The mass flow rate of furnace oil can be obtained using the following equation.

$$\dot{m}_f = V_f * \frac{\rho_f}{t} \dots\dots\dots\dots\dots\dots\dots\dots\dots\dots . \dots\dots\dots\dots\dots\dots\dots\dots . (4.12)$$

4.4.1.2. Determination of Mass Flow Rate of Feed Water

The mass flow rate can be determined based on the daily water supply data to preheater, number of working hour and the density of water. The mass flow rate of feed water can be obtained using the following equation.

$$\dot{m}_{pw} = V_{pw} * \frac{\rho_w}{t} \dots\dots\dots\dots\dots\dots\dots\dots\dots\dots\dots\dots\dots\dots\dots\dots\dots (4.13)$$

4.4.2. Energy Analysis of the Boiler

Thermal energy analysis of boiler must be conducted to know thermal energy supplied for industrial processes and the amount energy saved due to solar thermal design. The analysis is done based on the energy inputs and outputs of the boiler. All inputs and outputs of the boiler are shown in figure 4.4.

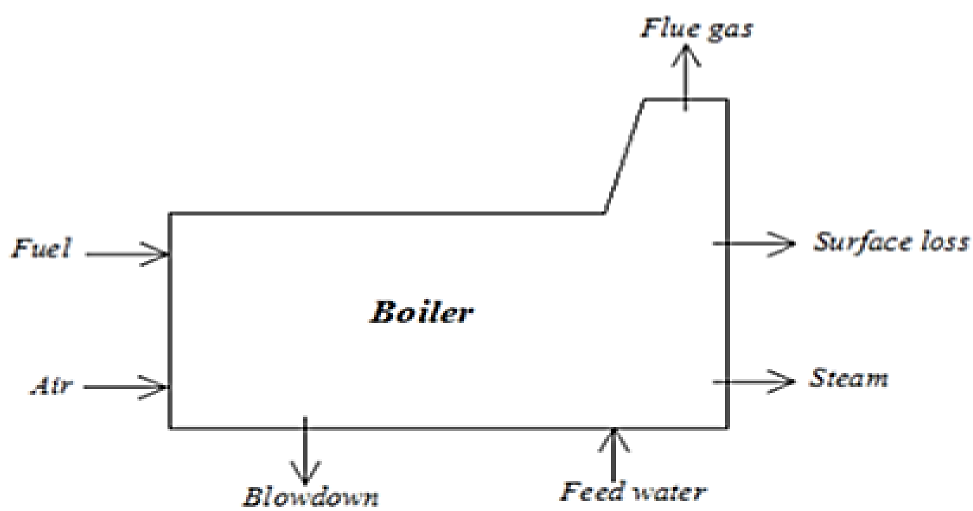

Figure 4. 4: Inputs and Outputs of Boiler

4.4.2.1. Determination of Input Energies

As illustrated in figure 4.4, heat due to chemical energy of furnace oil, combustion air and feed water are the input energies of the boiler.

I. Furnace Oil Energy

The furnace oil contains chemical energy and heat energy by virtue of its chemical constituents and pre-heating of the fuel at inlet to the furnace respectively.

a) Chemical Energy

The chemical energy of the furnace oil is quantified using its heating value. To calculate the energy efficiency of the boiler on GCV, the chemical energy of the furnace oil must be found. The chemical energy of the furnace oil is obtained by multiplying GCV of the fuel with the mass flow rate of the fuel.

$$\mathrm{Q_f} = \dot{\mathrm{m}} * \mathrm{GCV} \ldots\ldots\ldots\ldots\ldots\ldots\ldots\ldots\ldots\ldots\ldots\ldots\ldots\ldots\ldots\ldots\ldots. (4.14)$$

b) Energy due to Pre-heating

The energy due to fuel pre-heating is the enthalpy of furnace oil by virtue of its temperature elevation relative to the atmospheric temperature. The enthalpy of furnace oil due to its pre-heating from the ambient temperature to pre-heating temperature can be obtained using the following thermodynamic path. The energy due to pre-heating temperature can be obtained using the following equation.

$$\mathrm{Q_{pf}} = \dot{\mathrm{m}}_\mathrm{f}\mathrm{Cp_f}(\mathrm{T_f} - \mathrm{T_{am}}) \ldots\ldots\ldots\ldots\ldots\ldots\ldots.\ldots\ldots\ldots\ldots\ldots\ldots. (4.15)$$

II. Energy of Combustion Air

The inlet air temperature is at ambient temperature. Since the enthalpy of the flue gas is calculated relative to the temperature of the entering air, the relative enthalpy of combustion air is calculated by equation (4.16).

$$Q_a = \dot{m}_a * h_{ai} \ldots\ldots\ldots\ldots\ldots\ldots\ldots\ldots\ldots\ldots (4.16)$$

III. Energy of Feed Water

The energy of feed water is the enthalpy of water by virtue of its temperature elevation relative to the atmospheric temperature. The enthalpy of feed water due to its pre-heating from the ambient temperature to pre-heating temperature can be obtained using the following thermodynamic path. The energy due to pre-heating temperature can be obtained using the following equation (4.17).

$$Q_{pw} = \dot{m}_w * (h_{wo} - h_{wi}) \ldots\ldots\ldots\ldots\ldots\ldots\ldots\ldots\ldots\ldots\ldots (4.17)$$

4.4.2.2. Determination of the Output Energies

The output energy associated with the burning of furnace oil in the combustion includes:

- Loss of sensible heat of the dry flue gas,
- Loss due to the present of H2 in fuel (loss due to latent heat),
- Loss due to the moisture content of air,
- Loss of heat by radiation and convection from boiler surface,
- Loss due to the moisture content of the fuel,
- Boiler blowdown loss, and replaced
- Useful heat to steam.

All thermal energy output stated above are types of thermal energy losses except the last one (useful heat to steam) which is supplied for all thermal processes in the industry. The operation manual of the boiler indicated that the boiler efficiency is 80% [Catalogue].

4.4.2.3. Estimation of Thermal Energy by the Useful Water

One of the major energy output is the heat carried away by the steam. It is equal to the heat energy absorbed by processes without considering the heat losses in the delivery channel. The amount of heat energy absorbed by the useful water is obtained by multiplying the amount of mass flow rate of cold water supplied to the processes, enthalpy of water at outlet temperature and inlet temperature of water (which is equal to ambient temperate). The output energy can be obtained using equation (4.18) as follows.

$$Q_s = \dot{m}_w * (h_{wo} - h_{wi}) \ldots\ldots\ldots\ldots\ldots\ldots\ldots\ldots\ldots\ldots\ldots\ldots\ldots (4.18)$$

4.5. Analysis of Solar Thermal System

4.5.1. Design Parameters

The design parameters were quantified from the manufacturing specification for the selected type of heat pipe evacuated tube solar collector for water heating application. The type of collector is Mazdon 20 - TMA 600S which is manufactured by the Thermomax in China and supplied by SAT Solar Engineering in Ethiopia.

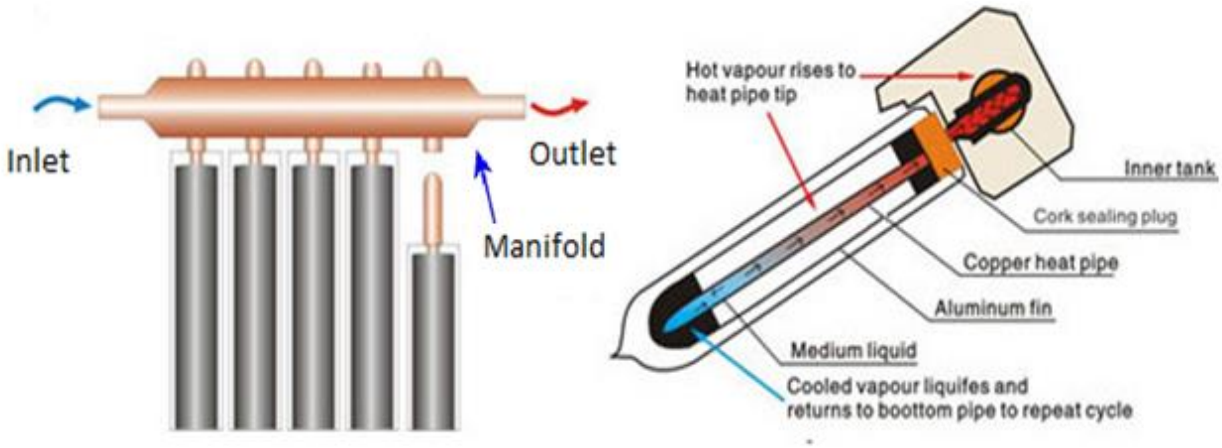

Table 4. 1: Heat Pipe Solar Collector Specification [54]

Figure 4. 5: Schematic Diagram of Heat Pipe Solar Collector [17]

Collector Dimensions	**Symbol**	**Unit**	**Value**
Space Between Evacuated Tubes (Center to Center)	W	m	0.080
Outer Diameter of Copper Heat Pipes	D_{cuo}	m	0.015
Inner Diameter of Copper Heat Pipes	D_{cui}	m	0.014
Thickness of Glasses	t_g	m	0.0012
Outer Diameter of Inner Glass Tube	D_p	m	0.049
Outer Diameter of Outer Glass Tube	D_g	m	0.058
Heat pipe length	L	m	1.8
Length of Evaporation Section	L_e	m	1.6
Length of Condensation Section	L_c	m	0.1
Length of Adiabatic Section	L_a	m	0.1
Number of Tubes	N		25
Volume of Heat Transfer fluid (Water) Per Heat Pipe	V_f	m^3	0.0001
Filling Ratio of Heat Transferring Fluid	V_t		0.333
Collector Area	A_c	m^2	3.2
Mass of Collector	M	Kg	53

4.5.2. Materials Properties

Table 4. 2: Materials Properties Data [55]

Collector Material Properties	Symbol	Unit	Value
Specific Heat Capacity of Water	C_p	J/Kg K	4179
Specific Heat of Glass	C_{pg}	J/kg K	835
Specific Heat of Absorber	C_{pp}	J/kg K	835
Specific Heat of Heat Pipe	C_{pcu}	J/kg K	385
Specific Heat of Heat Pipe	C_{pal}	J/kg K	903
Specific Heat of Fluid	C_{pl}	J/kg K	4180
Specific Heat of Condenser	C_{pco}	J/kg K	385
Thermal Conductivity of Heat Pipe	K_{hp}	W/m K	401
Latent Heat of Vaporization at 49 ^{0}C	h_{fg}	KJ/kg	2390
Viscosity of Fluid at 49 ^{0}C	μ	Ns/m^2	$0.558*10^{-3}$
Transitivity of Glass	τ_g		0.96
Absorptivity of Selective Coating	α		0.93
Emissivity of glass	ε_g		0.06
Emissivity of air	ε_a		0.02
Emissivity of Absorber Coating	ε_p		0.1
Emissivity of Copper	ε_{cu}		0.15

4.5.3. Energy Balance

Energy balance of each components in the system is the cumulative result of the thermal energy delivered into the component, released to the environment (heat loses) and the amount of heat absorbed by the component [13]. The transient heat energy balance equations of the system and the heat loss from the system can be stated as in the following sections.

4.5.3.1. Heat Loss in the System

Thermal energy in heat pipe evacuated tubes solar collector is transferred in the form of Radiation, convection and conduction. The majority of the energy transferred in the system is useful thermal energy. However, some parts of the thermal energy is released to the atmosphere is called heat losses. The amount of thermal energy losses are highly dependent on the heat loss coefficient, heat transferring surface area and temperature difference between two components. Figure 4.6 below shows thermal circuit representation of evacuated tubes solar water heater. The heat loss coefficient and thermal energy losses of radiation, convection and conduction processes are calculated as follows.

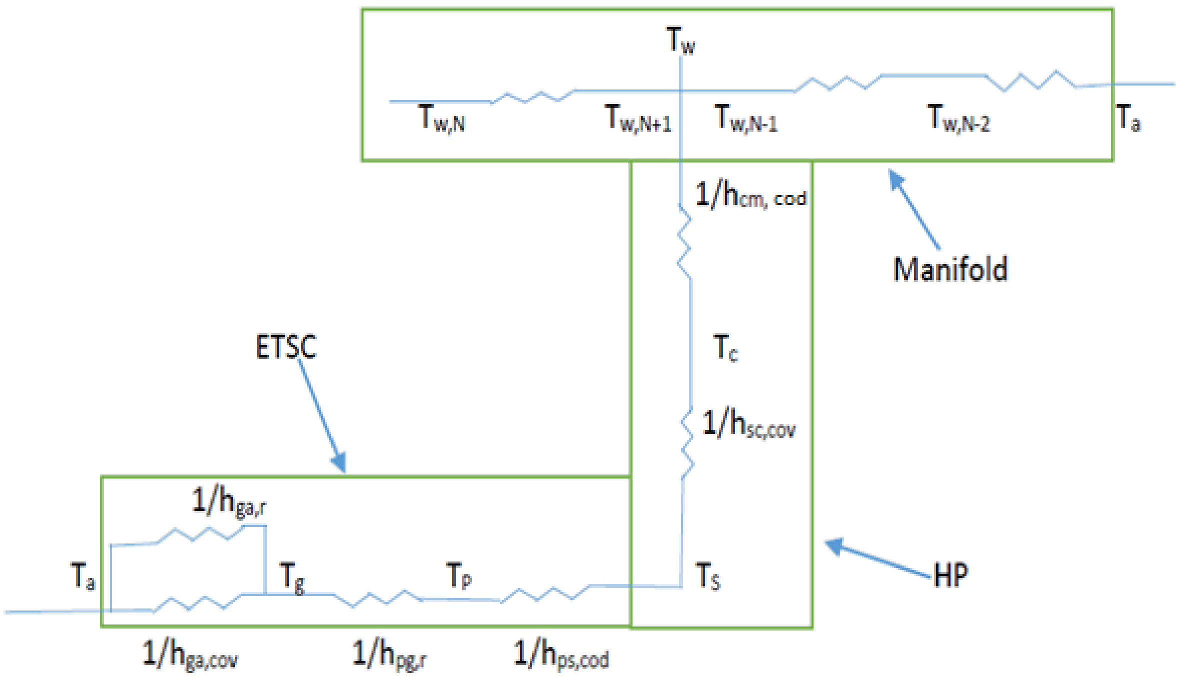

Figure 4. 6: Thermal Circuit Representation of Solar Water Heater

A, Radiation Heat Loss Coefficient: there are two radiation heat transfer in heat pipe evacuated tubes solar collector namely radiation heat transfer from inner glass tube to outer glass tube, and from outer glass tube to the atmosphere. Radiation heat transfer coefficient from inner glass tube to outer glass tube is calculated in equation (4.18) [13] and Radiation heat transfer coefficient from outer glass tube to the atmosphere is calculated in equation (4.19) [13].

$$\mathrm{h_{pg,r}} = \frac{\sigma(\mathrm{T_P^2}+\mathrm{T_g^2})(\mathrm{T_P}+\mathrm{T_g})}{(\frac{1}{\varepsilon_\mathrm{p}}+\frac{1}{\varepsilon_\mathrm{g}}-1)} \qquad (4.18)$$

$$h_{ga,r} = \varepsilon_g \sigma (T_g^2 + T_a^2)(T_g + T_a) \qquad (4.19)$$

Moreover, the thermal energy transfer in the form of radiation form inner tube ($Q_{pg,r}$) and outer tube ($Q_{ga,r}$) are given in equation (4.20) and equation (4.21) respectively [13].

$$\mathrm{Q_{Pg,r}} = \mathrm{h_{pg,r} D_p L_e (T_p - T_g)} \qquad (4.20)$$

$$Q_{ga,r} = h_{ga,r} D_g L_e (T_g - T_a) \qquad (4.21)$$

B, Convection Heat Loss Coefficient: there are two convection heat transfer in heat pipe evacuated tubes solar collector namely convection heat transfer between evaporation section and condensation section, and convection heat transfer between outer glass tube and the atmosphere. These are calculated by equation (4.22) [46] and (4.23) [13] respectively.

$$h_{sc,cov} = (0.997 - 0.334(\cos\beta)^{0.108})(\frac{K_l^2 \rho_w^2 g h_{fg}}{\mu L_c (T_s - T_c)})^{0.25} \left(\frac{L_c}{D_{cui}}\right)^{(0.254(\cos\beta))^{0.38}} \quad (4.22)$$

$$\mathrm{h_{ga,cov}} = 5.7 + 3.8\mathrm{V_w} \quad (4.23)$$

And, the thermal energy transfer in the form of convection from evaporation section to condensation section ($Q_{ec,cov}$), and outer glass tube to the atmosphere ($Q_{ga,cov}$) are given in equation (4.24) [46] and (4.25) [13] respectively.

$$\mathrm{Q_{sc,cov}} = \mathrm{h_{sc,cov}} \frac{\pi \mathrm{D_{cui}}}{4} (\mathrm{T_s} - \mathrm{T_c}) \quad (4.24)$$

$$\mathrm{Q_{ga,cov}} = \mathrm{h_{ga,cov}} \mathrm{D_g} \mathrm{L_e} \left(\mathrm{T_g} - \mathrm{T_a}\right) \quad (4.25)$$

C, Conduction Heat Loss Coefficient: there are two conduction heat transfer in this study. These are between the absorber tube and evaporation section (heat pipe tube) through the aluminum fin, and between the condensation section and manifold (water). The conduction heat transfer coefficient from absorber tube to evaporation section and conduction heat transfer coefficient from condensation section to water are determined by equation (4.26) [55] and (4.27) [46] respectively.

$$\mathrm{h_{ps,cod}} = \frac{\mathrm{k_{hp}} \mathrm{t_{cu}}}{\mathrm{D_{cu}} \mathrm{L_e}} \quad (4.26)$$

$$\mathrm{h_{cm,cod}} = \frac{\mathrm{k_{hp}} \mathrm{t_{cu}}}{\pi \mathrm{D_{cu}} \mathrm{L_c}} \quad (4.27)$$

Then, the conduction thermal energy transfer from absorber tube to evaporation section ($Q_{ps,cod}$) and from condensation section to water ($Q_{cm,cod}$) are calculated by equations (4.28) [55] and (4.29) [46] respectively.

$$\mathrm{Q_{ps,cod}} = \mathrm{h_{ps,cod}} \mathrm{D_p} \mathrm{L_e} \left(\mathrm{T_p} - \mathrm{T_{cu}}\right) \quad (4.28)$$

$$Q_{cm,cod} = \mathrm{h_{cm,cod}} \pi \mathrm{D_{coo}} \mathrm{L_c} (\mathrm{T_c} - \mathrm{T_w}) \quad (4.29)$$

4.5.3.2. Energy Balance Equations of Component

A. Absorber Tube: the transit heat energy balance equation of absorber tube of evacuated tubes heat pipe is written as.

$$\frac{\rho_p V_p (Cp)_p \, \partial T_p}{\partial t} = ItA_p\tau\alpha - h_{pg} * A_p(T_p - T_g) - h_{ps} * A_p(T_p - T_s) \dots\dots\dots\dots\dots\dots (4.30)$$

B. Outer Glass Cover: the transit heat energy balance equation of glass cover of evacuated tubes heat pipe is written as.

$$\frac{\rho_g V_g (Cp)_g \, \partial T_g}{\partial t} = ItA_g(1 - \tau) + ItA_p\tau\alpha + h_{pg} * A_p(T_p - T_g) - h_{ga} * A_g(T_g - T_a) \dots\dots\dots\dots\dots\dots\dots\dots\dots\dots\dots\dots\dots\dots\dots\dots (4.31)$$

C. **Evaporation Section (Saturated Liquid):** the transit heat energy balance equation of saturated liquid of evacuated tubes heat pipe is written as.

$$\frac{\rho_s V_s (Cp)_s \, \partial T_s}{\partial t} = h_{pg} * A_p(T_p - T_s) - h_{sc} * A_s(T_s - T_c) \dots\dots\dots\dots\dots\dots\dots\dots (4.32)$$

D. **Condensation Section:** the transit heat energy balance equation of condensed liquid of evacuated tubes heat pipe is written as.

$$\frac{\rho_c V_c (Cp)_c \, \partial T_c}{\partial t} = h_{sc} * A_s(T_s - T_c) - h_{cm} * A_c(T_c - T_w) \dots\dots\dots\dots\dots\dots\dots\dots\dots (4.33)$$

The temperature of each elements are varied with time until the system reached steady state condition. The initial temperature values for all elements in the above equation are guessed by following relationship.

$$T_p = T_a + 1.0 \dots\dots\dots\dots\dots\dots\dots\dots\dots\dots\dots\dots\dots\dots\dots (4.34)$$

$$T_g = T_a + 0.5 \dots\dots\dots\dots\dots\dots\dots\dots\dots\dots\dots\dots\dots\dots\dots\dots (4.35)$$

$$T_s = T_a + 0.75 \dots\dots\dots\dots\dots\dots\dots\dots\dots\dots\dots\dots\dots\dots\dots (4.36)$$

$$T_c = T_a + 0.5 \dots\dots\dots\dots\dots\dots\dots\dots\dots\dots\dots\dots\dots\dots\dots\dots (4.37)$$

This study developed Matlab script for numerical solution of ODE problems. This program uses iteration technique for computing the temperature of each component of the system. Fixed point iteration is one of the methods which used for solving of problems in the form of nonlinear differential equations [56]. This method was implemented for thermal analysis of each component of the system in this study.

4.5.4. Outlet Temperature of Fluid/ Water

Based on the transient analysis of heat energy balance equation, the Outlet temperature of each element of the system is obtained using integration of equation (4.30) up to (4.33) with time dt. In addition Matlab script is developed for numerical solution of PDE problems for thermal energy transfer analysis from condensation section of the system to the useful water (fluid) in the manifold (heat exchanger). The following central difference finite difference method is used to discretize the mathematical equations by sub-dividing the system in to a number of nodes with time and spaces [56]. The temperature gradient of inlet water in the manifold with time is calculated using finite difference methods [56].

$$\frac{\partial \mathrm{T}}{\partial \mathrm{t}} = \frac{(\mathrm{T}_{\mathrm{i}}^{\mathrm{n+1}} - \mathrm{T}_{\mathrm{i}}^{\mathrm{n}})}{\Delta \mathrm{t}} \ldots\ldots\ldots\ldots\ldots\ldots\ldots\ldots\ldots\ldots\ldots\ldots\ldots\ldots\ldots (4.38)$$

And, the temperature gradient of inlet water in the manifold along longitudinal axial is calculated using finite difference methods [56].

$$\frac{\partial T}{\partial x} = \frac{(T_{i+1}^{n} - T_{i}^{n})}{\Delta x} \ldots\ldots\ldots\ldots\ldots\ldots\ldots\ldots\ldots\ldots\ldots\ldots\ldots (4.39)$$

The outlet temperature of useful fluid is calculated by integration of the following with time dt [55].

$$\rho_{\mathrm{w}}\, \mathrm{V}_{\mathrm{w}}\, \mathrm{Cp}_{\mathrm{w}} \frac{\partial \mathrm{T}_{\mathrm{w}}}{\partial \mathrm{t}} = \mathrm{h}_{\mathrm{cm}} * \mathrm{A}_{\mathrm{c}}(\mathrm{T}_{\mathrm{c}} - \mathrm{T}_{\mathrm{w}}) - \frac{\dot{\mathrm{m}}\mathrm{Cp}_{\mathrm{w}}\, \partial \mathrm{T}_{\mathrm{w}}}{\partial \mathrm{x}} \ldots\ldots\ldots\ldots\ldots\ldots\ldots\ldots\ldots (4.40)$$

4.5.5. Energy Transfer to Water Storage Tank

Water storage tank and fluid conducting pipes are well covered with insulation materials. So that, the energy transfer to the storage tank is equal with the outlet temperature at the last node. The useful energy transfer to the working fluid (water) is calculated by the following equation (4.41) [13].

$$\mathrm{Q}_{\mathrm{u}} = \dot{\mathrm{m}}\mathrm{Cp}_{\mathrm{w}}(\mathrm{T}_{\mathrm{wo}} - \mathrm{T}_{\mathrm{wi}}) \ldots\ldots\ldots\ldots\ldots\ldots\ldots\ldots\ldots\ldots (4.41)$$

4.5.6. Instantaneous Efficiency of the System

The efficiency of a collector can be then defined: the ratio of useful energy transfer to the working fluid /water to solar irradiance collected by the absorber surface [13].

$$\eta_{\mathrm{i}} = \frac{\mathrm{Q}_{\mathrm{u}}}{\mathrm{I}_{\mathrm{t}} * \mathrm{A}_{\mathrm{c}}} \ldots\ldots\ldots\ldots\ldots\ldots\ldots\ldots\ldots\ldots\ldots\ldots\ldots\ldots\ldots (4.42)$$

4.6. Collector Arrangement and Size Determination

4.6.1. Collector Arrangement

The solar collectors must arrange parallel, series and both based on the supplied outlet temperature of the system, mass flow rate of water and the maximum operation temperature of the processes. In this study a single selected collector is too much for delivering hot water in to the processes and storage tank. So, all collectors were arranged in parallel with constant mass flow rate of water through manifold.

4.6.2. Size Determination

The number of evacuated tubes solar collector is determined depending on the daily average hot water consumption, mass flow rate of water through manifold of the collector and maximum operation temperature of the processes. This study identified three different mass flow rate (such as 0.0132, 0.0185 and 0.02) for three different maximum operation temperature (such as 80, 65 and 52) respectively. The average daily hot water consumption of all processes were mentioned in sub topics 4.2.2.1. The number of evacuated tubes solar collectors is calculated by:

$$\mathrm{N} = \frac{\text{Average Hot Water Consumption of the Process}\left(\frac{m^3}{\mathrm{S}}\right) * \text{Density of Water}\left(\frac{\mathrm{Kg}}{m^3}\right)}{\text{Mass Flow Rate of Water Through Manifold}\left(\frac{\mathrm{Kg}}{\mathrm{S}}\right)} \ldots\ldots\ldots\ldots\ldots.\ldots\ldots (4.43)$$

4.6.3. Micrositing of Solar Collectors

Micrositing of a solar collectors were done using AutCAD software. The site view of Harar Brewery Factory was identified and clipped from Google earth software. And then, AutCAD was devoted to show the installation of solar collectors in the industry compound.

4.7. Financial Analysis

The financial analysis of this study was performed with the help of RET Screen Software. In this software energy model, solar resource and heating load, cost analysis, GHG analysis and financial summary were analyzed. This software uses average monthly solar irradiance data for 12 months in the solar resource and heating load model and manufacturing specification data in energy model. In addition the cost of a single heat pipe evacuated tube solar collector and storage tanks are listed in cost analysis. Finally, financial summary is indicated the payback period, GHG reduction cost, saved conventional energy, money, and annual financial flow of the project. The analysis was executed for a base case scenario for a 20-year cash flow model. The base case scenario represents the anticipated financial terms for the investment in normal conditions with no incentives provided by the government.

Table 4. 3: Financial Analysis Parameters

Parameters	Value	Remark
Life Time (Investment Period)	20 years	The life time of heat pipe evacuated tubes solar collector is 20-30 years.
Inflation Rate	10%	This is the value of the inflation rate in Ethiopia for 2015.
Discount Rate	10%	
Salvage Value	10%	Conservative assumption for the value of the plant at the end of the lifetime
Debt Ratio	50%	% of the total capital cost to be borrowed
Debt Interest Rate	8.5%	Interest rate for DBE loan
Loan Period	10 years	
Avoided Cost of Heating Energy	$0.719/L	This is price of furnace oil per liter in Ethiopia market in 2015
Retail price of electricity	0.033$/KWhr	Price of electricity for industry supply in 2015.
Contingency	10%	

Table 4. 4: List of Price for Equipment's in Ethiopia Market by SAT Supplier (2015)

Energy Equipment (Fixed Costs)	*Single Price ($)*
Solar Collectors (m^2)	*246*
Solar Thermal Storage Tank (L)	*0.7*
Solar Loop Pipe Materials (m)	*27.00*
Circulating Pump (W)	*1.10*
Collector Support Structure (m^2)	*25*
Plumbing and Control (Project)	*300*

Table 4. 4: List of Price for Variable Costs in Ethiopia Market by SAT Supplier (Interview)

Variable Costs	**Price ($)**
Auxiliary Equipment Installation (Per Project)	5000
Operational & Maintenance Cost (Per Year)	1500
Transportation Cost (Per Project)	2000
Collector Installation (m^2)	5
Solar Loop Installation (m)	2
Auxiliary Equipment Installation (Project)	5

CHAPTER FIVE

5. Result and Discussion

5.1. Heat Transfer Limits of Heat Pipe and Developed Model Validation

5.1.1. Heat Transfer Limits of Heat pipe

Based on the design dimensions of collectors and heat pipe, the critical analysis criteria was considered to check the limits of the heat pipe heat transport. This study uses Mazdon 20 - TMA 600S heat pipe evacuated tube solar collector to analysis hourly outlet temperature of water, hourly useful energy harvested. A heat pipe evacuated tube solar collector specification has mentioned in table 4.1. The collector system was supposed to work in all conditions throughout the year and the maximum radiation level was considered as a critical value. A value of 1.17KW/m^2 maximum solar radiation is used for the collector on March 31 at 11:00 in the morning. With this radiation level, the maximum heat that the heat pipe transfer is 3.19KW. Table 5.1 shows a summary of the heat transfer limits for the heat pipe. The values obtained are well above the critical analysis value and the heat pipe is safe for operation.

Table 5. 1: Heat Transfer Limit of Heat Pipe

Type	Value
Sonic Limit	3.46KW
Entrainment Limit	5.88KW
Boiling Limit	4.18KW
Capillary Limit	3.6KW

5.1.2. Developed Mathematical Model Validation

The developed model was evaluated against simulation result of a previous study that is extracted from M. Arab, A. Abbas et al. (2013) [57]. The design data of the SWH and the built-in heat pipes data are presented in table 5.2. A comparison between the simulations results of this study and M. Arab et al. (2013) show in figure 5.1.

Table 5. 2: Technical Details of Heat Pipe and Collector [57]

Technical Details of Heat Pipes Inside the Evacuated Tubes.	**Values**	**Technical Details of The Collector.**	**Values**
Wick structure	Grooved Wick	Type	Evacuated Tube
Casing	Copper	Tilt angle	35
Do,HP (mm)	8.67	Do;g(mm)	47
Di,HP (mm)	7.17	Di,g (mm)	37
Le (m)	1.25	N	30
La	0.12	Lmani:(m)	1.5
Lc (m)	0.13	Lcon.pipes (m)	3.9

The simulations were executed for six different hours at 0.8 kg/min water mass flow rates, and the same inlet water temperatures and solar irradiation data. As shown in Figure 5.1 although there is a small difference between the previous result and the simulated temperature of circulating water at the end of the manifold which was predicted by the developed model.

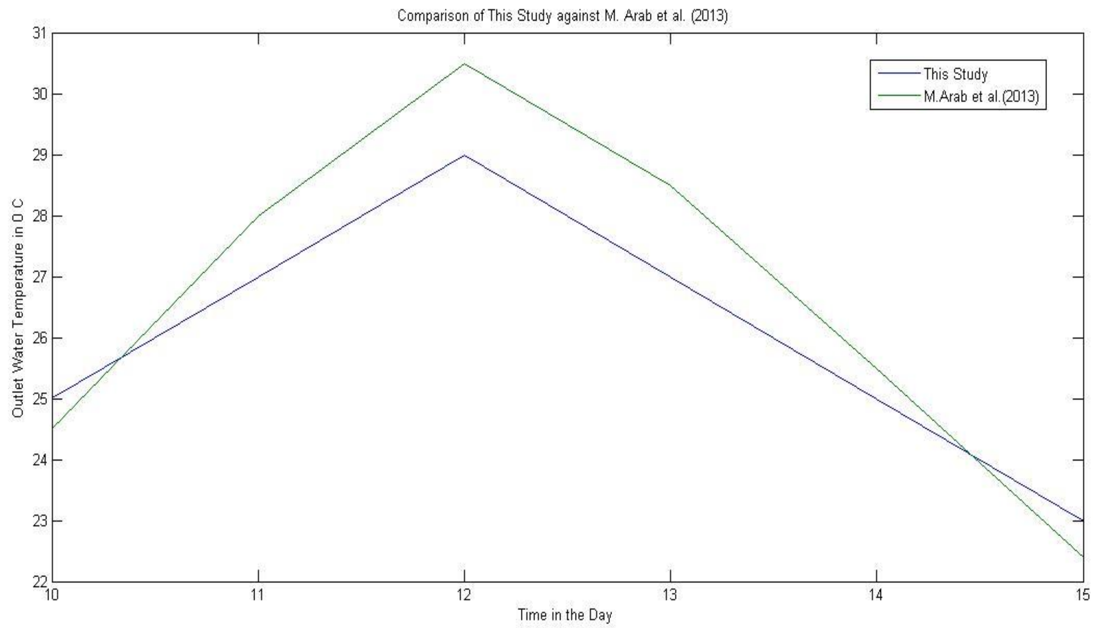

Figure 5. 1: Comparison between the Simulations Results of This Study and M. Arab Et Al. (2013)

Furthermore, as shown in Figure 5.1, all of the predicted temperatures are within 93% confidence interval. The calculated error percentage for temperature of water at the last evacuated tube solar collector is in the range of [-2.67%, 5.26%] with a total average of 1.83%. Therefore, it can be concluded that there is a very good agreement between the M. Arab et al. (2013) and this study simulation results.

5.2. Conventional Thermal System in the Industry

The conventional thermal energy consumption was analyzed for the selected processes in the industry. The energy consumption profile of the selected processes such as mashing (at 78^0C and 52^0C), feed water pre heating, bottle cleaning, kegging and CIP, are mentioned in the next sections.

The hourly conventional thermal energy consumption highly affected by the inlet temperature of water to the processes. Figure 5.2 shows hourly conventional thermal energy consumption graph for six selected processes and the total conventional thermal energy consumption for selected processes in the industry. X-axis indicated that the number of hours in the year, Y-axis is conventional thermal energy consumption in MW.

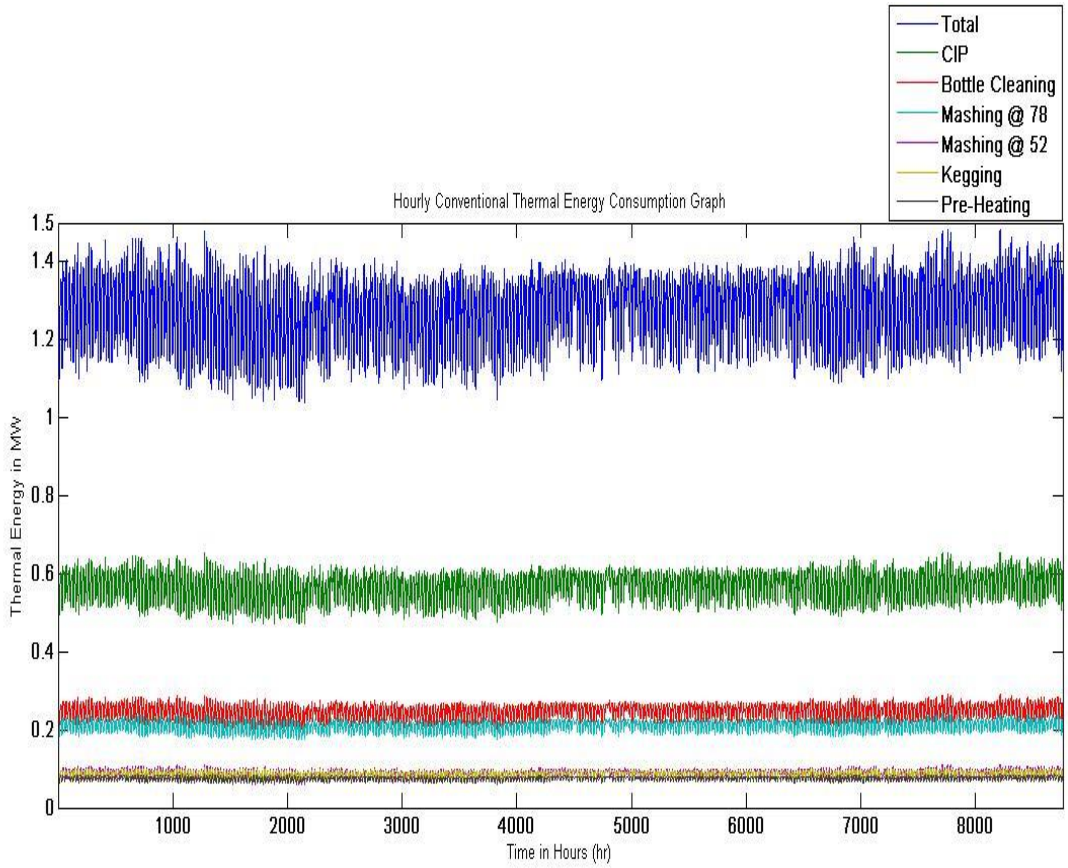

Figure 5. 2: Hourly Conventional Thermal Energy Consumption Graph

Figure 5.2 above shows the highest hourly conventional thermal energy consumption is on November 20 at 5:00 in the morning and the lowest hourly conventional thermal energy consumption is on March 31 at 2:00 in the afternoon. The highest and the lowest conventional thermal energy consumption for mashing process at 78^0C are 0.24MW and 0.17MW respectively. Moreover, the annual conventional thermal energy consumption for mashing at 78^0C is 1841.69MWthr. And, the highest and the lowest conventional thermal energy consumption for mashing at 52^0C are 0.11MW on November 20 and the lowest is 0.06MW on March 31. Moreover, the annual conventional thermal energy consumption for mashing at 52^0C is 757.18MWthr.

Based on the figure 5.2 the maximum hourly conventional thermal energy consumption for feed water pre heating is 0.09MW and the minimum energy consumption is 0.06MW. Moreover, the annual conventional thermal energy consumption for feed water pre heating process is 653.72MWthr.

The highest and the lowest conventional thermal energy consumption for bottle cleaning process are 0.29MW and the lowest is 0.20MW respectively. Moreover, the annual conventional thermal energy consumption for bottle cleaning process is 2170.84MWthr.

Based on figure 5.2 shows above the highest hourly conventional thermal energy needed for kegging process is 0.10MW and the lowest is 0.07MW. Moreover, the annual conventional thermal energy consumption for kegging process is 770.94MWthr.

The highest and the lowest conventional thermal energy consumption for CIP process are 0.65MW and the lowest is 0.47MW respectively. Moreover, the annual conventional thermal energy consumption for CIP process is 4981.81MWhr.

Figure 5.2 shows that the maximum conventional thermal energy is required when low ambient temperature is recorded which means at dark time. And, the minimum thermal energy is needed at solar noon. The highest conventional thermal energy needed for all selected processes is 1.48MW on November 20 and the lowest is 1.04MW on March 31. Besides, the highest daily conventional thermal energy consumption for all selected processes on July 19 is 31.00MWthr and the lowest daily thermal energy consumption for all selected processes on March 29 is 27.38MWthr. Moreover, the annual conventional thermal energy consumption for all selected processes is 11176.18MtWhr.

5.3. Result of Thermal Analysis of HPETSCs

5.3.1. Hourly Outlet Water Temperature

Hourly outlet water temperature result indicated that the outlet temperature depends on the total solar irradiance on tilted surface and the mass flow rate of water. Figure 5.3 shows the outlet water temperature graph at the end of a manifold for three different water mass flow rate. X-axis indicated that the number of hours in the year and Y-axis is the outlet water temperature variation in ^{0}C.

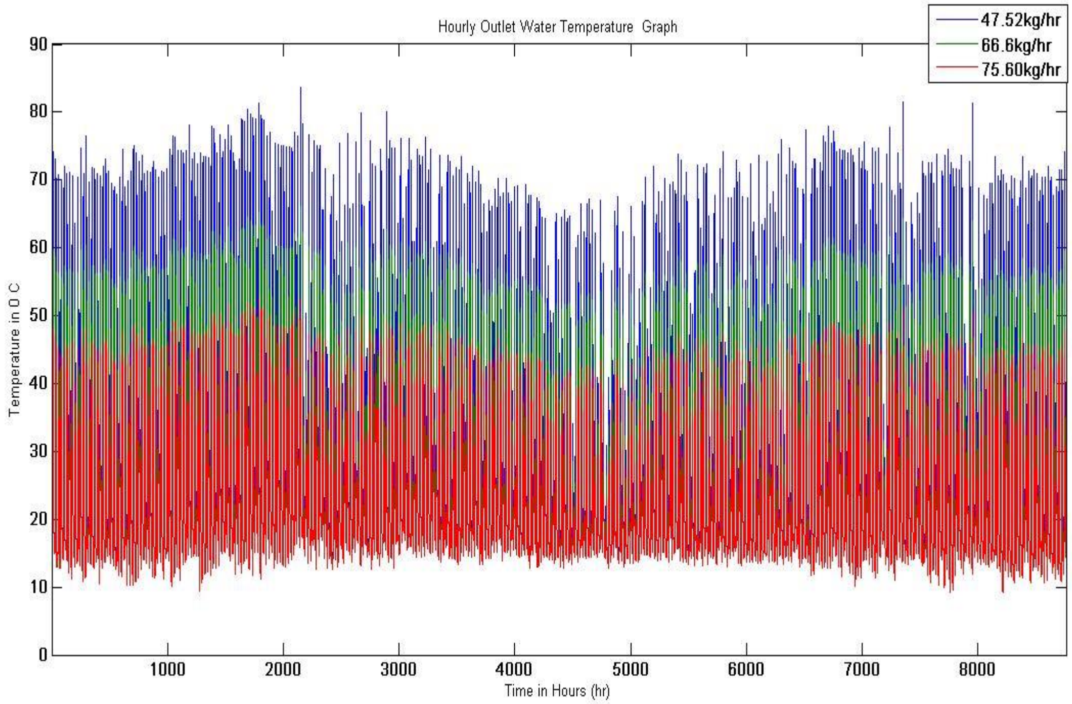

Figure 5. 3: Outlet Water Temperature Graph at the End of the Manifold

Figure 5.3 shows that the outlet water temperatures at the end of a manifold have a parabolic shape which bends downward for all days of the year. However, the outlet temperature is nearly equal with ambient temperature during the night. The highest outlet water temperature is recorded on March 31 at 11:00 in the morning. The maximum outlet water temperature is 80^0C for mass flow rate of 47.52 kg/hr through the manifold. This flow rate is designed for thermal processes such as Mashing at 78^0C, CIP, Kegging and Preheating of makeup water. Nevertheless, the maximum outlet water temperature for Mashing at 52^0C process is 52^0C in which the mass flow rate must be 75.60kg/hr. The maximum outlet water temperature for Bottle cleaning is 65^0C in which it should have a mass flow rate of 66.6kg/hr.

Figure 5.4 shows the hourly outlet temperature of water graph at the ends of a manifold for two days of the year which are March 16 and April 15. These days are representative days of the month for March and April. X-axis indicated the number of hours in the year and Y-axis is the outlet water temperature in ^{0}C.

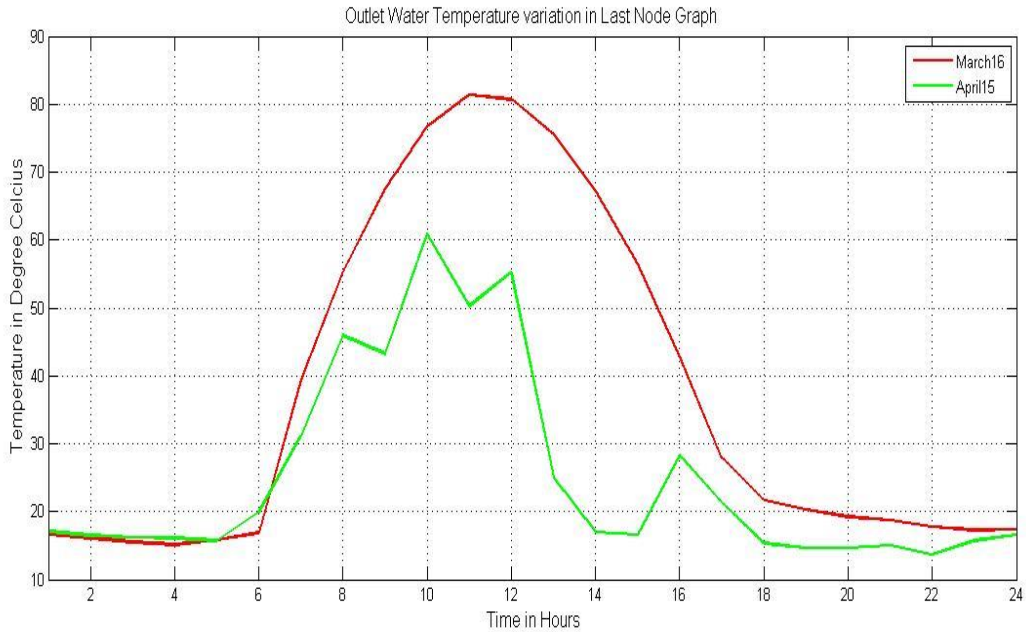

Figure 5. 4: Hourly Outlet Temperature of Water Graph at the End of the Manifold for March 16 and April 15

Based on figure 5.4 shows above the maximum outlet water temperature is 80^0C on March 16 at 11:00 in the morning for water mass flow rate of 47.52 kg/hr. The maximum and minimum outlet water temperature on April 15 are 60^0C at 10:00 in the morning and 16^0C at 3:00 in the afternoon respectively. The outlet water temperature on April 15 is fluctuated hour to hour due to the indistinct sky cover.

5.3.2. Instantaneous Efficiency of the System

The instantaneous efficiency of the system depends on the mass flow rate of water through the manifold and hourly solar irradiance on the tilted surface. Figure 5.5 shows the instantaneous efficiency graph of solar collector for representative days of the months. When solar radiation absorbed on tilted surface is less than one the instantaneous efficiency on this study is going to greater than 100%. This study omits the result when the instantaneous efficiency value out of the boundary. X-axis indicated the number of hours in the day from 6:00 in the morning to 6:00 in the afternoon and Y-axis is instantaneous efficiency in percentage.

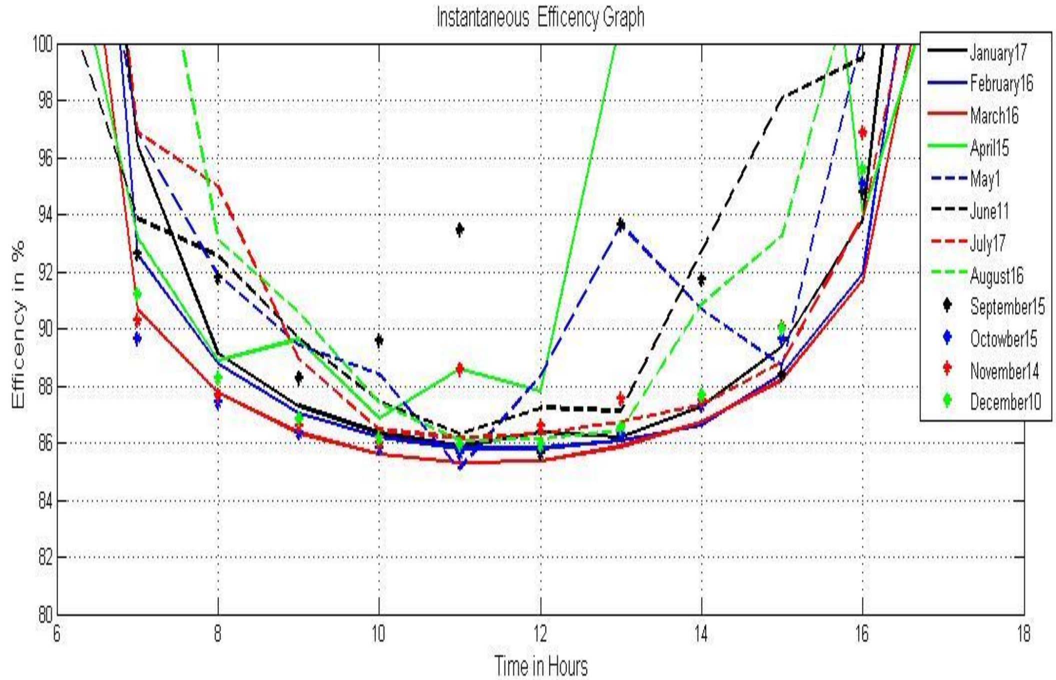

Figure 5. 5: Instantaneous Efficiency Graph by a Single Collector for Representative Days of the Month

Figure 5.5 shows that the instantaneous efficiency of the collector ranging between 84.96-100%. The maximum instantaneous efficiency is during sunshine and sunset hours. And, the minimum instantaneous efficiency is 84.96% on March 31 at 11:00 in the morning for the mass flow rate of 47.52kg/hr. However, the minimum instantaneous efficiency is 83.02% when the mass flow rate is 66.6kg/hr. And, the minimum instantaneous efficiency of the system is 62.19% when the mass flow rate of water 75.60kg/hr.

5.3.3. Hourly Useful Energy Harvest of the System

Solar thermal energy governs by the solar radiation, mass flow rate and outlet water temperature. Figure 5.6 shows an hourly solar thermal energy harvest graph of a single solar collector. X-axis indicated that the number of hours in the year and Y-axis is solar thermal energy in W.

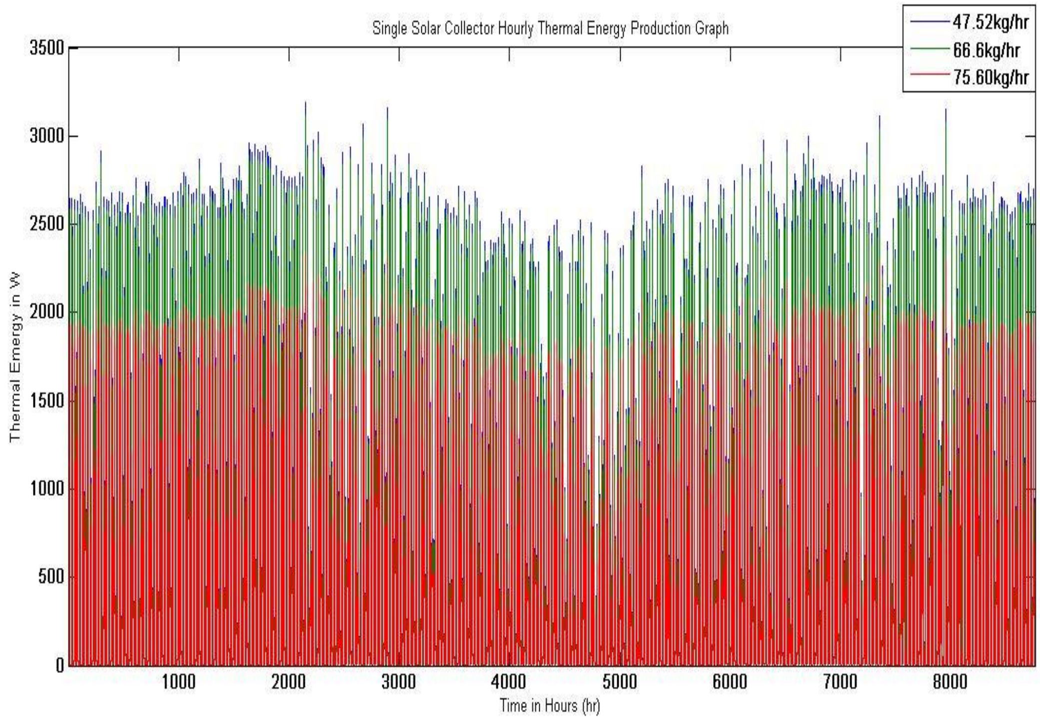

Figure 5. 6: Hourly Solar Thermal Energy Harvest Graph of a Single Collector

Figure 5.6 shows a plot of the hourly solar thermal energy production by a single collector. It has a parabolic shape which bends downward for all days of the year. A single collector produces a maximum hourly solar thermal energy on March 31 at 11:00 in the morning. The maximum solar thermal energy production of a single collector is 3.19KW at 80^0C outlet water temperature and the mass flow rate of 47.52kg/hr. However, the maximum thermal energy production is 2.33KW at 52^0C of outlet water temperature and the mass flow rate of 75.60kg/hr. And, the maximum thermal energy production is 3.12KW at 65^0C of outlet water temperature and the mass flow rate of 66.6kg/hr.

Figure 5.7 shows the hourly solar thermal energy production graph by a single collector for March 12 and July 19. These days are the highest and the smallest solar thermal energy production day of the year for Harar Weather condition respectively. X-axis indicated the number of hours in the day and Y-axis is solar thermal energy in W.

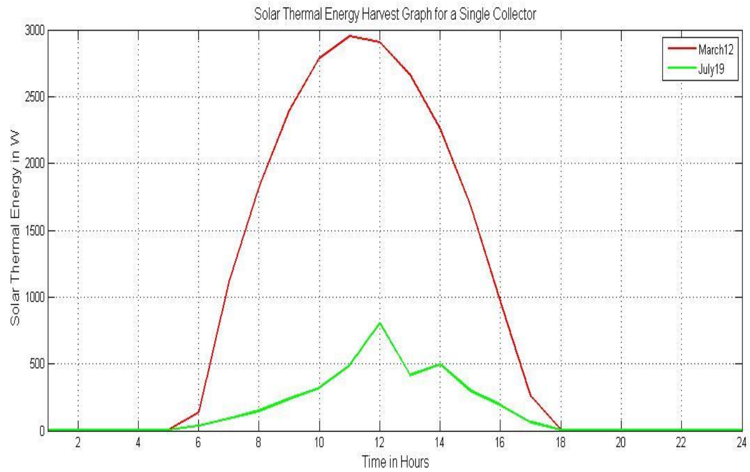

Figure 5. 7: Hourly Solar Thermal Energy production Graph by a Single Collector for March 12 and July 19.

Figure 5.7 shows above the hourly solar thermal energy production on March 12 and July 19 for the mass flow rate of 47.50kg/hr. The highest daily solar thermal energy produced on March 12 is 22.01KWthr and the lowest daily solar thermal energy produced on July 19 is 3.66KWthr.

5.4. Size, Arrangement and Micrositting of Solar Collectors

The optimal number of solar collector was determined for all processes based on maximum operation temperature of processes, mass flow rate and ambient temperature. And, the appropriate location of solar collector was identified to harness the maximum possible solar energy. The optimal number of collectors were calculated for each process.

5.4.1. Collector Arrangement and Size

Table 5. 3: Design Mass Flow Rate and Number of Collector for Each Process

Processes	**Daily Average Water Consumption in m^3**	**Mass Flow Required in Kg/s**	**Design Mass Flow Rate in Kg/s**	**Number of Collectors**
Mashing at 52 ^{0}C	53.27	0.62	0.0210	30.00
Cleaning at 65^{0}C	93.41	1.08	0.0185	59.00
Mashing at 78^{0}C	70.61	0.82	0.0132	62.00
Preheating	25.09	0.29	0.0132	22.00
CIP	191.10	2.21	0.0132	168.00
Kegging	29.56	0.34	0.0132	27.00
	463.03			**368.00**

Table 5.3 indicates that the number of solar collectors needed for supply parts of the thermal energy demand in the industry. The number of collectors required for mashing processes are 92 (30 for mashing at 52^0C and 62 for mashing at 78^0C). And, for processes bottle cleaning, feed water pre-heating, CIP, and kegging are 59, 22,168 and 27 respectively. So, the total number of solar collectors required are 368. All of the collectors should have arranged in parallel.

5.4.2. Micrositting of Solar Collectors

Solar collector installation site was identified on the roof of bottle cleaning section in the industry. Figure 5.8 shows the site view of Harar Brewery factory production section.

Figure 5. 8: Site View of Harar Brewery Factory

The bottle cleaning section is the safest place for solar collectors' installation. It has a total roof area of 2925m^2 (39m width by 75m length). However, the total solar collectors' area required for the selected processes is 2504.2m^2 (including pipe area and clearance). There is too much space for micrositting of all collector for solar thermal energy harvesting in the industry.

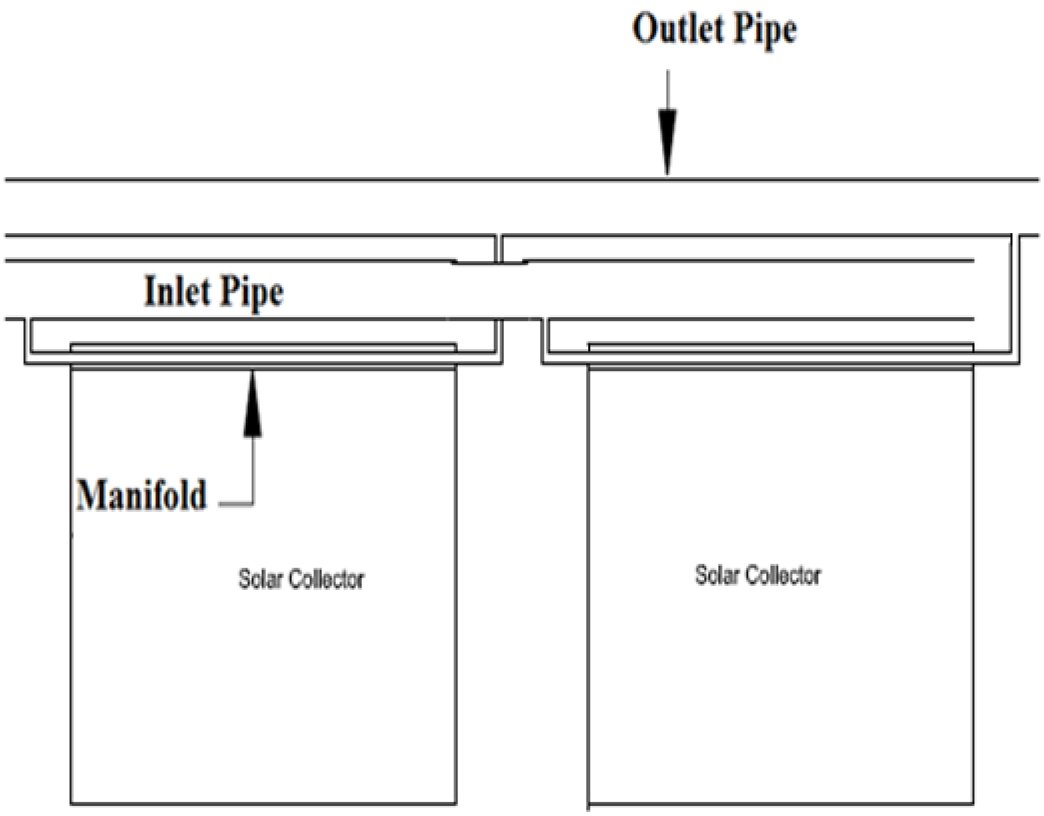

Figure 5. 9: Parallel Arrangement of Solar Collectors

Figure 5.9 shows above parallel arrangement of solar collectors on the roof of bottle cleaning section. In addition, the solar collector arrangement shows in Appendix D.

5.5. Solar Thermal Energy

The outputs of solar thermal energy are divided in to three different section based on the maximum operation temperature of the processes in the industry. The first section is the solar thermal energy harvesting for mashing process. In this process the maximum outlet water temperature at the last node is 52^0 C. The second section is the solar thermal energy harvesting for bottle cleaning process. It has a maximum outlet water temperature of 65^0 C at the last node. And, the last section includes solar thermal energy harvesting for feed water pre heating, kegging, CIP and mashing at 78^0 C. The maximum outlet water temperature production at the last node for these processes are $78^{-}80^0$ C.

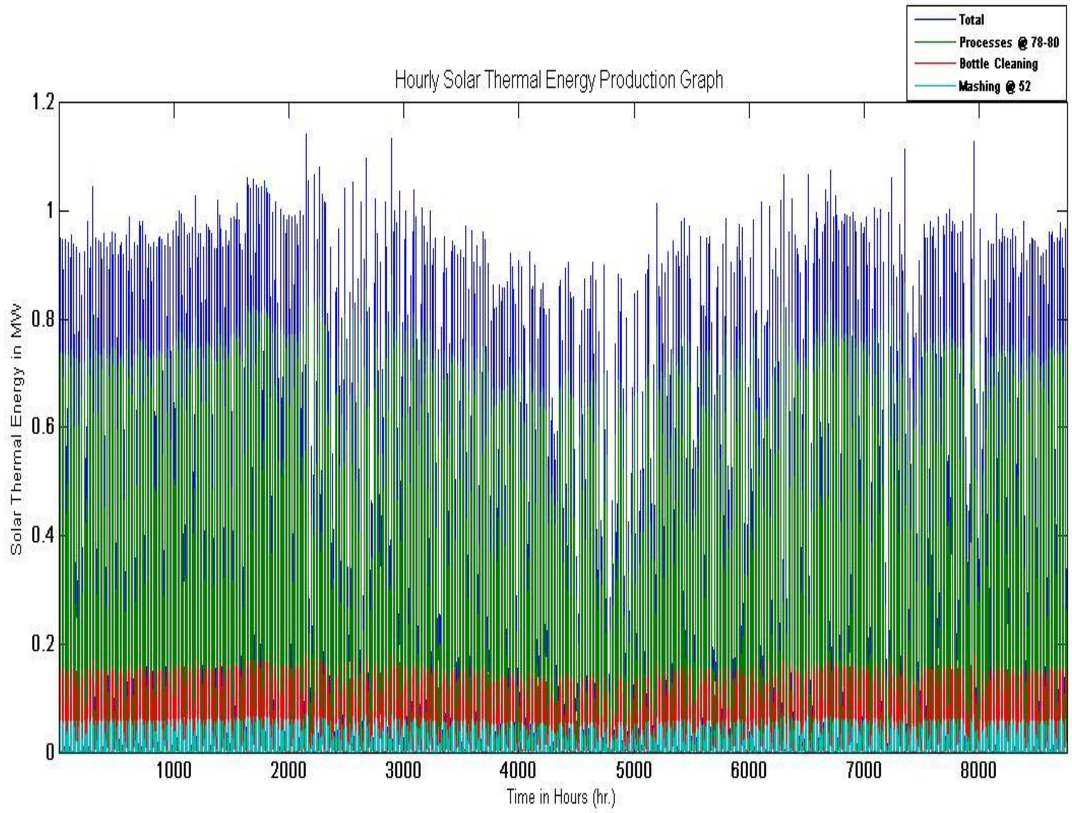

Figure 5. 10: Hourly Solar Thermal Energy Production

Figure 5.10 above shows the highest hourly solar thermal energy production on March 31 at 11:00 in the morning. It has 0.89MW, 0.18MW, 0.07MW and 1.14MW for thermal processes at maximum operation temperature 78-80^{0}C, bottle cleaning, Mashing at 52^{0}C and total solar thermal energy production for all selected processes in the industry, respectively. The highest daily solar thermal energy produced for all selected processes on March 12 is 7.89MWhr and the lowest daily solar thermal energy produced for all selected processes on July 19 is 1.31MWhr.

The annual solar thermal energy production for mashing process at 52^{0}C is 127.03MtWhr. The integration strategy of solar thermal system for Mashing process at 52^{0}C is integration of the solar thermal into the process heat with thermal storage tank of 20m^3.

The annual solar thermal energy production for bottle cleaning process at 65^{0}C is 333.47Mtwhr. The solar thermal energy integration stratagem for bottle cleaning is integration of the solar thermal into the process heat with thermal storage tank of 30m^3.

Figure 5.10 shows hourly solar thermal energy production graph for processes at a temperature of 78-80^0 C such as feed water pre heating, kegging, CIP and mashing at 78^{0}C. The annual solar thermal energy production for these processes is 1613.98MtWhr (358.66 for mashing at 78^0 C, for CIP 971.86, for Kegging 156.19 and for pre heating 127.27). The integration strategy of solar thermal system for feed water pre heating is integration of the solar thermal into the pre heating without thermal storage. However, the integration strategy for other processes (such as kegging, CIP and mashing at 78^{0}C) is integration of the solar thermal into the process heat with thermal storage tank 30m^3.

The annual solar thermal energy production for all selected processes in the industry is 2074.48MWhr.

5.6. Integrated System Thermal Energy Consumption

The result of the integration of solar thermal system in the industry shows that how much the conventional thermal energy consumption reduced throughout the year. Figure 5.11 shows hourly conventional thermal energy consumption integrated with SWH, conventional thermal energy consumption without integrated with SWH and solar thermal energy production using SWH system for one year time period. X-axis indicated the number of hours in the year and Y-axis is hourly thermal energy consumption and production in MW.

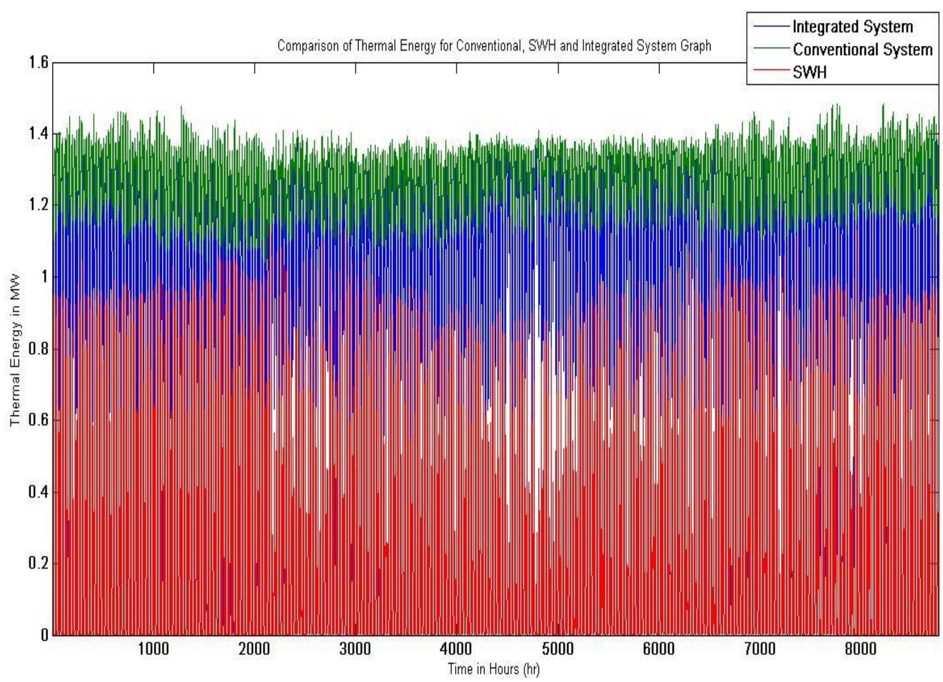

Figure 5. 11: Hourly Conventional Thermal Energy Consumption Integrated With SWH, Conventional Thermal Energy Consumption without Integrated With SWH and Solar Thermal Energy Generation

Figure 5.11 shows that the maximum conventional thermal energy required when low ambient temperature is recorded which means at dark time. And, the minimum conventional thermal energy is needed at solar noon.

Figure 5.12 shows hourly conventional thermal energy consumption of integration system, SWH system energy production and conventional thermal energy consumption for March 12, March 29 and July 19. X-axis indicated the number of hours in the day and Y-axis is hourly thermal energy consumption and production in MW.

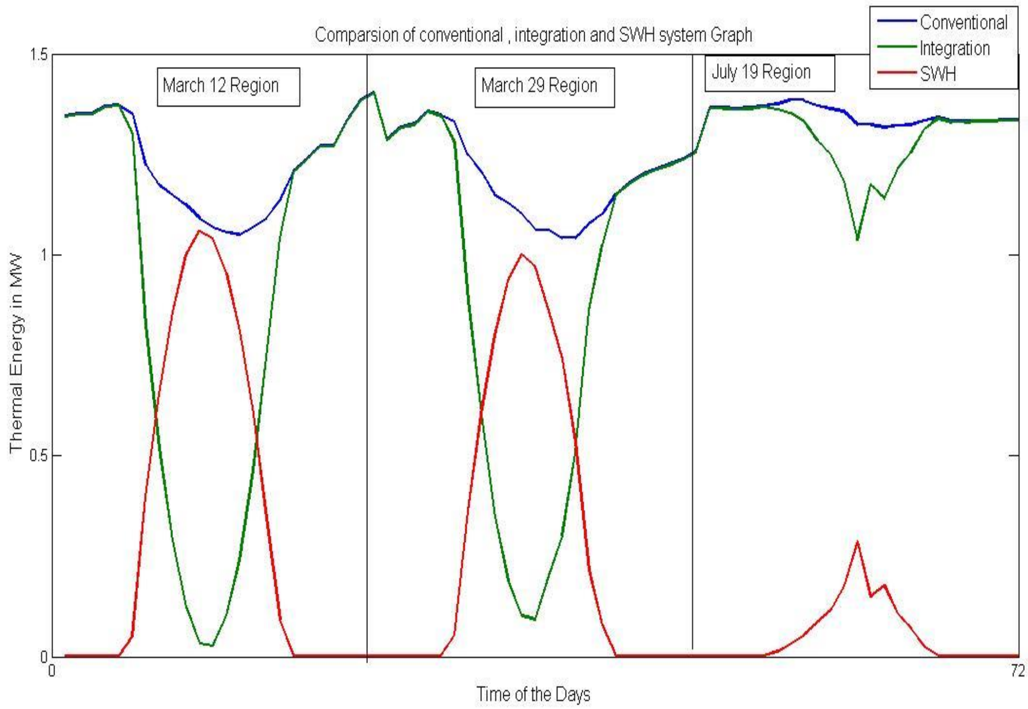

Figure 5. 12: Hourly Conventional Thermal Energy Consumption of Integration System, Conventional Thermal Energy Consumption and Solar Thermal Energy Production in for March 12, March 29 and July 19

Based on figure 5.12 shows above the highest daily conventional thermal energy consumption for all selected processes on July 19 which is 31.00MWthr and the lowest daily thermal energy consumption for all selected processes on March 29 is 27.38MWthr. The highest daily solar thermal energy produced for all selected processes on March 12 is 7.89MWhr and the lowest daily solar thermal energy production for all selected processes on July 19 is 1.31MWhr. However, thermal energy consumption for integrated system on March 12, March 29 and July 19 are 20.22Mwthr, 20.20MWthr and 29.69MWthr respectively.

Based on figure 5.12 shows above the maximum solar thermal energy harvested at 11:00 in the morning but the conventional thermal energy consumption is minimum. And, during the night solar thermal production is not available, that way all thermal energy demand is covered by conventional thermal energy system.

Table 5. 4: Annual Thermal Energy Analysis of Conventional System and Integration System

S.N	Processes	Annual Conventional Energy Supply (MWthr)	Annual Solar Energy Supply (MWthr)	Energy Save(MWthr)	Integration System Conventional Energy Consumption (MWthr)	Conventional Energy Supply (%)	Integration System Conventional Energy Supply (%)	Total Industry Energy Save (%)
1.	Mashing 52	757.18	127.03	127.03	630.15	3.67	3.05	0.62
2.	Mashing 78	1841.69	358.66	358.66	1483.03	8.92	7.19	1.74
3.	CIP	4981.81	971.86	971.86	4009.95	24.14	19.43	4.71
4.	Kegging	770.94	156.19	156.19	614.75	3.74	2.98	0.76
5.	Make Up	653.72	127.27	127.27	526.45	3.17	2.55	0.62
6.	Washing	2170.84	333.47	333.47	1837.37	10.52	10.12	0.39
	Total (Selected Processes)	**11176.18**	**2074.48**	**2074.48**	**9101.70**	**54.15**	**44.10**	**10.05**
7.	Pre Heating of Fuel	25.41		2.55	24.32	0.10	0.09	0.01
8.	Overall Heat Loss	4127.65		414.90	3712.75	20.00	17.99	2.01
9.	Other Processes (Pasteurization, Evaporation Etc.)	5314.63			5314.63	25.75	25.75	0.00
10.	Pump			-1.46	1.46	0.00	0.00	0.00
	Total	**20638.23**		**2490.47**	**18147.76**	**100.00**	**87.93**	**12.07**

Table 5.4 indicated that the summary of annual energy distribution for thermal processes in the industry. The total annual thermal energy consumption of the industry is 20638.23MWthr. This thermal energy distribution are 54.15% to the selected thermal processes, 0.1% to pre heating of furnace oil, 25.75% to other thermal processes (not included in this study) and the remaining 20% is heat loss. Due to the integration of solar thermal system in low temperature industrial processes, the consumption of conventional thermal energy for the selected processes are reduced from 11176.18MtWhr/year to 9101.70MWhr/year. Which means 18.56% of thermal energy consumption for selected processes in the industry could be saved. However, the total annual thermal energy consumption of the industry is reduced to 18147.76MWthr. This means 2490.47 MWthr/ year or 12.07% (10.05% from selected processes, 2.01% from overall heat loss and 0.01% from pre heating of fuel) of the fuel consumption in the industry is saved. In other way, 205,840.65 liter of furnace oil could be saved every year.

5.7. Result of Financial Analysis

Figure 5.13 shows the project cumulative cash flow of integrated solar thermal system for financial analysis of section 4.9. X-axis is the number of years and Y –axis is the cumulative financial flow of the project.

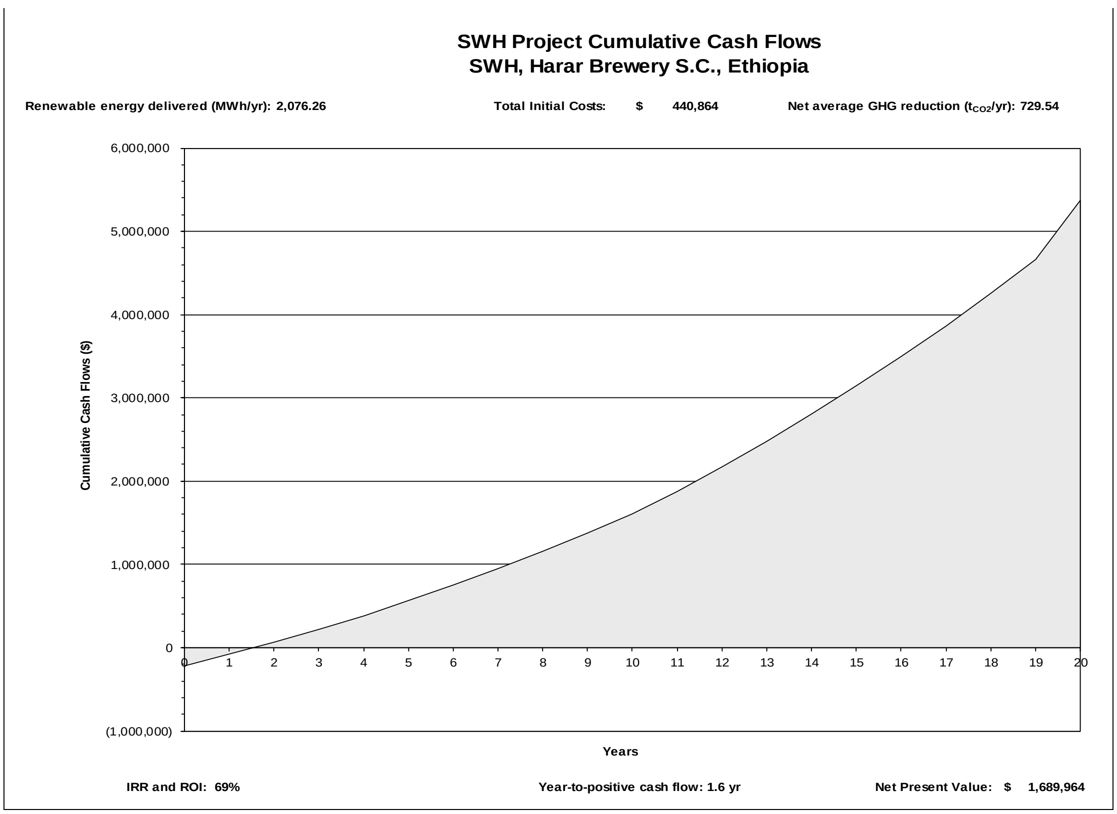

Figure 5. 13: Project Cumulative Cash Flow of Integrated Solar Thermal System

Based on figure 5.13 shows above the analysis of RETScreen software, the total initial investment cost is $440,864 out of which 50% is project equity and the remaining is project debt. This project has 20 years life time. The system produces 2076.26MWthr annual solar thermal energy. This project will reduce $165,813 of the cost for thermal energy application and 729.54 tons of carbon dioxide (CO_2) emission per year. The project equity is returned back with 1.6 years. However, this financial model doesn't include the amount of energy saved due to reduction of annual fuel consumption in the industry. Which means, in addition to the annual solar thermal energy harvest, 1.09MWthr and 414.90MWthr energy are saved from pre-heating of furnace oil and the overall heat loss of the system respectively. Therefore, the industry could save 2492.25MWthr annually (2490.47 MWthr based on Matlab analysis). The input parameters and the financial analysis of the RETScreen software are showed in Appendix C.

CHAPTER SIX

6. Conclusion and Recommendation

6.1. Conclusion

This work describes an integration of solar thermal system for improved energy consumption in low temperature industrial processes case study Harar brewery S.C. The approaches to achieve the objective of the research involve data collection, synthesis with understanding the conventional thermal energy supply, knowing distribution of steam for different processes in the industry and analysis of heat pipe evacuated tube solar collector with the development of mathematical model which approximates physical law with literation and finite difference method.

In this thesis, the performance of heat pipe evacuated tube solar collectors was predicted. A mathematical model is developed for simulation of hourly outlet water temperature, instantaneous efficiency, solar thermal energy, conventional thermal energy and integrated conventional thermal energy for one year period in the Matlab program. A fully integrated model for a heat pipe type evacuated tube solar water heater was developed and validated against M. Arab et al. (2013). All of the predicted temperatures are within 93% confidence interval. The calculated error percentage for water temperature at the ends of the manifold is in the range of [- 2.67%, 5.26%] with a total average of 1.83%.

Six low temperature processes, such as feed water pre-heating, kegging, CIP, Mashing at 78^0C, bottle cleaning and mashing at 52^0C were selected in the industry for solar thermal integration. Annual conventional thermal energy consumption was calculated for all processes. Those are 1841.69MWthr, 4981.81MWthr, 770.94MWthr, 653.72MWthr, 2170.84MWthr, 757.18MWthr for the processes of Mashing at 78^0C, CIP, kegging, feed water pre heating, bottle cleaning and mashing at 52^0C respectively. A total of 11,176.18MWhr annual conventional thermal energy is needed for all selected processes. The selected processes covers 54.15% of the annual total thermal energy consumption from the chemical energy of fuel which is 20638.23MWthr. The remaining 45.85% thermal energy are distributed 20% for overall heat losses, 0.10% for pre-heating of fuel and 25.75% for other thermal processes which were not part of this study.

Hourly outlet water temperature result shows that the outlet temperature depends on the total solar irradiance on tilted surface. And the maximum outlet temperature is recorded during solar noon which is 80^0C for mass flow rate of 47.52 kg/hr through the manifold. However, the maximum outlet temperature is 52^0C in mashing process and the mass flow rate must be 75.60kg/hr. and, bottle cleaning process operates at a range of 65-85^0C, but, this paper designs SWH for the minimum operation temperature which is at 65^0C. It should have a mass flow rate of 66.6kg/hr.

The maximum instantaneous efficiency is during sun shine and sun set hours. And, the minimum instantaneous efficiency is 84.96% on March 31 at 11:00 in the morning for the mass flow rate of 47.52kg/hr. However, the minimum instantaneous efficiency is 83.02% when the mass flow rate is 66.6kg/hr. And, the minimum instantaneous efficiency of the system is 62.19% when the mass flow rate of water is 75.60kg/hr. Solar thermal energy also dependent on the solar radiation, mass flow rate and operation temperature of the processes. The maximum solar thermal energy is harvested for the processes at 80^0C, which is 3.19KW on March 31 at 11:00 in the morning form a single collector. However, the highest daily solar thermal energy produced on March 12 is 22.01KWhr and the lowest daily solar thermal energy produced on July 19 is 3.66KWhr.

The optimal number of solar collector was determined for all processes based on the maximum operation temperature of the processes, mass flow rate and ambient temperature. And, the appropriate location of solar collector is identified to harness the maximum possible solar energy. The optimal number of collectors are calculated for each process. The total number of collectors are 368 which means 30 for mashing at 52^0C, 62 for mashing at 78^0C, 59 for bottle cleaning, 22 for feed water pre heating, 168 for CIP and 27 for kegging.

Annual solar thermal energy production was analyzed for all processes. Those are 127.03MWhr, 333.47Mwhr and 1613.98MWhr for mashing at 52^0C, bottle cleaning and other thermal processes at 78-80^0C respectively. The total annual solar thermal energy harvested for all selected processes is 2074.48MWhr.

Due to the integration of solar thermal system in low temperature industrial processes, the consumption of conventional thermal energy for the selected processes are reduced from 11176.18MtWhr/year to 9101.70MWhr/year. Which means 18.56% of thermal energy consumption for selected processes in the industry could be saved. However, the total annual thermal energy consumption of the industry is reduced from 20638.23MWthr to 18147.76MWthr. This means 12.07% (10.05% from selected processes, 2.01% from overall heat loss and 0.01% from pre heating of fuel) of the fuel consumption in the industry is saved. In other way, 205,840.65 liter of furnace oil is saved every year.

The total initial investment cost is $440,864 out of which 50% is project equity and the remaining is project debt. This project has 20 years life time. The system produces 2076.26MWthr annual solar thermal energy. This project will reduce $165,813 of the cost for thermal energy application and 729.54 tons of carbon dioxide (CO2) emission per year. The project equity is returned back with 1.6 years.

6.2. Recommendation

This presented study forms a foundation and should be considered as a starting point for further studies. In the future with required developments and research, these systems can be more viable for industrial energy saving, and cost of energy saving opportunity. Suggestions to improve on this developed mathematical model and integration work are as follows:

- This study does not include thermal energy storage for the night time energy consumption in the industry due to lack of suitable place for installation of additional solar collectors. It is suggested to use thermal Storage system for other industrial application can be increased the energy saving opportunity of this system.
- The current work is validated against other study with similar design specification and solar radiation on tilted surface. It is recommended to study experimental test for this theoretical analysis.
- Future studies should consider a variety of improvements to the existing results that should include primarily data collection for thermal devices in the industry and additional study on the steam energy delivering pipes and boiler combustion.
- This study focuses on hourly outlet water temperature on the end of manifold. However it should be suggested additional study about stratification in thermal storage tank.
- Further study should consider on other suitable solar thermal processes in the industry like pasteurization (which is not part of this study).
- This study focuses on non-tracking heat pipe evacuated tube solar collector. However, further studies should be done on tracing solar collector design.

References

1. Cleaner Production – Energy Efficiency Manual for GERIAP, UNEP, Bangkok prepared by National Productivity Council
2. Christina Galitsky, Nathan Martin, Ernst Worrell and Bryan Lehman**,** *Energy Efficiency Improvement and Cost Saving Opportunities for Breweries*, Environmental Energy Technologies Division (Sept 2003), LBNL-50934.
3. International Energy Agency. 2011. Co-generation and Renewables: Solution for a Low Carbon Future. International Energy Agency. http://www.iea.org/ papers /2011/ CHP_ Renewables. Pdf (accessed December 1, 2011).
4. U.S. Department of Energy, Office of Energy Efficiency and Renewable Energy, Industrial Technologies Program. January 2006. *Best Practices: Process Heating*. U.S. Department of Energy. http://www1.eere.energy.gov/industry/bestpractices/pdfs/39155.pdf (accessed December 1, 2011).
5. Martin J. Atkins, Michael R.W. Walmsley, Andrew S. Morrison, *Integration of solar thermal for improved energy efficiency in low-temperature-pinch industrial processes*. Energy 35 (2010) 1867–1873.
6. A. Freina, M. Calderonia, M. Mottaa, *Solar thermal plant integration into an industrial process.* Energy Procedia 48 (2014) 1188 – 1193.
7. International Energy Agency, Solar Heating and Cooling Program. 2008. Potential for Solar Heating in Industrial Processes. International Energy Agency. http://www.iea-shc.org/publications/downloads/task33 Potential_for_Solar_Heat_in_Industrial_Processes.pdf (accessed December 1, 2011).
8. Kalogirou S. *The potential of solar industrial process heat applications*. Applied Energy 2003; 76(4):337–61.
9. Benz N, Gut M, Rub W. *Solar process heat in breweries and dairies*. Portoroz, Slovenia: Eurosun 1998; 1998.
10. H. Müllera, S. Brandmayra, W. Zörnera, *Development of an evaluation methodology for the potential of solar-thermal energy use in the food industry*. Energy Procedia 48 (2014) 1194 – 1201.
11. Ministry of water and Energy, Ethiopian national energy policy (2nd draft), Ethiopia, Addis Ababa, 2013, February.
12. Ministry of Water and Energy Scaling Up Renewable Energy Program Ethiopia Investment Plan (Draft Final), January 2012.
13. J.A.Duffie and W.A.Beckman *Solar Engineering of Thermal Processing* 4th. Edition.

14. R. Shukla, K.Sumathy and P. Erickson, J. Gong, *Recent advances in the solar water heating systems: A review*. Renewable and Sustainable Energy Reviews 19 (2013) 173–190.
15. S. Arora1, S. Chitkara1, R. Udayakumar1 and M. Ali, *Thermal analysis of evacuated solar tube collectors*, Journal of Petroleum and Gas Engineering Vol. 2(4), pp. 74-82, April 2011.
16. Dr.S.P.Vendan, L.P.A.Shunmuganathan, T.Manojkumar, and C.Shiva Thanu, *Study on Design of an Evacuated Tube Solar Collector for High Temperature Steam Generation.* International Journal of Emerging Technology and Advanced Engineering, Volume 2, Issue 12, December 2012).
17. /http://www.solarpanelsplus.com/evacuated-tube-collectors/S.
18. Hossain MS, Saidur R, Fayaz H, Rahim NA, Islam MR and Ahamed JU, *Review on solar water heater collector and thermal energy performance of circulating pipe*. Renewable and Sustainable Energy Reviews 2011; 15: 3801–12.
19. Ogueke NV, Anyanwu EE, and Ekechukwu OV. *A review of solar water heating systems.* Renewable Sustainable Energy 2009; 1:043-106.
20. Kalogirou SA. *Solar thermal collectors and applications* .Prog Energy Combust Sci 2004; 30:231–95.
21. G. Morrison, I. Budihardjo and M. Behnia, *Water-In-Glass Evacuated Tube Solar Water Heaters*. Sol Energy 2004; 76:135–40.
22. Zubriski SE and Dick K. *Measurement of the Efficiency of Evacuated Tube Solar Collectors under Various Operating Conditions*. College Publishing; 2012.p. 114–130.
23. Ayompe L, Duffy A, Mckeever M, Conlon M, and McCormack S. *Comparative field performance study of flat plate and heat pipe evacuated tube collectors (ETCs) for domestic water heating systems in a temperate climate*. Energy 2011; 36:3370–8.
24. Dr. Ludwig Scheller, Dr. Rudolf Michel, and Udo Funk, 2008, *Efficient Use of Energy in the Brew house***,** MBAA TQ vol. 45, no. 3, pp. 263–267,
25. Kalogirou S. *Solar thermal collectors and applications*. Progress in Energy and Combustion Science 2004; 30:231–95.
26. Schnitzer H, Brunner C, and Gwehenberger G. *Minimizing greenhouse gas emissions through the application of solar thermal energy in industrial processes.* Journal of Cleaner Production 2007; 15(13–14):1271–86.
27. J. Atkins, Michael R., W. Walmsley and Andrew S., *Integration of solar thermal for improved energy efficiency in low-temperature-pinch industrial processes*. Energy 35 (2010) 1867–1873.
28. Nicolas Cottret, Emanuela Menichetti, *Technical Study Report on Solar Heat for Industrial Processes.* SSFA/2010/GFL 5070-4A54-2647-2101.

29. Zubriski SE and Dick K. *Measurement of the efficiency of evacuated tube solar collectors under various operating conditions*. College Publishing; 2012.p. 114–130.].
30. Shah LJ and Furbo S. *Vertical evacuated tubular-collectors utilizing solar radiation from all directions*. Apply Energy 2004:78:371–95.
31. Garcıa AF, Zarza E, Valenzuela L and Perez M. *Parabolic-trough solar collectors and their applications.* Renew Sustain Energy Rev 2010; 14:1695–721.
32. Siddharth Suman, and Kaleem Khan, *Performance enhancement of solar collectors; review.* Renewable and Sustainable Energy Reviews 49 (2015) 192–210.
33. Mousazadeh H, Keyhani A,J avadi A,Mobli H, A brinia K, Sharifi A. *A review of principle and sun-tracking methods for maximizing solar systems output*. Renew Sustain Energy Rev 2009; 13:1800–18.
34. Perez R, Seals R, Anderson J, Menicucci D. *Calculating solar radiation received by tubular collectors.* Journal of Solar Energy Engineering 1995; 117:341–4.
35. Morrison GL, Budihardjo I and Behnia M, *Water-in-glass evacuated tube solar water heaters.* Proceedings of ISES Solar World Congress, Adelaide, Australia, p. 545–550.
36. Liang R, Zhang J and Zhao D. *Theoretical and experimental investigation of the filled-type evacuated tube solar collector with U tube.* Solar Energy 2011; 85:1735–44.
37. Rittidech S, Donmaung A and Kumsombut K. *Experimental study of the performance of a circular tube solar collector with closed-loop oscillating heat-pipe with check valve*. Renewable Energy 2009; 34:2234–8.
38. Dunn P.D and Reay D.A., *Heat Pipes*, Fourth Edition (1994), Elsevier Science Ltd.
39. Azad E., *Theoretical and experimental investigation of heat pipe solar collector*. Experimental Thermal and Fluid Science 2008, 32:1666–1672.
40. Mathioulakis E. and Belessiotis V., *a new heat-pipe type solar domestic hot water system*. Solar Energy 2002, 72: 13–20.
41. Johane Bracamonte, José Parada, Jesús Dimas, and Miguel Baritto, Effect *of the collector tilt angle on thermal efficiency and stratification of passive water in glass evacuated tube solar water heater.* Applied Energy 155 (2015) 648–659.
42. Runsheng Tang, Wenfeng Gao, Yamei Yu and Hua Chen, *Optimal tilt-angles of all-glass evacuated tube solar collectors*. Energy 34 (2009) 1387–1395.
43. Yan Gao, Qunli Zhang, Rui Fan, Xinxing Lin and Yong Yu, *Effects of thermal mass and flow rate on forced-circulation solar hot-water system: Comparison of water-in-glass and U-pipe evacuated-tube solar collectors.* Solar Energy 98 (2013) 290–301.
44. Alireza Hobbi and Kamran Siddiqui, *Optimal design of a forced circulation solar water heating system for a residential unit in cold climate using TRNSYS.* Solar Energy 83 (2009) 700–714.

45. Y. Gao, R. Fan, X.Y. Zhang and Y.J. AN, *Thermal performance and parameter analysis of a U-pipe evacuated solar tube collector.* Solar Energy 98 (2013) 290–301
46. Reay D.A. and Kew P.A., *Heat Pipes,* 5th Edition 2006, Butterworth-Heinemann publisher, Oxford, UK.
47. Hussein H.M.S., *Theoretical and experimental investigation of wickless heat pipes flat plate solar collector with cross flow heat exchanger.* Energy Conversion and Management, 48 (2007):1266–1272.
48. Hussein H.M.S., Mohamad M.A. and El-Asfouri A.S., *Optimization of a wickless heat pipe flat plate solar collector*. Energy Conversion & Management, 40 (1999):1949-1961.
49. Mathioulakis E. and Belessiotis V., 2002, *a new heat-pipe type solar domestic hot water system*. Solar Energy, 72: 13–20.
50. Chien C.C., Kung C.K., Chang C.C., Lee W.S., Jwo C.S. and Chen S.L., *Theoretical and experimental investigations of a two-phase thermosyphon solar water heater*. Energy, 36 (2011): 415-423.
51. Ismail K.A.R, and Abogderah M. M., *Performance of a heat pipe solar collector*, Transaction of ASME, 120 (1998): 51-59.
52. Taherian H., Rezania A., Sadeghi S. and Ganji D.D., *Experimental validation of dynamic simulation of the flat plate collector in a closed thermosyphon solar water heater*. Energy Conversion and Management, 52 (2011): 301–307.
53. http://en.wikipedia.org/wiki/Harar Brewery S. Co.
54. http://www.alibaba.com/product-detail/Vacuum-tube-solar-panels-system-evacuated.
55. Incropera, DeWitt, Bergman and Lavine *Fundamental of Heat and Mass Transfer* 6th Edition.
56. Steven C. Chapra, *Applied Numerical Methods with MATLAB for Engineers and Scientists* 3rd Edition.
57. Mobin Arab, Ali Abbas, *Model-based design and analysis of heat pipe working fluid for optimal performance in evacuated tube solar water heater*, Solar Energy 94 (2013) 162–176.

Appendix

Appendix A: MATLAB Codes

```
Clear

% Given Radiation and ambient temperature values for a year
% Consider a glass cover and circular absorber tubes
% Design Parameters
N=25;          %number of tubes
tg=0.0012;     %thickness of glasses[m]
tp=0.0008;     %thickness of absorber coating[m]
tcu=0.0005;    %thickness of heat pipe[m]
tco=0.0005;    %thickness of condenser[m]
L=1.8;         %length of collector [m]
Le=1.6;        %length of evaporation section[m]
Lc=0.1;        %length of condensation section[m]
La=0.1;          %length 0f adiabatic section[m]
w=0.08 ;       %center distance b/n tubes[m]
Dg1=0.0556;     %inner diameter of outer glass[m]
Dp=0.0466;      %inner diameter of inner glass[m]
Dcu=0.015;        %inner diameter of heat pipe [m]
Dcuo=Dcu+2*tcu;   %outer diameter of heat pipe [m]
Dpo=Dp+2*tp;   %outer diameter of heat pipe [m]
Dg1o=Dg1+2*tg;   %outer diameter of heat pipe [m]
Dco=0.04;        %inner diameter of condenser [m]
Dcoo=Dco+2*tco;   %outer diameter of condenser [m]
Dm=0.039;           % inner diameter of manifold for 80 c processes[m]
rog=2250;         %density  of gasses at room temperature[kg/m^3]
roal=2702;         %density  of gasses at room temperature[kg/m^3]
rop=2250;         %density  of absorber tube[kg/m^3]
rocu=8933;        %density  of heat pipe/copper[kg/m^3]
rol=988;          %density  of fluid[kg/m^3]
roco=8933;        %density  of condenser[kg/m^3]
row=1000;         %density  of water[kg/m^3]
Cpg=835;          %specific heat of glass [J/kg K]
Cpp=835;          %specific heat of absorber [J/kg K]
Cpcu=385;         %specific heat of heat pipe [J/kg K]
Cpal=903;         %specific heat of heat pipe [J/kg K]
Cpl=4180;         %specific heat of fluid [J/kg K]
Cpco=385;         %specific heat of condenser [J/kg K]
Cpw=4179;         %specific heat of water [J/kg K]
kl=1.2;           %thermal conductivity of fluid at 49 0c [w/m K]
kHP=401;          %thermal conductivity of heat pipe[W/m K]
hfg=2390*10^3;    % specific heat of vaporization at 49 0c[J/kg]
muel=0.558*10^-3;  %viscosity of fluid at 49 0c[Ns/m2]
mdot=0.0132; % mass flow rate of water through manifold for processes
@ 80 0c[kg/s]
mdotp=0.0185;        % mass flow rate of water through manifold for
bottle cleaning @ 65 0c[kg/s]
```

```
mdotb=0.021; % mass flow rate of water through manifold for Mashing @
52 0c[kg/s]
Eg1=0.85;            %Emissivity of glass
Ep=0.1;              %Emissivity of absorber coating
Ecu=0.15;            %Emissivity of copper
Vt=1/3;               % filling ratio of fluid
Pabso=0.92 ;          %absorptivity of absorber coating
Gtrans=0.96;          %transitivity of glass
rho=0.2;              %ground reflectivity factor
sigma=5.67e-8;       %Boltzman constant [ W/m2K4 ]
Vw=7.8;            %wind speed [ m/s2 ]
beta=9*pi/180;      %Collector slope  [ rad ]
phi=9.31.*pi/180;    %latitude of Harar [ rad ]
gama=20*pi/180;     %surface azimuth [ rad ]
dt=60;              %time step
g=9.81;             % gravitational acceleration [m/s2]
% % % % % % % % % % % % % % % % % % % % % % % % % % % % % % % % % % % %
% % %

%%%%%%%%%%%%%%%%%%%%%%%%%%%%%%%%%%%%%%%%%%%%%%%%%%%%%%%%%%%%%%%%%%%%%%
%%%%%%

 load Dataa.m;

   data=zeros(24,3,365);

for j=1:365;

    data(:,:,j)=Dataa(j+(23*(j-1)):j*24,:);

end

%======================================================================
=====

 % Calculation of the declination angle for each day of the year.

  for N=1:365

     decl(N)=(pi/180)*(23.45*sin((2*pi/365.5)*(284+N)));

   end

%======================================================================
=====

 % Calculation of the hour angle for each hour of the day.
```

```
 for  ii=1:24

    omega(ii)=(12-ii)*pi/12;

end %%%%%%%%%%%%%%%%%%%%%%%%%%%%%%%%%%%%%%%%%%%%%%%%%%%%%%%%%%%%%

It11=zeros(365,24); Tp11=zeros(365,24); Tg111=zeros(365,24);
Ts11=zeros(365,24);

Tco11=zeros(365,24); Ta11=zeros(365,24); eff1=zeros(365,24);

  for i=1:365          % number of days of the year

     Grr=data(:,1,i);   Drr=data(:,2,i);  Taa=data(:,3,i);

 for j=1:24            % number of hours of the day

         Gr=Grr(j);      Dr=Drr(j) ;     Ta=Taa(j);

         Ta0=Ta+273; %initial ambient temperature [ K ]

% calculation of beam ratio

Rb=((sin(decl(i))*sin(phi)*cos(beta)-
sin(decl(i))*cos(phi)*sin(beta)*cos(gama)+cos(decl(i))*cos(phi)*cos(be
ta)*cos(omega(j))+...cos(decl(i))*sin(phi)*sin(beta)*cos(gama)*cos(ome
ga(j))+cos(decl(i))*sin(beta)*sin(gama)……*sin(omega(j)))/((cos(phi)*co
s(decl(i))*cos(omega(j)))+(sin(decl(i))*sin(phi))));

% calculation of total irradiance [W/m2] on the tilted surface

It=Rb*(Gr-Dr)+(Dr*0.5*(1+cos(beta)))+(0.5*rho*((1-cos(beta))*Gr));

Tg10=Ta0+0.25; %initial outer glass temperature [ K ]

Tp0=Ta0+1;      %initial inner glass temperature [ K ]

Ts0=Ta0+0.75;   %initial saturated fluid temperature [ K ]

Tco0=Ta0+0.5;   %initial condensed fluid temperature [ K ]

Tw0=Ta0+0.5;    %initial useful water temperature [ K ]

Twi=Ta0;        %initial water temperature at inlet [ K ]

Tsky=0.0552.*Ta0^1.5;   % sky temperature [ K]
```

```
 % heat transfer coefficient calculation

for k=1:60

Upg1r=sigma.*(Tp0.^2+Tg10.^2).*(Tp0+Tg10)/(1/Ep+1/Eg1-1);   %
Radiation heat loss coefficient inner glass to outer glass [W/m2K]

Upg1=Upg1r;  % total heat loss coefficient inner glass to outer glass
[W/m2K]

Ug1ar=sigma.*Eg1*(Tg10.^2+Tsky.^2).*(Tg10+Tsky);    % Radiation heat
loss coefficient outer glass to ambient [W/m2K]

Ug1acov=5.7+3.8*Vw;         % convention heat loss coefficient outer
glass to ambient [W/m2K]

Ug1a=Ug1ar+Ug1acov;         % total heat loss coefficient outer glass
to ambient [W/m2K]

Ufi=kHP*tcu/(pi.*Dcu.*Lc);   % convection heat loss coefficient
condensation section to manifold [W/m2K]

Ups=(kHP*tcu/(Dcu.*Le));     % conduction heat loss coefficient
absorber surface to evaporation section [W/m2K]

% convection heat loss coefficient evaporation section to condensation
section [W/m2K]

Uco=(0.997-0.334.*(cos(9))^0.108).*(kl^3*rol^2*g*hfg/(muel*Lc*(Ts0-
Tco0)))^0.25.*(Lc/Dcu)^(0.254*(cos(9))^0.385);

Ut1=((1/Upg1)+(1/Ug1a))^-1; %overall heat loss coefficient

%%%%%%%%%%%%%%%%%%%%%%%%%%%%%%%%%%%%%%%%%%%%%%%%%%%%%%%%%%%%%%%

%% transient temperature variation of elements

Tp0=(Dpo*dt/((rop.*pi*Dp.*tp.*Cpp)+((roal/4)*pi*(Dp-
Dcuo)^2*Cpal)))*(It.*Pabso.*Gtrans-Upg1.*(Tp0-Tg10)-Ups.*(Tp0-
Ts0))+Tp0;

Tg10=(dt/(rog.*pi*Dg1.*tg.*Cpg)).*(It*Dg1o*(1-Gtrans)+Upg1.*Dpo.*(Tp0-
Tg10)-Ug1a.*Dg1o.*(Tg10-Ta0))+Tg10;
```

```
Ts0=(4.*dt/(rol.*Dcu^2.*Le.*Vt.*Cpl)).*(Ups.*Dp.*Le.*(Tp0-Ts0)-
Uco.*Dcu^2.*0.25.*(Ts0-Tco0))+Ts0;

Tco0=(4.*dt/(roco.*(Dco-Dcuo)^2.*Lc.*Cpco)).*(Uco.*Dcuo^2.*0.25.*(Ts0-
Tco0)-Ufi.*Dcuo.*Lc.*(Tco0-Tw0))+Tco0;

q1=(Ut1)*Dpo*Le*(Tp0-Ta);     % overall heat loss

end

% matrix for ambient temperature, solar irradiance and temperature of
elements

Ta1=Ta0;      It11(i,j)=It;          Ta11(i,j)=Ta1-273;
Tp11(i,j)=Tp0-273;      Tg111(i,j)=Tg10-273;

Ts11(i,j)=Ts0-273;              Tco11(i,j)=Tco0-273;

 end

  end

%======================================================================
=====

 load Dataa.m;

   data=zeros(24,3,365);

for j=1:365;

    data(:,:,j)=Dataa(j+(23*(j-1)):j*24,:);

end

%%%%%%%%%%%%%%%%%%%%%%%%%%%%%%%%%%%%%%%%%%%%%%%%%%%%%%%%%%%%%%%%%%%%%%
%%%%%%%%%%%%%

T11=zeros(365,24);  Ta11=zeros(365,24);Taaa1=zeros(365,24);
Tco1=zeros(365,24);

Qub1=zeros(365,24); Qb1=zeros(365,24); Qbint1=zeros(365,24);

Qucip1=zeros(365,24); Qcip1=zeros(365,24); Qcipint1=zeros(365,24);

Quke1=zeros(365,24); Qke1=zeros(365,24); Qkeint1=zeros(365,24);
```

```
Qumu1=zeros(365,24); Qmu1=zeros(365,24); Qmuint1=zeros(365,24);

Qu1=zeros(365,24);

Qupa1=zeros(365,24); Qpa1=zeros(365,24); Qpaint1=zeros(365,24);

Qu31=zeros(365,24);

Qub21=zeros(365,24); Qb21=zeros(365,24); Qbint21=zeros(365,24);

Qu21=zeros(365,24);

Quto1=zeros(365,24); Qto1=zeros(365,24); Qtoint1=zeros(365,24);

eff11=zeros(365,24);eff21=zeros(365,24); eff31=zeros(365,24);

 for i=1:365

     Grr=data(:,1,i);          Drr=data(:,2,i);
Taa=data(:,3,i);

 for j=1:24

         Gr=Grr(j);            Dr=Drr(j);                Ta=Taa(j);

   Ta0=Ta+273;  Ta11(i,j)=Ta0;

Rb=((sin(decl(i))*sin(phi)*cos(beta)-
sin(decl(i))*cos(phi)*sin(beta)*cos(gama)+cos(decl(i))*cos(phi)*cos(be
ta)*cos(omega(j))+........cos(decl(i))*sin(phi)*sin(beta)*cos(gama)*co
s(omega(j))+cos(decl(i))*sin(beta)*sin(gama)*sin(omega(j)))/((cos(phi)
*cos(decl(i))*cos(omega(j)))+(sin(decl(i))*sin(phi))));

It=Rb*(Gr-Dr)+(Dr*0.5*(1+cos(beta)))+(0.5*rho*((1-cos(beta))*Gr));

% Define input variables

Lm  =2.08; %Length of manifold space[m]    n  = 26 ; % Number of nodes

del_i= Lm/(n-1) ; %Spacing of nodes   T_2= Ta0; %Temperature of Cold
side [K]

t_2   =  120 ;   % Seconds Stopping time    pt_spc = 6 ; % Number of
iterations between lines plotted
```

```
V  =(pi*0.034^2/4)*(Lm-0.08) ;  % volume of manifold [m3]   del_t  =
t_2/(n-1); % seconds  Change in time each iteration

t(1)  = 0;        %seconds  Initial time

% Temperature variation matrix of condensation section, saturated
section and

% ambient temperature and irradiance

Tco=Tco11(i,j);   Ts=Ts11(i,j);     Itt=It11(i,j);    Taaa=Ta11(i,j);

 T(1:n,:)=Ta0;  %inlet water temperature for processes at 80 0c

Tp(1:n,:)=Ta0;  %inlet water temperature bottle cleaning

Tm(1:n,:)=Ta0;  %inlet water temperature mashing at 52 0c

% Loop to generate x position matrix

for z = 1:n

    x(z) = del_i*(z-1)          ;

end

% Initiate iteration variables

m                       = 1                  ; %""       Time counter

mm                      = 1                   ;

 %Start While loop to run until convergence it met

 while t(m) < t_2

    %Loop to calculate updated temperature based on governing equation

    for k = 1:n

    %cold initial point

        if k == 1
```

```
T(k,m+1)= T(k,m) +
4.*del_t/(rol*Cpw*pi*0.1^2*del_i)*(Ufi*pi*Dcuo*Lc/del_i*(Tco+273-T_2)-
mdot*Cpw/del_i*(T(k,m)-T_2));

Tp(k,m+1)= Tp(k,m) +
4.*del_t/(rol*Cpw*pi*0.1^2*del_i)*(Ufi*pi*Dcuo*Lc/del_i*(Tco+273-T_2)-
mdotp*Cpw/del_i*(Tp(k,m)-T_2));

Tm(k,m+1)= Tm(k,m) +
4.*del_t/(rol*Cpw*pi*0.1^2*del_i)*(Ufi*pi*Dcuo*Lc/del_i*(Tco+273-T_2)-
mdotb*Cpw/del_i*(Tm(k,m)-T_2));

    % hot External Surface

        elseif k == n

T(k,m+1)= T(k,m) +
4*del_t/(rol*Cpw*pi*0.1^2*del_i)*(k*Ufi*pi*Dcuo*Lc/del_i*(Tco+273-T(k-
1,m))-mdot*Cpw/del_i*(T(k,m)-T(k-1,m)));

Tp(k,m+1)= Tp(k,m) +
4*del_t/(rol*Cpw*pi*0.1^2*del_i)*(k*Ufi*pi*Dcuo*Lc/del_i*(Tco+273-
Tp(k-1,m))-mdotp*Cpw/del_i*(Tp(k,m)-Tp(k-1,m)));

Tm(k,m+1)= Tm(k,m) +
4*del_t/(rol*Cpw*pi*0.1^2*del_i)*(k*Ufi*pi*Dcuo*Lc/del_i*(Tco+273-
Tm(k-1,m))-mdotb*Cpw/del_i*(Tm(k,m)-Tm(k-1,m)));

    %internal nodes

         Else

T(k,m+1)= T(k,m) +
4*del_t/(rol*Cpw*pi*0.1^2*del_i)*(k*Ufi*pi*Dcuo*Lc/del_i*(Tco+273-T(k-
1,m))-mdot*Cpw/del_i*(T(k,m)-T(k-1,m)));

Tp(k,m+1)= Tp(k,m) +
4*del_t/(rol*Cpw*pi*0.1^2*del_i)*(k*Ufi*pi*Dcuo*Lc/del_i*(Tco+273-
Tp(k-1,m))-mdotp*Cpw/del_i*(Tp(k,m)-Tp(k-1,m)));

Tm(k,m+1)= Tm(k,m) +
4*del_t/(rol*Cpw*pi*0.1^2*del_i)*(k*Ufi*pi*Dcuo*Lc/del_i*(Tco+273-
Tm(k-1,m))-mdotb*Cpw/del_i*(Tm(k,m)-Tm(k-1,m)));
```

```
        end % (if statement)

     end %(i loop)

     t(m+1)                  = t(m) + del_t                    ; %seconds
Time

  %Important to put all the (m+1) variables before the m = m +1 line

    m                      = m + 1        ; %       Update check counter

    mm                     = mm + 1       ; %         plot counter

 %Conditional statement to check and make sure while loop does not run

    %indefinitely (Use Control C to stop infinite loop)

    if m == 20001

        fprintf('Autobreak')   %Print notice to announce auto stopping

        break

    end % (Check loop)

    Ut4=(1/(n*Ufi));

  q4=Ut4*pi*Dcuo*Lc*((Tco+273-T(k,m)));
qp4=Ut4*pi*Dcuo*Lc*((Tco+273-Tp(k,m)));

  qm4=Ut4*pi*Dcuo*Lc*((Tco+273-Tm(k,m)));

% solar thermal energy production for all selected thermal processes

% conventional thermal energy consumption for all processes

% integrated system conventional thermal energy consumption

% processes at 80 0C

Qub=62*mdot*Cpw*(T(k,m)-Taaa); Qb=0.817*Cpw*(80+273-Taaa);  Qbint=Qb-
Qub;

 Qucip=168*mdot*Cpw*(T(k,m)-Taaa); Qcip=2.21*Cpw*(80+273-Taaa);
Qcipint=Qcip-Qucip;
```

```
  Quke=27*mdot*Cpw*(T(k,m)-Taaa); Qke=0.342*Cpw*(80+273-Taaa);
Qkeint=Qke-Quke;

  Qumu=22*mdot*Cpw*(T(k,m)-Taaa); Qmu=0.29*Cpw*(80+273-Taaa);
Qmuint=Qmu-Qumu;

  Qu=mdot*Cpw*(T(k,m)-Ta0);

% bottle cleaning Processes at 650C

 Qupa=59*mdotp*Cpw*(Tp(k,m)-Taaa); Qpa=1.08*Cpw*(73.33+273-Taaa);
Qpaint=Qpa-Qupa;

  Qu3=mdotp*Cpw*(Tp(k,m)-Taaa);

%mashing at 520C

 Qub2=30*mdotb*Cpw*(Tm(k,m)-Taaa); Qb2=0.616*Cpw*(52+273-Taaa);
Qbint2=Qb2-Qub2;

  Qu2=mdotb*Cpw*(Tm(k,m)-Taaa);

% instantaneous efficiency

 eff1=Qu*100/(3.2*It); eff2=Qu2*100/(3.2*It); eff3=Qu3*100/(3.2*It);

 % total thermal energy production and total conventional thermal
energy consumption

Qto=Qb+Qcip+Qke+Qmu+Qpa+Qb2; Quto=Qub+Qucip+Quke+Qumu+Qupa+Qub2;
Qtoint=Qto-Quto;

 end

T11(i,j)=T(k,m)-273; Ta11(i,j)=Ta0-273; Taaa1(i,j)=Taaa;Tco1(i,j)=Tco;

Qub1(i,j)=Qub;      Qb1(i,j)=Qb;      Qbint1(i,j)=Qbint;

Qucip1(i,j)=Qucip; Qcip1(i,j)=Qcip; Qcipint1(i,j)=Qcipint;

Quke1(i,j)=Quke;    Qke1(i,j)=Qke;    Qkeint1(i,j)=Qkeint;

Qumu1(i,j)=Qumu;    Qmu1(i,j)=Qmu;    Qmuint1(i,j)=Qmuint;

Qu1(i,j)=Qu;
```

```
Qupa1(i,j)=Qupa;  Qpa1(i,j)=Qpa;  Qpaint1(i,j)=Qpaint;

Qu31(i,j)=Qu3;

Qub21(i,j)=Qub2; Qb21(i,j)=Qb2; Qbint21(i,j)=Qbint2;

Qu21(i,j)=Qu2;

eff11(i,j)=eff1; eff21(i,j)=eff2; eff31(i,j)=eff3;

Quto1(i,j)=Quto;  Qto1(i,j)=Qto;  Qtoint1(i,j)=Qtoint;

 end

 end

%Print the number of iteration used to command window

fprintf('Number of Iterations was %0.2f \n\n',m)

%%%%%%%%%%%%%%%%%%%%%%%%%%%%%%%%%%%%%%%%%%%%%%%%%%%%%%%%%%%%%%%%%%%%%%
%%%%

% Generate figure and plot results
figure(1)

plot (Qto1,Qcip1,Qke1,Qmu1,Qb1,Qb21,Qpa1);
plot (T11,Tm11,Tp11);

TM16=T11(75,:);TA15=T11(105,:);


 jj=1:24;

 plot(jj,real(TM16),'r-',jj,real(TA15),'g-','linewidth',2);
    xlabel(' Time in Hours','fontsize',12)
   ylabel('Temperature in Degree Celcius','fontsize',12)
   title('Outlet Water Temperature variation in Last Node
Graph','fontsize',12)
   legend('March16','April15')
   grid on
  pause
   clf


effJ17=eff1(17,:);effF16=eff1(47,:);effM16=eff1(75,:);effA15=eff1(105,
:);....
   effM1=eff1(121,:);effJ11=eff1(162,:);
effJu17=eff1(198,:);effA16=eff1(228,:);....
```

```
effS15=eff1(258,:);effO15=eff1(288,:);effN14=eff1(318,:);effD10=eff1(3
44,:);

 jj=1:24;

 plot(jj,real(effJ17),'k-',jj,real(effF16),'b-',jj,real(effM16),'r-
',jj,real(effA15),'g-',jj,real(effM1),'b--',...
    jj,real(effJ11),'k--',jj,real(effJu17),'r--',jj,real(effA16),'g--
',jj,real(effS15),'k*',jj,real(effO15),'b*',...
jj,real(effN14),'r*',jj,real(effD10),'g*','linewidth',2);
    xlabel(' Time in hours','fontsize',12)
   ylabel(' efficency in %','fontsize',12)
   title(' efficency ','fontsize',12)

legend('January17','February16','March16','April15','May1','June11','J
uly17',.....
 'August16','September15','Octowber15','November14','December10')
   grid on
  pause
   clf

   plot( Qu1,Qu21,Qu31);

QuM12=Qu1(71,:);QuJ19=Qu1(200,:);

  jj=1:24;

 plot(jj,real(QuM12),'r-',jj,real(QuJ19),'g-','linewidth',2);
    xlabel(' Time in Hours','fontsize',12)
   ylabel('Solar Thermal Energy in W','fontsize',12)
   title(' Solar Thermal Energy Harvest Graph','fontsize',12)
   legend('March12','July19')
   grid on
  pause
   clf
  plot (Quto1, Qucip1,Quke1,Qumu1, Qub1, Qub21, Qupa1);
 plot (Quto1, Qto1, Qtoint1);

  QutoM12=Quto1(71,:); QtoM12=Qto1(71,:); QtointM12=Qtoint1(71,:);

 jj=1:24;

 plot(jj,real(QutoM12),'k-',jj,real(QtoM12),'r-
',jj,real(QtointM12),'b-','linewidth',2);
    xlabel(' Time in hours','fontsize',12)
   ylabel('hourly Solar thermal energy','fontsize',12)
   title(' energy ','fontsize',12)
   legend('Quto','Qto','Qtoint')
   grid on
  pause
   clf
```

```
QutoM29=Quto1(88,:); QtoM29=Qto1(88,:); QtointM29=Qtoint1(88,:);

 jj=1:24;

 plot(jj,real(QutoM29),'k-',jj,real(QtoM29),'r-
',jj,real(QtointM29),'b-','linewidth',2);
    xlabel(' Time in hours','fontsize',12)
   ylabel('hourly Solar thermal energy','fontsize',12)
   title(' energy ','fontsize',12)
   legend('Quto','Qto','Qtoint')
   grid on
  pause
   clf

QutoJ19=Quto1(200,:); QtoJ19=Qto1(200,:); QtointJ19=Qtoint1(200,:);

 jj=1:24;

 plot(jj,real(QutoJ19),'k-',jj,real(QtoJ19),'r-
',jj,real(QtointJ19),'b-','linewidth',2);
    xlabel(' Time in hours','fontsize',12)
   ylabel('hourly Solar thermal energy','fontsize',12)
   title(' energy ','fontsize',12)
   legend('Quto','Qto','Qtoint')
   grid on
  pause
   clf
```

Appendix B: Thermal Energy Analysis

Appendix B-1: Monthly Furnace Oil Consumption Data

Monthly Furnace Oil Consumption Data			
Months	**Years**	**Unit**	**Consumption**
Jan	2014	Lt	130643.00
Feb	2014	Lt	123058.00
Mar	2014	Lt	123058.00
Apr	2014	Lt	121548.00
May	2014	Lt	126073.00
Jun	2014	Lt	119941
Jul	2014	Lt	143627
Aug	2014	Lt	162431
Sep	2014	Lt	159908
Oct	2014	Lt	165277
Nov	2014	Lt	78845
Dec	2014	Lt	154597
Jan.	2015	Lt	148460
Feb.	2015	Lt	150117
Mar.	2015	Lt	170570
Apr.	2015	Lt	159141
May	2015	Lt	161082
Jun.	2015	Lt	159710
Average Annual Oil Consumption		**Lt**	**1705390.667**

Appendix B-2: Furnace Oil Energy Analysis

Furnace Oil Analysis		
Parameters	**Unit**	**Amount**
Annual Operation Hour of Boiler	hr	8344
Average Daily Oil Consumption	Lt	4905.25
Oil Flow Rate	m3/sec	5.67737E-05
Gross Calorific Value of Oil	KJ/Kg	43962
Density of Fuel Oil	Kg/m3	991
Chemical Energy of Oil	KW	2473.42
Annual Chemical Energy of Oil	**MWthr**	**20638.23**
Specific Heat of Fuel	KJ/KgK	0.879
Annual Energy For Pre Heating of Fuel	MWthr	25.41
Annual Heat Loss	MWthr	4127.65
Pump Power	W	350
Annual Pump Energy	MWhr	1.46

Appendix C: RETScreen Analysis

RETScreen® Energy Model - Solar Water Heating Project

Training & Support

Site Conditions		Estimate	Notes/Range
Project name		SWH	See Online Manual
Project location		Harar Brewery S.C., Ethiopia	
Nearest location for weather data		Harar, Ethiopia	Complete SR&HL sheet
Annual solar radiation (tilted surface)	MWh/m²	2.22	
Annual average temperature	°C	18.7	-20.0 to 30.0
Annual average wind speed	m/s	7.5	
Desired load temperature	°C	77	
Hot water use	L/d	463,033	
Number of months analysed	month	12.00	
Energy demand for months analysed	MWh	11,181.03	

System Characteristics		Estimate	Notes/Range
Application type		Service hot water (with storage)	
Base Case Water Heating System			
Heating fuel type	-	**#6 oil - L**	
Water heating system seasonal efficiency	%	80%	50% to 190%
Solar Collector			
Collector type	-	Evacuated	See Technical Note 1
Solar water heating collector manufacturer		Thermomax	See Product Database
Solar water heating collector model		Mazdon 20 - TMA 600S	
Gross area of one collector	m²	3.20	1.00 to 5.00
Aperture area of one collector	m²	2.32	1.00 to 5.00
Fr (tau alpha) coefficient	-	0.89	0.40 to 0.80
Fr UL coefficient	(W/m²)/°C	1.07	0.30 to 3.00
Temperature coefficient for Fr UL	(W/(m·°C)²)	0.00	0.000 to 0.010
Suggested number of collectors		1467	
Number of collectors		368	
Total gross collector area	m²	1177.6	
Storage			
Ratio of storage capacity to coll. area	L/m²	93.7	37.5 to 100.0
Storage capacity	L	80,000	
Balance of System			
Heat exchanger/antifreeze protection	yes/no	No	
Suggested pipe diameter	mm	N/A	8 to 25 or PVC 35 to 50
Pipe diameter	mm	25	8 to 25 or PVC 35 to 50
Pumping power per collector area	W/m²	0	3 to 22, or 0
Piping and solar tank losses	%	0%	1% to 10%
Losses due to snow and/or dirt	%	0%	2% to 10%
Horz. dist. from mech. room to collector	m	100	5 to 20
# of floors from mech. room to collector	-	10	0 to 20

Annual Energy Production (12.00 months analysed)		Estimate	Notes/Range
SWH system capacity	kW_{th}	598	
	MWth	0.598	
Pumping energy (electricity)	MWh	**1.48**	
Specific yield	kWh/m²	1,763	
System efficiency	%	80%	
Solar fraction	%	19%	
Renewable energy delivered	MWh	**2,076.26**	
	GJ	7,474.54	
			Complete Cost Analysis sheet

RETScreen® Solar Resource and Heating Load Calculation - Solar Water Heating Project

Site Latitude and Collector Orientation		Estimate	Notes/Range
Nearest location for weather data		Harar, Ethiopia	See Weather Database
Latitude of project location	°N	9.3	-90.0 to 90.0
Slope of solar collector	°	9.0	0.0 to 90.0
Azimuth of solar collector	°	20.0	0.0 to 180.0

Monthly Inputs

(Note: 1. Cells in grey are not used for energy calculations; 2. Revisit this table to check that all required inputs are filled if you change system type or solar collector type or pool type, or method for calculating cold w ater temperature).

Month	Fraction of month used (0 - 1)	Monthly average daily radiation on horizontal surface (kWh/m²/d)	Monthly average temperature (°C)	Monthly average relative humidity (%)	Monthly average wind speed (m/s)	Monthly average daily radiation in plane of solar collector (kWh/m²/d)
January	1.00	6.16	17.8	100.0	11.3	6.65
February	1.00	6.78	19.5	66.0	11.8	7.12
March	1.00	7.51	20.7	66.0	9.8	7.64
April	1.00	5.54	18.8	71.0	5.4	5.45
May	1.00	6.40	20.2	67.0	5.4	6.13
June	1.00	5.50	20.8	74.0	5.0	5.23
July	1.00	2.84	17.5	83.0	4.4	2.99
August	1.00	5.68	18.0	85.0	5.3	5.53
September	1.00	4.72	16.5	79.0	4.3	4.72
October	1.00	6.92	19.5	69.0	6.4	7.20
November	1.00	6.72	17.5	66.0	8.7	7.23
December	1.00	6.45	17.2	69.0	12.2	7.06

		Annual	Season of Use
Solar radiation (horizontal)	MWh/m²	2.16	2.16
Solar radiation (tilted surface)	MWh/m²	2.22	2.22
Average temperature	°C	18.7	18.7
Average wind speed	m/s	7.5	7.5

Water Heating Load Calculation		Estimate	Notes/Range
Application type	-	Service hot water	
System configuration	-	With storage	
Building or load type	-	Industrial	
Number of units	-	-	
Rate of occupancy	%	-	50% to 100%
Estimated hot water use (at ~60 °C)	L/d	N/A	
Hot water use	L/d	463032.943	
Desired water temperature	°C	77.25	
Days per week system is used	d	7	1 to 7
Cold water temperature	-	User-defined	
Minimum	°C	13.0	1.0 to 10.0
Maximum	°C	28.0	5.0 to 15.0
Months SWH system in use	month	12.00	
Energy demand for months analysed	MWh	11,181.03	
	GJ	40,251.69	

Return to Energy Model sheet

RETScreen® Cost Analysis - Solar Water Heating Project

Type of project:	Pre-feasibility	Currency:	$
		Second currency:	Ethiopia
Cost references:	Second currency	Rate: $/ETB	0.04760

Initial Costs (Credits)	Unit	Quantity	Unit Cost	Amount	Relative Costs	% Foreign	Foreign Amount
Feasibility Study							
Other - Feasibility study	Cost	0	$ -	$ -		0%	ETB -
Sub-total :				**$ -**	0.0%	-	ETB -
Development							
Other - Development	Cost	0	$ -	$ -		0%	ETB -
Sub-total :				**$ -**	0.0%	-	ETB -
Engineering							
Other - Engineering	Cost	0	$ -	$ -		0%	ETB -
Sub-total :				**$ -**	0.0%	-	ETB -
Energy Equipment							
Solar collector	m²	1,177.6	$ 246	$ 289,690		100%	ETB 6,085,916
Solar storage tank	L	80,000	$ 0.70	$ 56,000		100%	ETB 1,176,469
Solar loop piping materials	m	313	$ 27.00	$ 8,456		100%	ETB 177,655
Circulating pump(s)	W	350	$ 1.10	$ 385		100%	ETB 8,089
Heat exchanger	kW	0.0	$ -	$ -		100%	ETB -
Transportation	project	1	$ 2,000	$ 2,000		100%	ETB 42,017
Other - Energy equipment	Cost	2	$ 400	$ 800		100%	ETB 16,807
Sub-total :				**$ 357,331**	81.1%	100%	ETB 7,506,953
Balance of System							
Collector support structure	m²	1,177.6	$ 25	$ 29,440		100%	ETB 618,487
Plumbing and control	project	1	$ 300	$ 300		100%	ETB 6,303
Collector installation	m²	1,177.6	$ 5	$ 5,888		100%	ETB 123,697
Solar loop installation	m	313	$ 2.00	$ 626		100%	ETB 13,160
Auxiliary equipment installation	project	1	$ 5,000	$ 5,000		100%	ETB 105,042
Transportation	project	1	$ 1,000	$ 1,000		100%	ETB 21,008
Other - Balance of system	Cost	0	$ -	$ -		100%	ETB -
Sub-total :				**$ 42,254**	9.6%	100%	ETB 887,697
Miscellaneous							
Training	p-h	6	$ 200	$ 1,200		100%	ETB 25,210
Contingencies	%	10%	$ 400,785	$ 40,079		100%	ETB 841,986
Sub-total :				**$ 41,279**	9.4%	100%	ETB 867,196
Initial Costs - Total				**$ 440,864**	100.0%	100%	**ETB 9,261,846**

Annual Costs (Credits)	Unit	Quantity	Unit Cost	Amount	Relative Costs	% Foreign	Foreign Amount
O&M							
Property taxes/Insurance	project	0	$ -	$ -		100%	ETB -
O&M labour	project	1	$ 1,500	$ 1,500		100%	ETB 31,513
Other - O&M	Cost	0	$ -	$ -		100%	ETB -
Contingencies	%	10%	$ 1,500	$ 150		100%	ETB 3,151
Sub-total :				**$ 1,650**	97.1%	100%	ETB 34,664
Electricity	kWh	1,483	**$ 0.0330**	**$ 49**	2.9%	100%	ETB 1,028
Annual Costs - Total				$ 1,699	100.0%	100%	ETB 35,692

Periodic Costs (Credits)		Period	Unit Cost	Amount	% Foreign	Foreign Amount
Valves and fittings	Cost	20 yr	$ 250	**$ 250**	100%	ETB 5,252
Pool heat pump compressor	Credit	10 yr	$ -	**$ -**	100%	ETB -
				$ -	0%	ETB -
End of project life		-	$ 41,943	**$ (41,943)**		

Go to GHG Analysis sheet

RETScreen® Greenhouse Gas (GHG) Emission Reduction Analysis - Solar Water Heating Project

Use GHG analysis sheet? Yes

Type of analysis: Standard

Background Information

Project Information

Project name	SWH
Project location	Harar Brewery S.C., Ethiopia

Global Warming Potential of GHG

1 tonne CH_4 =	21 tonnes CO_2	(IPCC 1996)
1 tonne N_2O =	310 tonnes CO_2	(IPCC 1996)

Base Case Electricity System (Baseline)

Fuel type	Fuel mix (%)	CO_2 emission factor (kg/GJ)	CH_4 emission factor (kg/GJ)	N_2O emission factor (kg/GJ)	Fuel conversion efficiency (%)	T & D losses (%)	GHG emission factor (t_{CO2}/MWh)
Large hydro	100.0%	0.0	0.0000	0.0000	100.0%	8.0%	0.000
#6 oil	0.0%	77.4	0.0030	0.0020	30.0%		0.000
Electricity mix	100%	0.0	0.0000	0.0000		8.0%	0.000

Base Case Heating System (Baseline)

Fuel type	Fuel mix (%)	CO_2 emission factor (kg/GJ)	CH_4 emission factor (kg/GJ)	N_2O emission factor (kg/GJ)	Fuel conversion efficiency (%)	GHG emission factor (t_{CO2}/MWh)
Heating system						
#6 oil	100.0%	77.4	0.0030	0.0020	80.0%	0.351

Proposed Case Heating System (Solar Water Heating Project)

Fuel type	Fuel mix (%)	CO_2 emission factor (kg/GJ)	CH_4 emission factor (kg/GJ)	N_2O emission factor (kg/GJ)	Fuel conversion efficiency (%)	GHG emission factor (t_{CO2}/MWh)
Heating system						
Electricity	0.1%	0.0	0.0000	0.0000	100.0%	0.000
Solar	99.9%	0.0	0.0000	0.0000	100.0%	0.000
Heating energy mix	100.0%	0.0	0.0000	0.0000		0.000

GHG Emission Reduction Summary

	Base case GHG emission factor (t_{CO2}/MWh)	Proposed case GHG emission factor (t_{CO2}/MWh)	End-use annual energy delivered (MWh)		Annual GHG emission reductio (t_{CO2})
Heating system	0.351	0.000	2,076.26		729.54
			Net GHG emission reduction	t_{CO2}/yr	**729.54**

Complete Financial Summary sheet

RETScreen® Financial Summary - Solar Water Heating Project

Annual Energy Balance

Project name		SWH	Electricity required	MWh	1.48
Project location		Harar Brewery S.C., Ethiopia			
Renewable energy delivered	MWh	2,076.26	Net GHG reduction	t_{CO2}/yr	729.54
Heating fuel displaced	-	#6 oil - L	Net GHG emission reduction - 20 yrs	t_{CO2}	14,590.86

Financial Parameters

Avoided cost of heating energy	$/L	0.719	Debt ratio	%	50.0%
			Debt interest rate	%	8.5%
			Debt term	yr	10
GHG emission reduction credit	$/$t_{CO2}$	-	Income tax analysis?	yes/no	No
Retail price of electricity	$/kWh	0.033			
Energy cost escalation rate	%	5.0%			
Inflation	%	10.0%			
Discount rate	%	10.0%			
Project life	yr	20			

Project Costs and Savings

Initial Costs				**Annual Costs and Debt**		
Feasibility study	0.0%	$	-	O&M	$	1,650
Development	0.0%	$	-	Electricity	$	49
Engineering	0.0%	$	-	Debt payments - 10 yrs	$	33,596
Energy equipment	81.1%	$	357,331	**Annual Costs and Debt - Total**	**$**	**35,294**
Balance of system	9.6%	$	42,254			
Miscellaneous	9.4%	$	41,279	**Annual Savings or Income**		
Initial Costs - Total	100.0%	**$**	**440,864**	Heating energy savings/income	$	165,813
Incentives/Grants		$	-			
				Annual Savings - Total	**$**	**165,813**
Periodic Costs (Credits)						
Valves and fittings		$	250	Schedule yr # 20		
Pool heat pump compressor		$	-			
		$	-			
End of project life -		$	(41,943)	Schedule yr # 20		

Financial Feasibility

Pre-tax IRR and ROI	%	69.0%	Calculate GHG reduction cost?	yes/no	Yes
After-tax IRR and ROI	%	69.0%	GHG emission reduction cost	$/$t_{CO2}$	(272)
Simple Payback	yr	2.7	Project equity	$	220,432
Year-to-positive cash flow	yr	1.6	Project debt	$	220,432
Net Present Value - NPV	$	1,689,964	Debt payments	$/yr	33,596
Annual Life Cycle Savings	$	198,503	Debt service coverage	-	5.13
Benefit-Cost (B-C) ratio	-	8.67			

Appendix D: Sample Solar Collector Installation

Appendix E: Input Data for Heat Transfer Limit Calculation

Parameters	Symbol	Units	Value
Liquid Density	ρ_l	kg/m^3	988
Vapor Density	ρ_v	kg/m^3	0.08
Liquid Viscosity	μ_l	Ns/m^2	0.0005588
Surface Tension	σ	N/m	0.0679
Heat Pipe Total Length	l_t	m	1.8
Evaporator Length	l_e	m	1.6
Condenser Length	l_c	m	0.1
Adiabatic Length	l_a	m	0.1
Internal Pipe Diameter ,	D_{cui}	mm	14
External Pipe Diameter	D_{cuo}	mm	15
Temperature of Vaporization	T_s	^{0}C	49
Latent Heat of Vaporization	h_{fg}	KJ/kg	2390
Pipe Material Thermal Conductivity	k_{hp}	$W \cdot m^{-1} \cdot 0C^{-1}$	401
Equivalent Thermal Conductivity Wick Materials	k_e	$W \cdot m^{-1} \cdot 0C^{-1}$	1.2
Weak Permeability	K_p	m^2	1.29E-09
Mesh Wire Diameter,	d_{meshw}	mm	0.2
Effective Radius of Heat Pipe	r_e	mm	0.25
Vapor Specific Heat Ratio	γ_v		1.32
Wick Area	A_w	mm^2	0.19
Vapor Core Diameter ,	D_v	mm	13.4
Hydraulic Radius of Porous Medium	r_h	mm	0.014
Wick Porosity	ε		0.7
Filling Ratio			33%
Gravitational Acceleration	g	m/s^2	9.81
Angel of Inclination	β		9
Gas Constant	R_v	J/kg .K	461.5
Vapor Core Area	A_v	m^2	0.02412
Working Pressure	p_o	Kpa	600